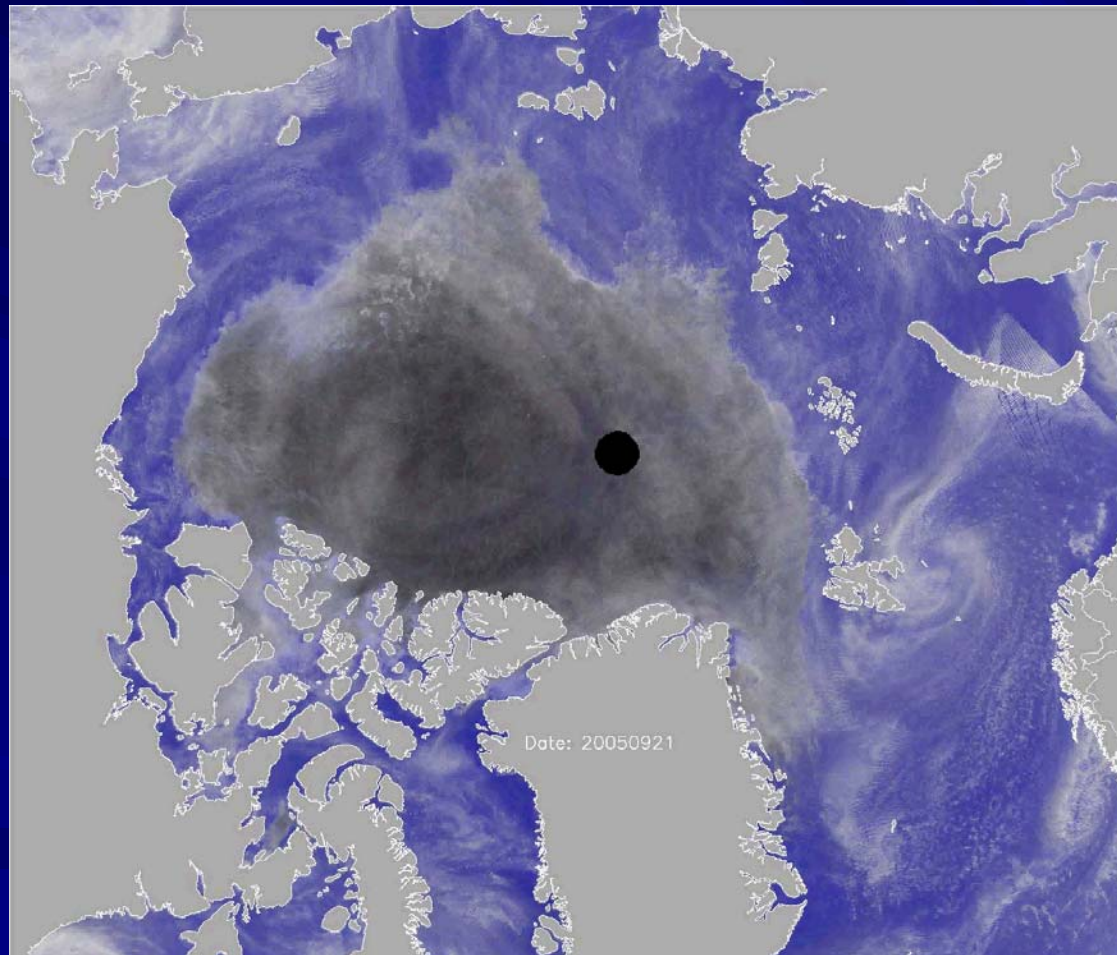


Arctic seaice Sept 2005-May 2006 *Tom Agnew*



(i) Optical alimetry: imaging a rotating fluid

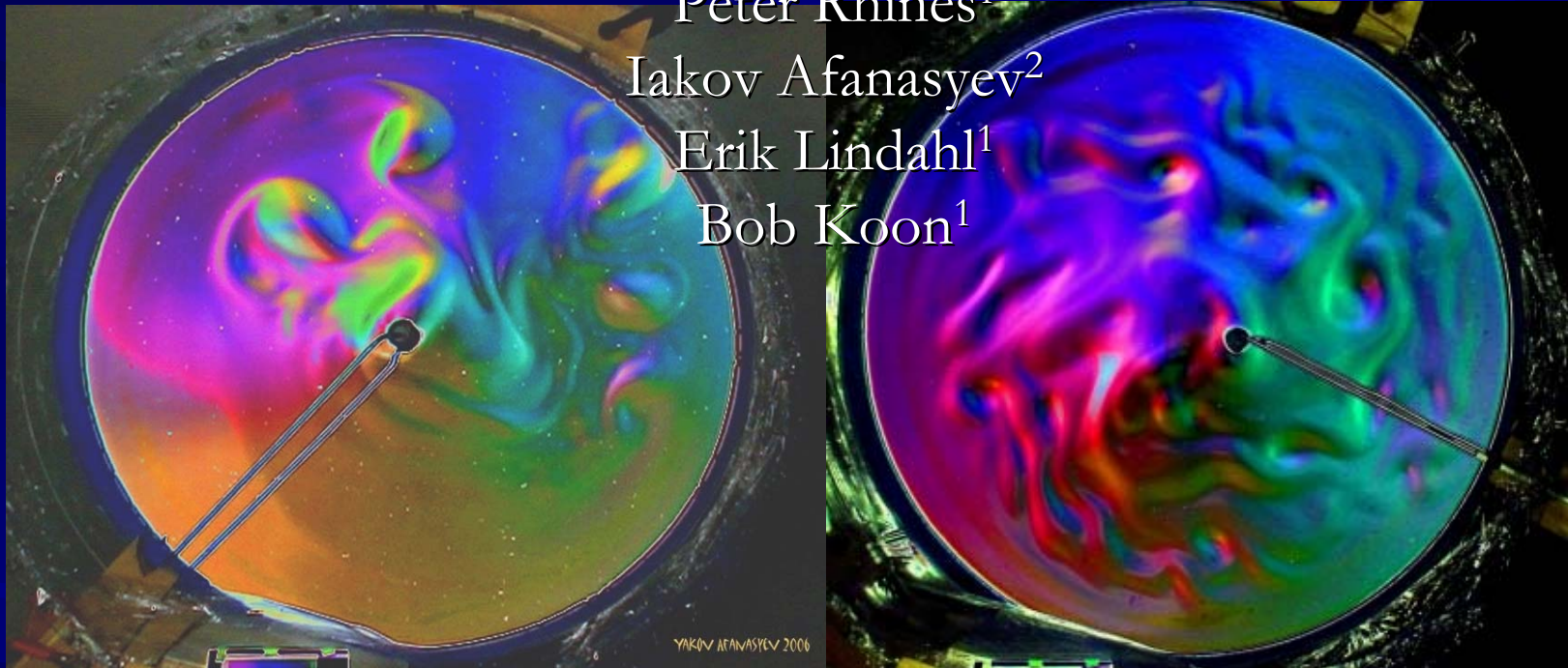
(ii) Teaching about global environment and energy in the lab

Peter Rhines<sup>1</sup>

Iakov Afanasyev<sup>2</sup>

Erik Lindahl<sup>1</sup>

Bob Koon<sup>1</sup>



<sup>1</sup>*Oceanography & Atmospheric Sciences, University of Washington*

<sup>2</sup>*Physics, Memorial University, St Johns Newfoundland*

View from above: SSH field in 1m diameter rotating cylinder, configured as a polar-cap ocean and excited by a buoyant source of upper-ocean water at center

## ■ Two aspects of a fluids lab:

- teaching graduate students about rotating, stratified fluids
- teaching undergraduates about the scientific basis for understanding the global environment

angular momentum, Coriolis, buoyancy, potential vorticity

energy as a focus: solar forcing of climate => biological energy => human mining of energy resources => lives of Arctic natives

We physical scientists have to admit that biology, ecosystems and human prosperity are the end-game of our science. We must relate to them in our teaching.

Whaling by the Inupiat natives of Alaska's north slope (image by Charles Wohlforth, author of *The Whale and the Supercomputer*). These bowhead whales weight about 100,000 lbs and may live in excess of 200 years. This says something about the stability of their environment.





- A modern aspect of fluids labs is their connections with field observations....both through scale-model simulations but also shearly through technique and technology. For example:
  - satellite altimetry and GFD lab altimetry
  - buoyancy driven ocean circulation and turbulent mixing via robotic Seagliders and lab simulations
  - jet stream dynamics and cyclogenesis from atmospheric reanalyzed global observations, and the family of classic jets in the lab



## The Jet-Stream Conundrum

Mark P. Baldwin, Peter B. Rhines, Hwei-Ping Huang, Michael E. McIntyre

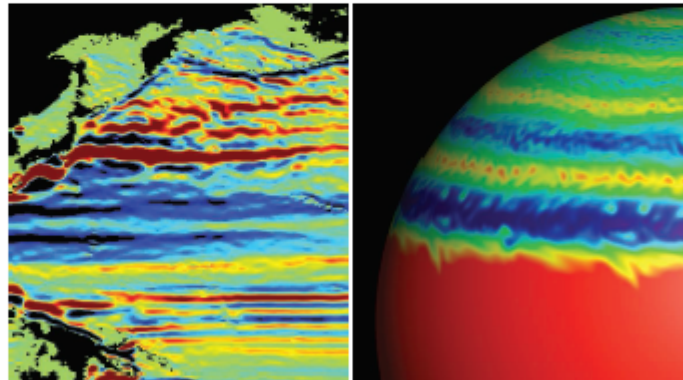
Jet streams, or “jets” for brevity, are concentrated, intense, elongated flows that often contain most of the kinetic energy in a flowing fluid. They are pervasive features of Earth’s atmosphere and oceans, where they transport heat, chemicals, and even biota such as krill, and they are also abundant on other planets (see the figure).

Jets are observed to occur spontaneously on rotating planets whenever stratified atmospheres or oceans are forced into turbulent motion. Yet there is a mystery as to why jets exist at all—why is there this propensity to concentrate energy and momentum? A second mysterious property of jets is that they can act as flexible material barriers, inhibiting mixing across their axes. The strongest eastward jets provide expressways for the transport of chemicals and biota along their axes but severely inhibit mixing across their axes. A

new theoretical paradigm (*1*) explains the abundance of jets, in any planetary atmosphere or ocean, in a simple manner. The paradigm combines field theory with chaotic (turbulent) fluid motion; in doing so, it captures long-range interactions that are crucial for forming and stabilizing jets. It shows that mix-

ing a fluid on a rotating planet will invariably produce jets and that the two mysteries, jet formation and the inhibition of mixing, formerly regarded as two separate phenomena, are intimately related to each other.

Both jet formation and the inhibition of mixing are completely enigmatic in terms of



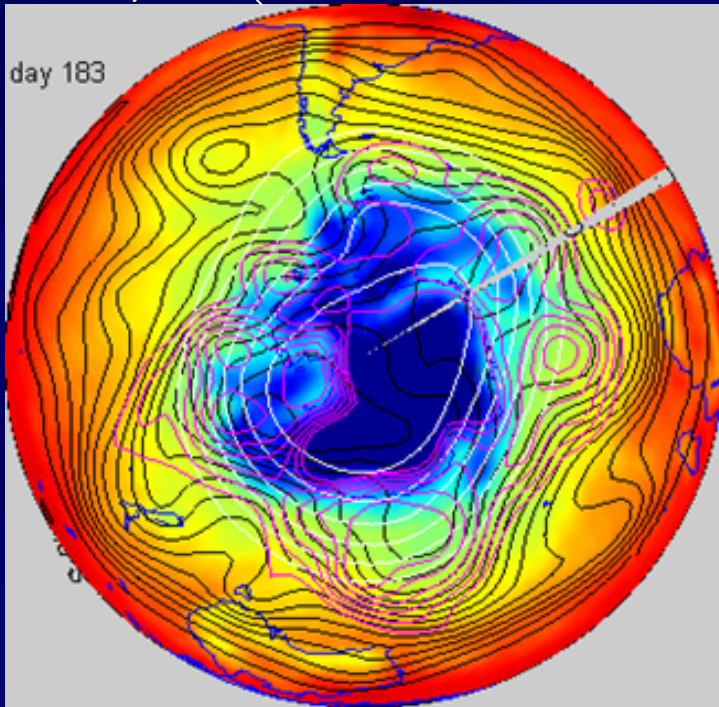
Jets near and far. (Left) Map of east-west current speeds at 400-m depth, simulated by an eddy-resolving ocean model. Red and blue indicate eastward and westward flows. [Adapted from Richards *et al.* (11)] (Right) Snapshot of a simulation for Jupiter, with red and blue indicating eastward and westward flows. [Adapted from Heimpel *et al.* (16)]

M. P. Baldwin is at Northwest Research Associates, Bellevue, WA 98009, USA. E-mail: mark@nra.com. P. B. Rhines is in the Department of Oceanography, University of Washington, Seattle, WA 98195, USA. E-mail: rhines@ocean.washington.edu. H.-P. Huang is at the Lamont-Doherty Earth Observatory, Palisades, NY 10964, USA. E-mail: hwei@ldeo.columbia.edu. M. E. McIntyre is in the Department of Applied Mathematics and Theoretical Physics, University of Cambridge, Cambridge CB3 0WA, UK. E-mail: m.e.mcintyre@damp.cam.ac.uk

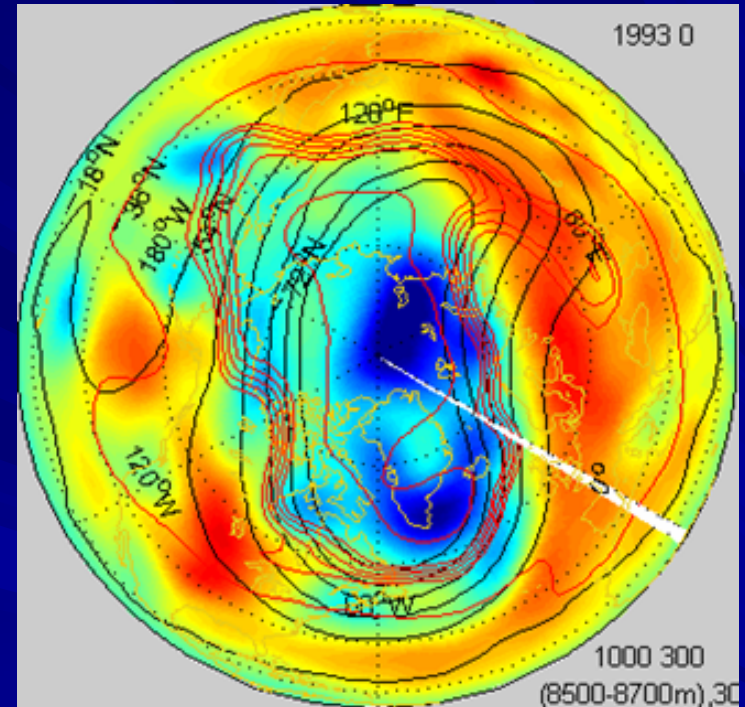
..the wave-turbulence-mean flow jig-saw puzzle

Southern hemisphere and northern hemisphere circulations: weather introduces new time-scales into high latitude life. Left is south polar view, right is north polar view. There are natural cycles over 10 years and longer, as well as global warming related change in weather patterns, temperature and rainfall. The jet streams are seen at the 300 HPa level (where just a few contours are selected to highlight the jets). There is a *strong* symbiosis between the synoptic highs and lows at the surface, the jet, and the smoother, faster stratospheric polar vortex above. Note the much more zonal nature of the SH flow. One glitch: colors in the NH are SLP while colors in SH are 850 HPa temperature....sorry for this confusion!

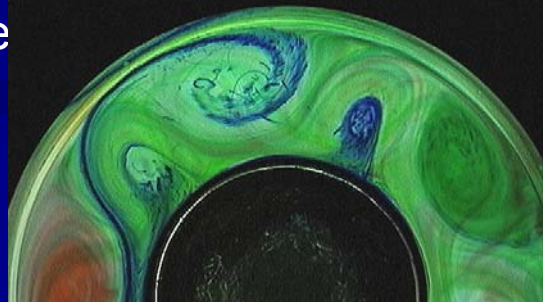
(dynamic height at 1000 Hpa (colors: blue = low pressure cyclones, red=high pressure anticyclones), 300 Hpa, 30 Hpa 1993 (NH), 1996 (SH) winters, 100 days each



southern hemisphere



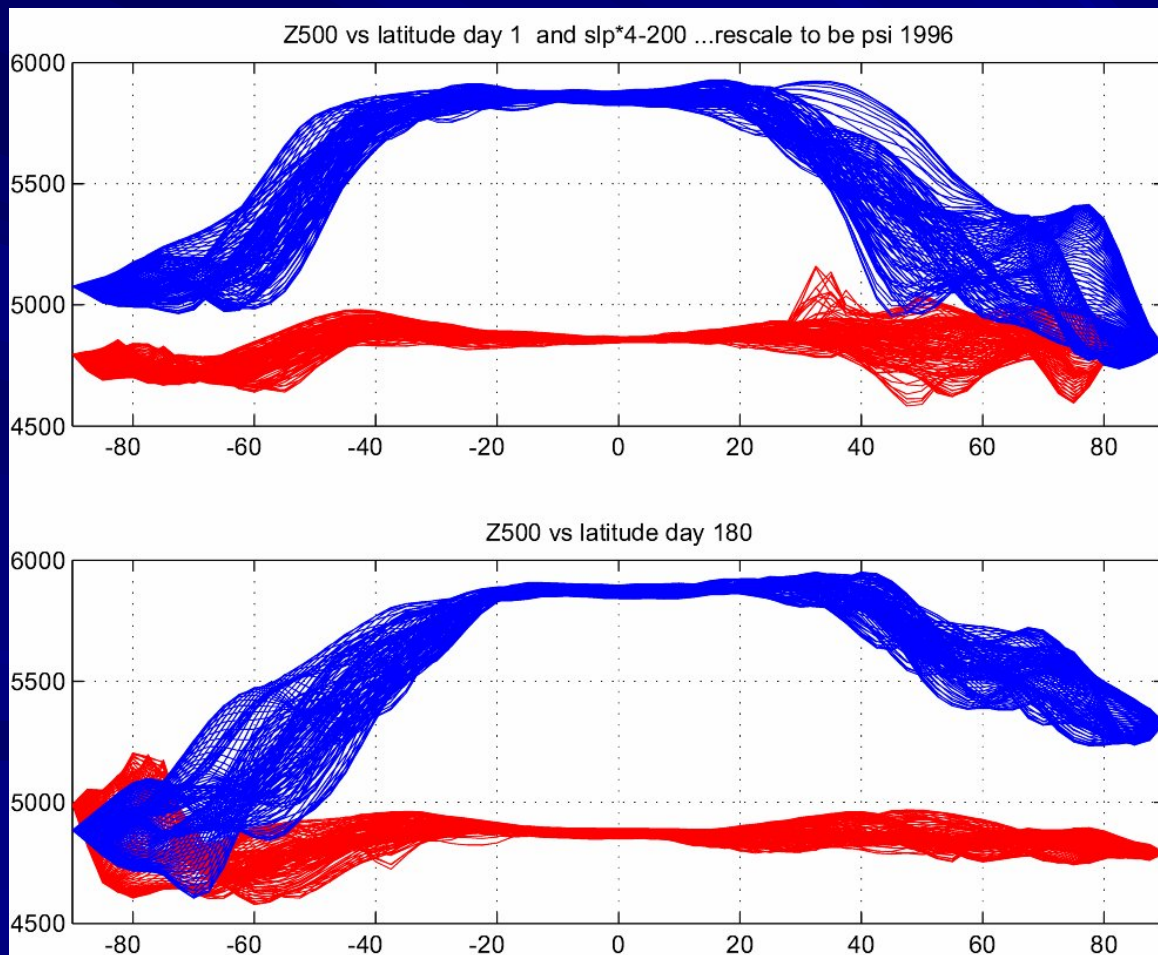
northern hemisphere



UW-GFD lab hemisphere



On the first day of 1996, this (upper) is the dynamic height as a function of latitude for all the longitudes, 500 hPa (blue) and sea-level pressure (red). The wintertime high-latitude jet stream appears in the chaotic, steeply sloped pressure gradient in 40N-60N. The southern hemisphere has a rather strong jet even in summer. Lower panel is day 180 of 1996, with a stronger southern jet. If we plotted streamfunction instead of height it would begin to show the low latitude circulation which is suppressed here.



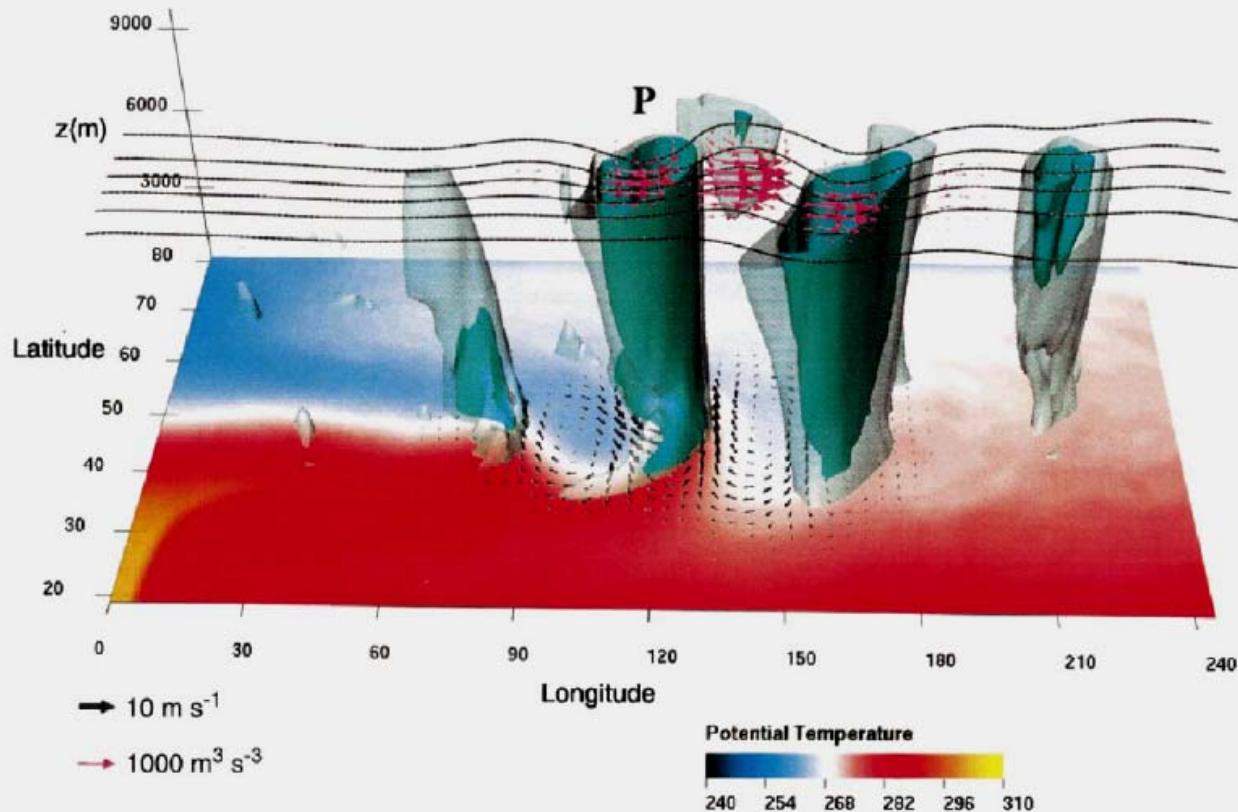
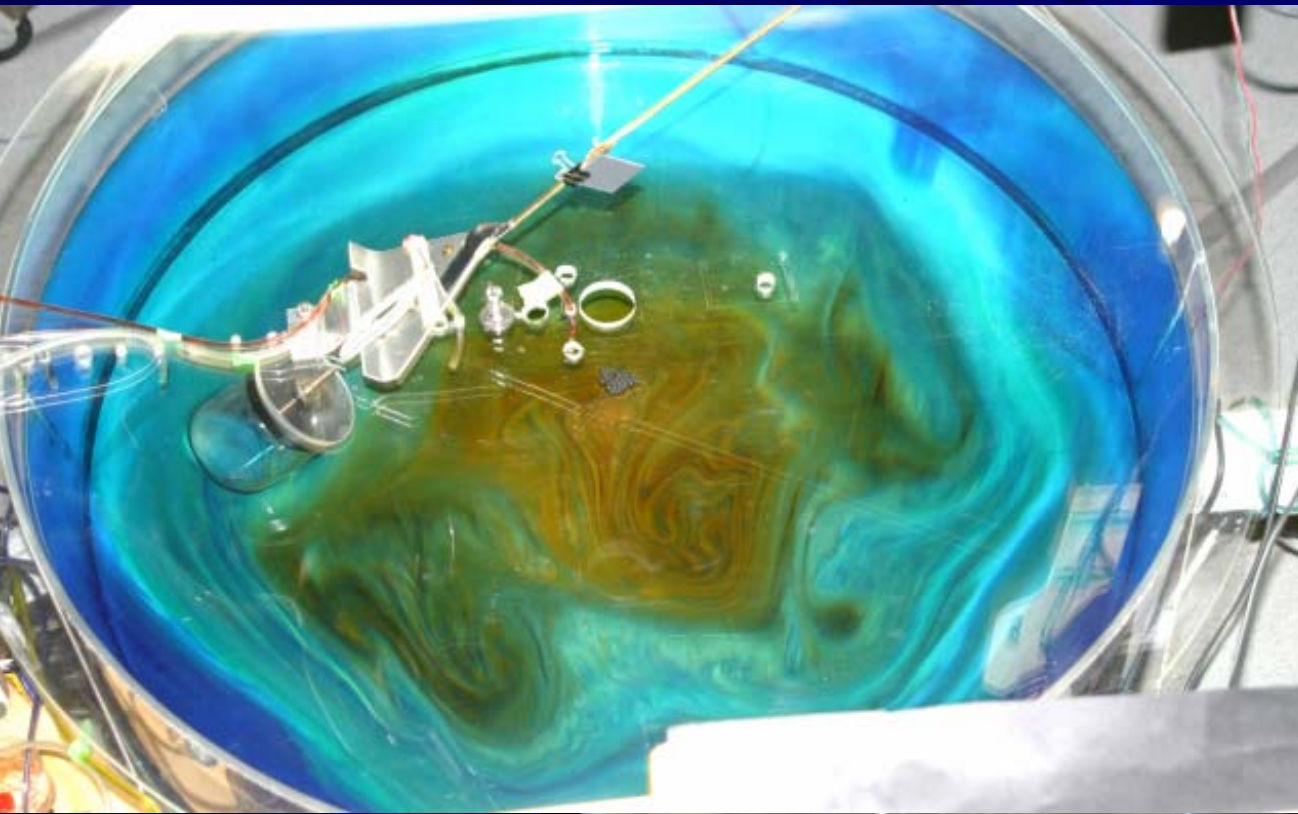


FIG. 3. Regression with zero time lag of the cyclonic relative vorticity (light blue  $3 \times 10^{-6} \text{ s}^{-1}$  and dark blue  $7 \times 10^{-6} \text{ s}^{-1}$  isosurfaces), surface potential temperature (color shading in K), surface wind (black vectors), ageostrophic geopotential fluxes at 10 km (magenta vectors), and geopotential at 10 km (contours every  $2190 \text{ m}^2 \text{ s}^{-2}$ ). The largest surface wind vector corresponds to about  $8 \text{ m s}^{-1}$ , and the largest geopotential flux vector corresponds to about  $1500 \text{ m}^3 \text{ s}^{-3}$ . "P" denotes the principal eddy.

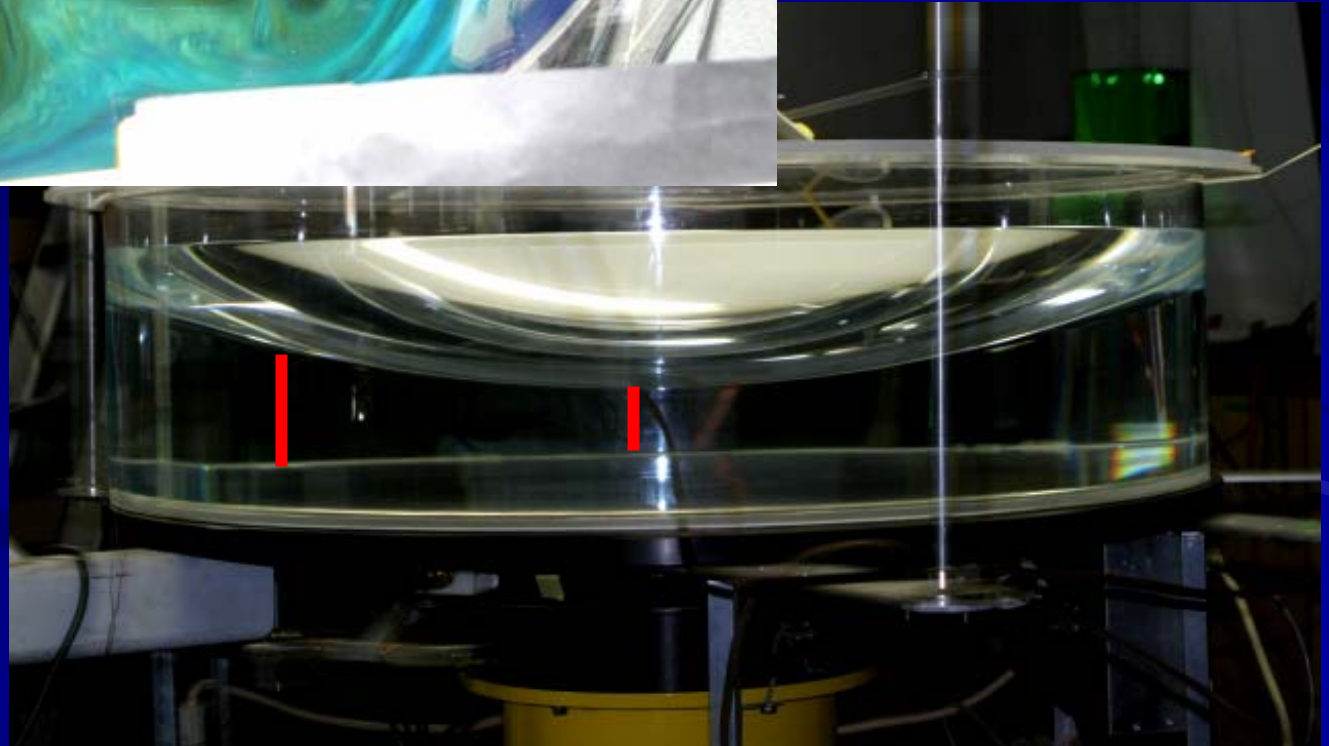
At the entrance of the storm track, a growing eddy is observed within which baroclinicity generates the low-level vorticity. The vorticity surface is tilted westward, a well-known feature of unstable baroclinic eddies. As this system matures, the upper and lower relative vorticity centers undergo a rotation, during which the low-level cyclone center moves poleward during its roll-up, whereas the upper-level center moves equatorward. These features are apparent in the principal eddy, centered at  $120^\circ$  longitude and denoted by "P," which shows features typical of a mature eddy, including the cold frontal structure behind warm (red) air advected from the south, and the associated cyclonic surface circulation. The open cone shape of the vorticity isosurface at 10 km indicates that the upper-level vorticity has considerable meridional structure, with its center south of the surface center. As the low-level cyclonic circulation rolls up the potential temperature field to produce the gradient reversal in the poleward flank, energy fluxes (magenta vectors) predominate at upper levels, consistent with the downstream development mechanism. These energy fluxes tend to be quite dispersive, that is, with a considerable equatorward component, which produces an upper-level disturbance that tends to move equatorward, as in the third vorticity center (referred to hereafter as the downstream eddy). As will be discussed below, the principal eddy and the downstream eddy can be considered a distinctly nonmodal couplet, where the principal eddy is maintained by baroclinicity and the downstream eddy by geopotential fluxes from the principal eddy. The anticyclonic shear on the equatorward side of the jet shreds the downstream eddy, which breaks anticyclonically. Inspecting different time lags in the regression reveals that the downstream system will evolve without further regeneration because at this point in the storm track surface baroclinicity has been severely depleted. In these experiments this is in part an artifact





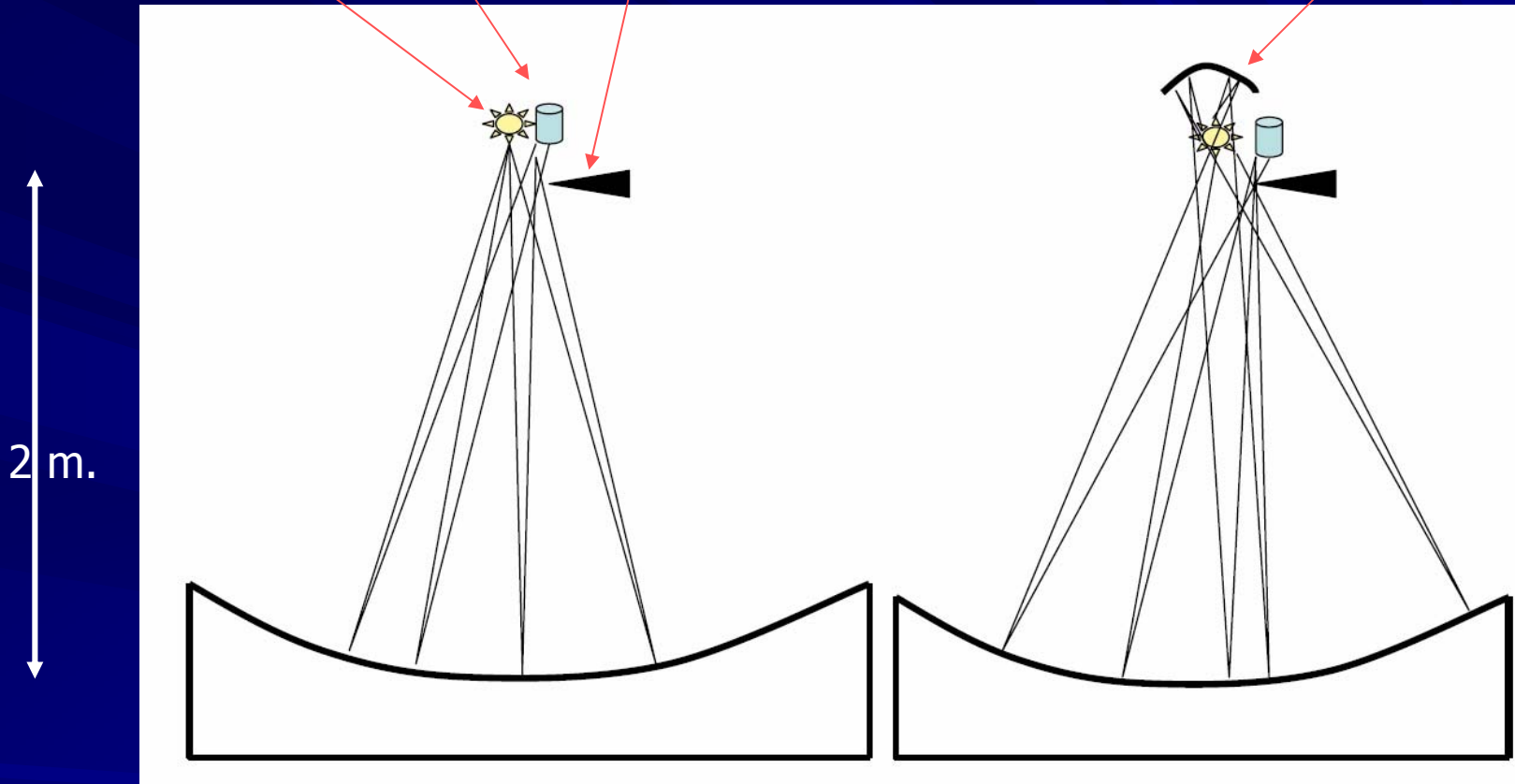
*the laboratory polar  
 $\beta$ -plane  
(GFD lab, Univ. of Washington)*

*stiffness along  
the rotation axis:  
2D ribbons of  
tracer*



Simple set-up  
light camera knife-edge

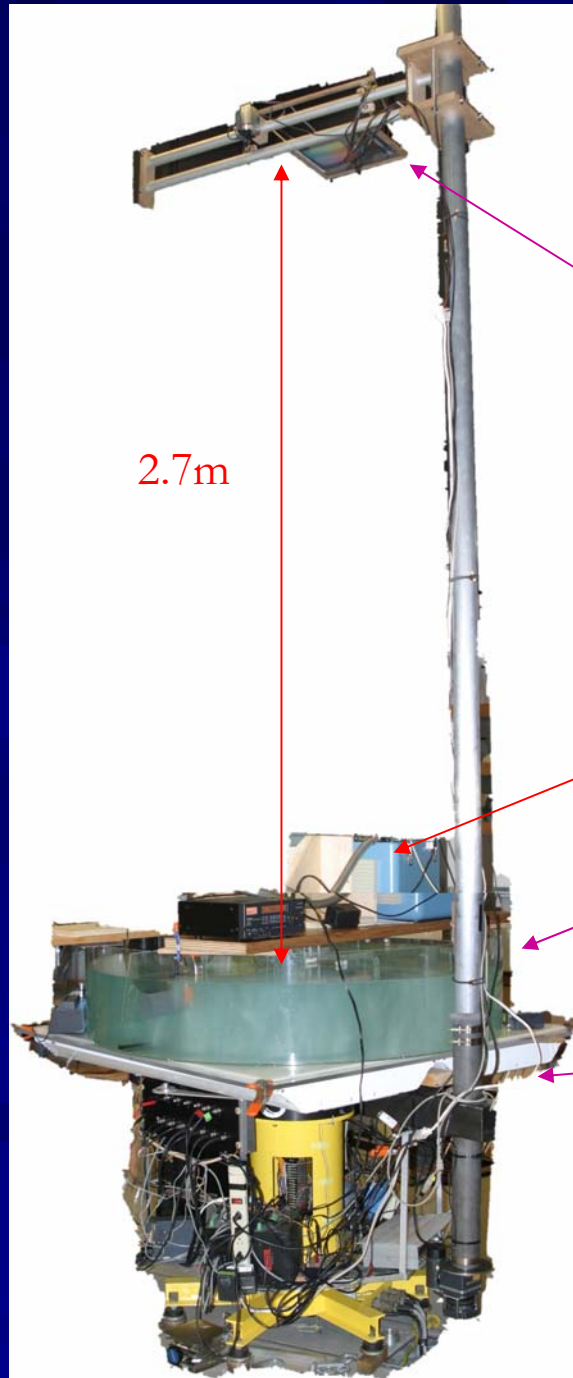
improved by a  
spherical correction mirror



$$h(r) = H_0 + \frac{\Omega^2}{2g} \left( r^2 - \frac{a^2}{2} \right)$$

focus at  $z = g/2\Omega^2 \sim 1 \text{ m}$  for  $\Omega = 2.2 \text{ s}^{-1}$





2.7m

robotically positioned  
light source and camera

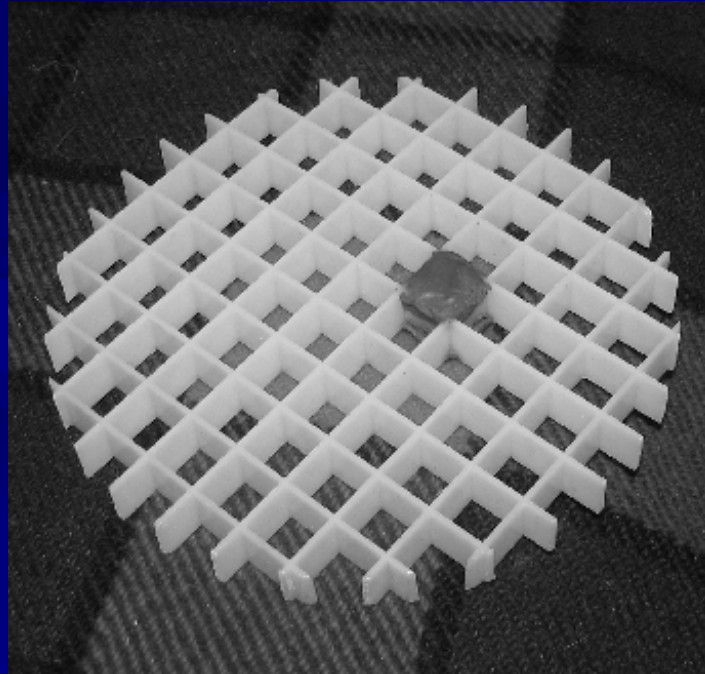
laser velocimeter

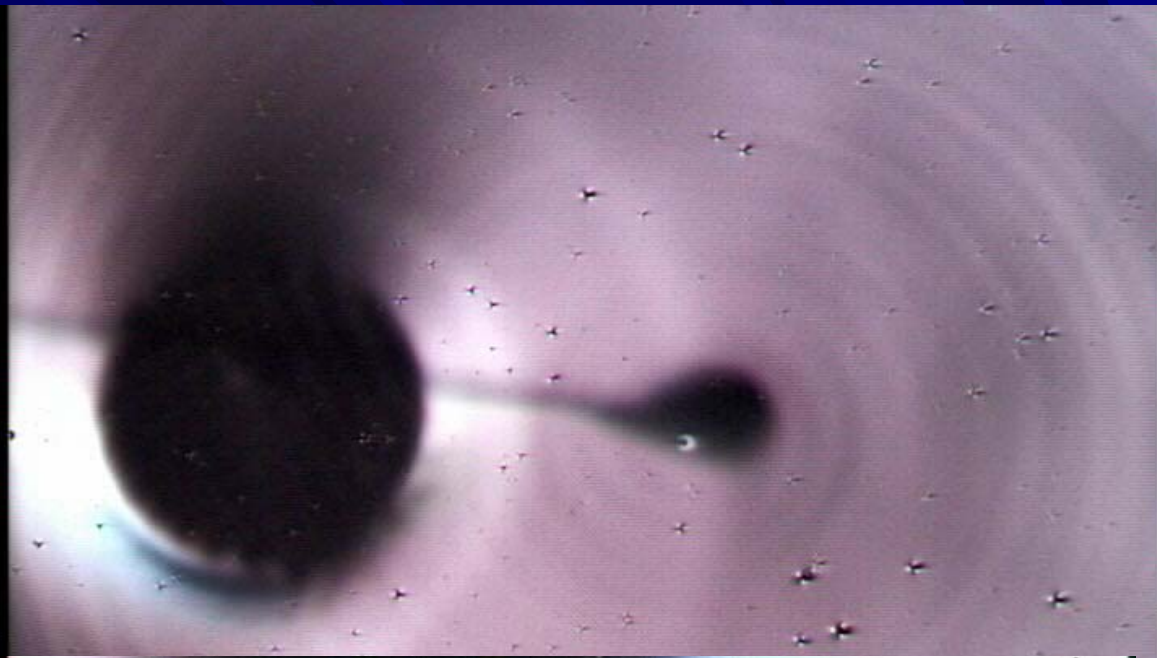
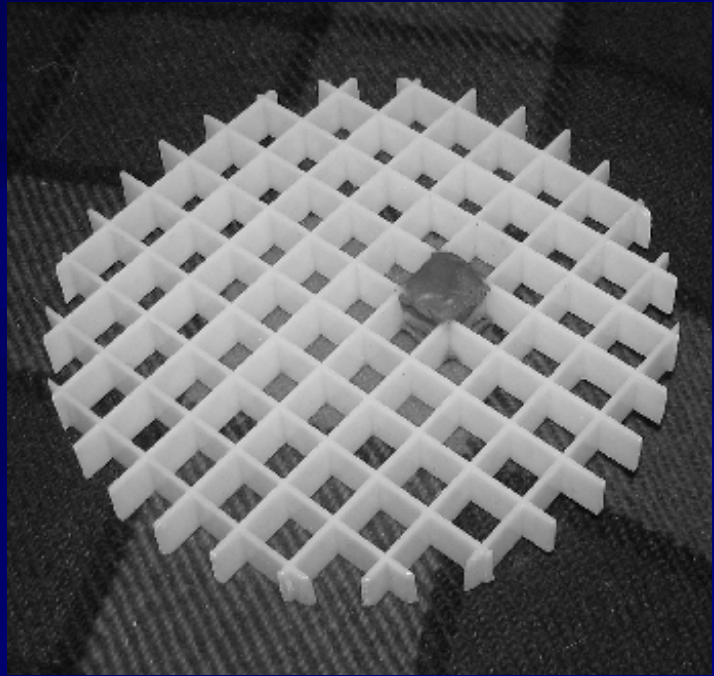
test fluid

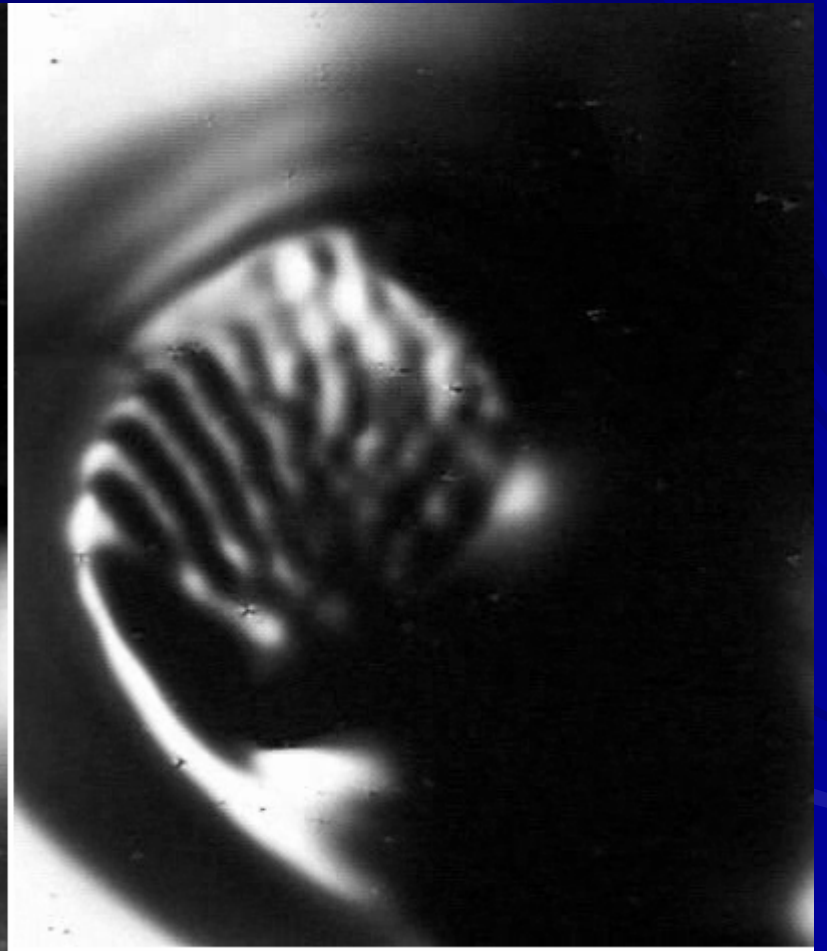
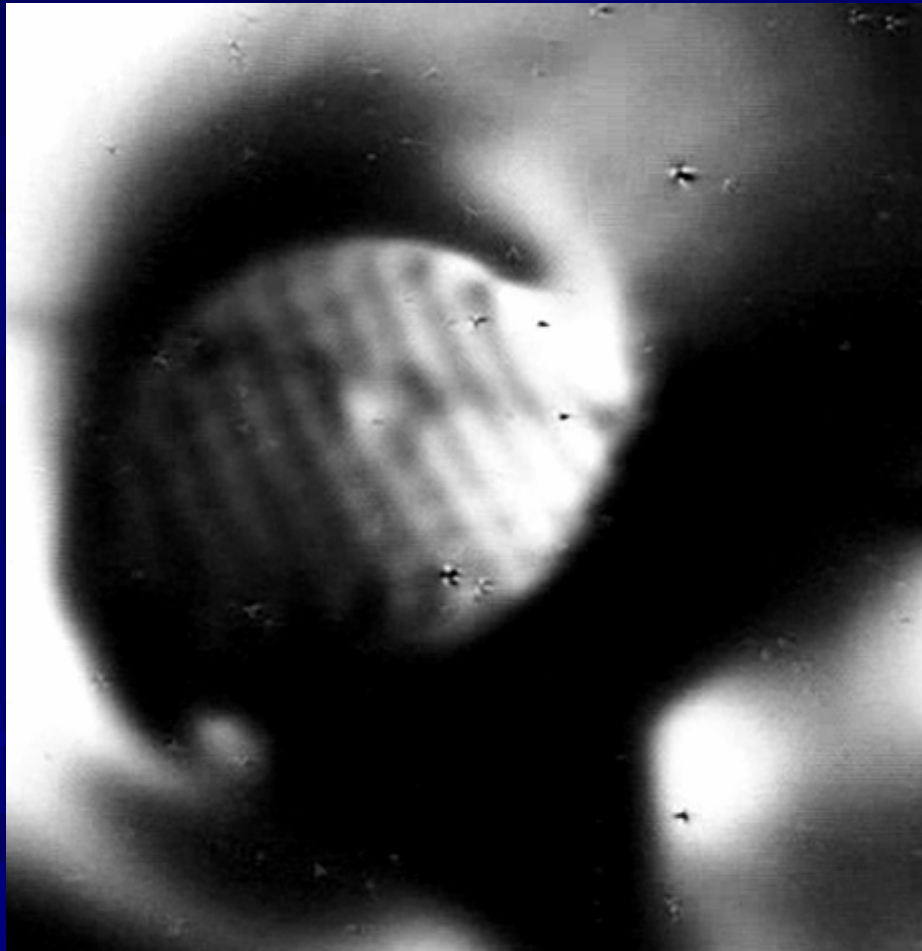
light box to illuminate  
fluid from below

note: this 2.7m height configuration  
corresponds to a rotation rate of  $1.9 \text{ rad sec}^{-1}$   
yet a lesser height can be used at higher  
rotation. Using a mirror above and camera/light  
below one can double the path length.

a high-wavenumber 'test mountain', a panel of  $\sim 1$  cm squares beneath 15 cm of mean water depth

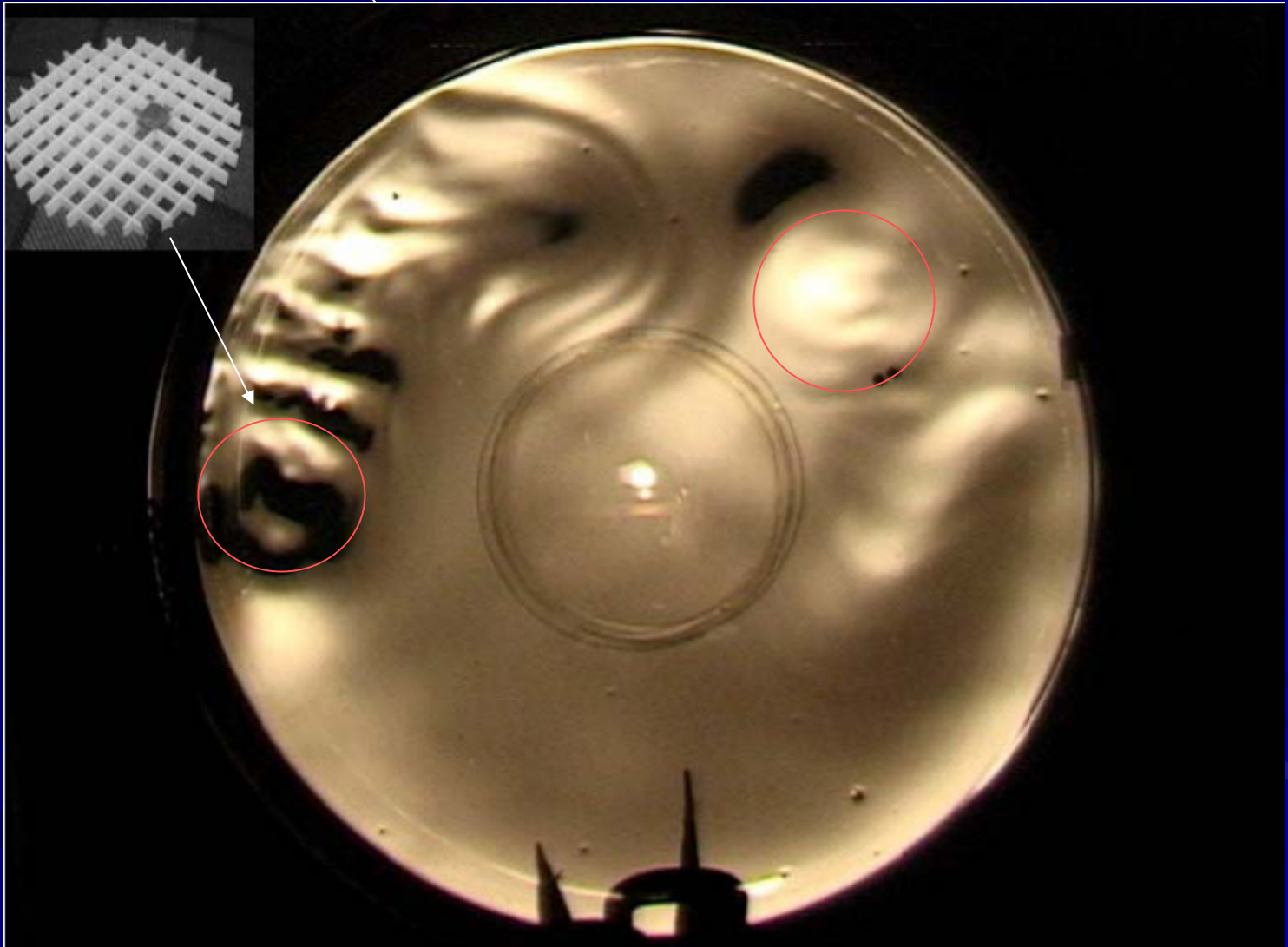






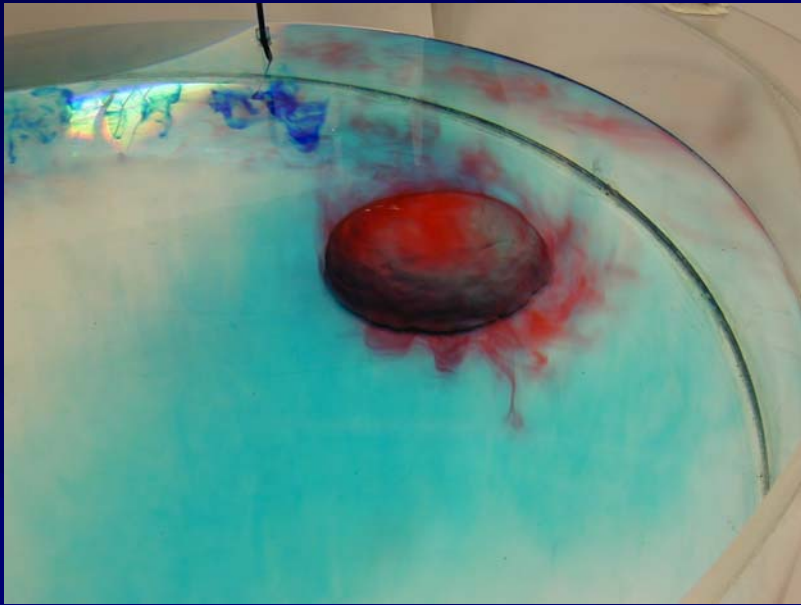


Two 'test mountains' (red circles) with azimuthal flow forced over them yield a pattern of near-inertial waves and turbulent yet geostrophic eddies

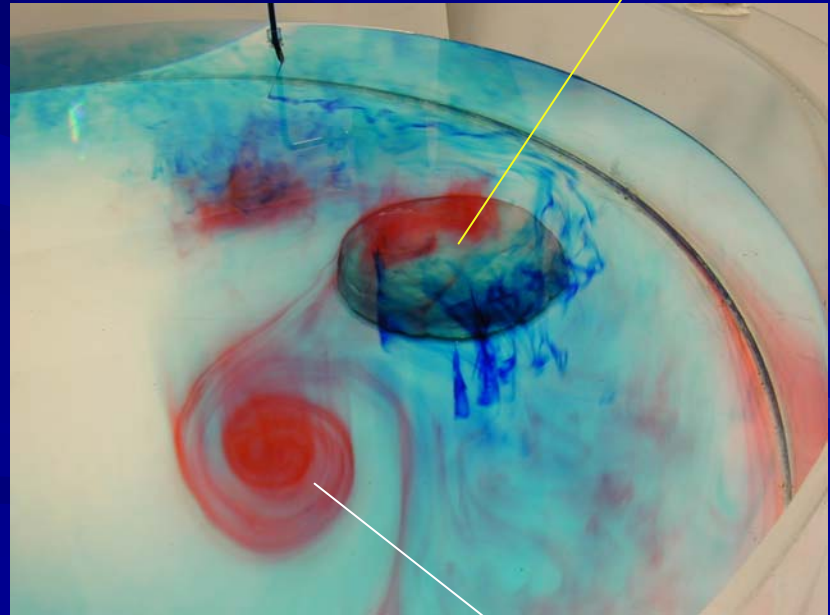
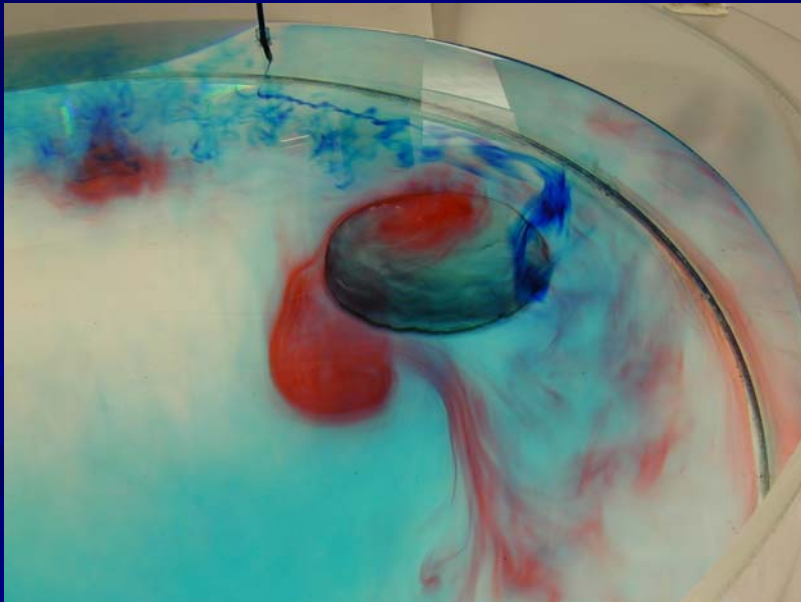


Waves: Kelvin (long gravity waves coastally trapped by rotation) and inertial (3-dimensional waves for which gravity is irrelevant) plus mountain-shed vortices



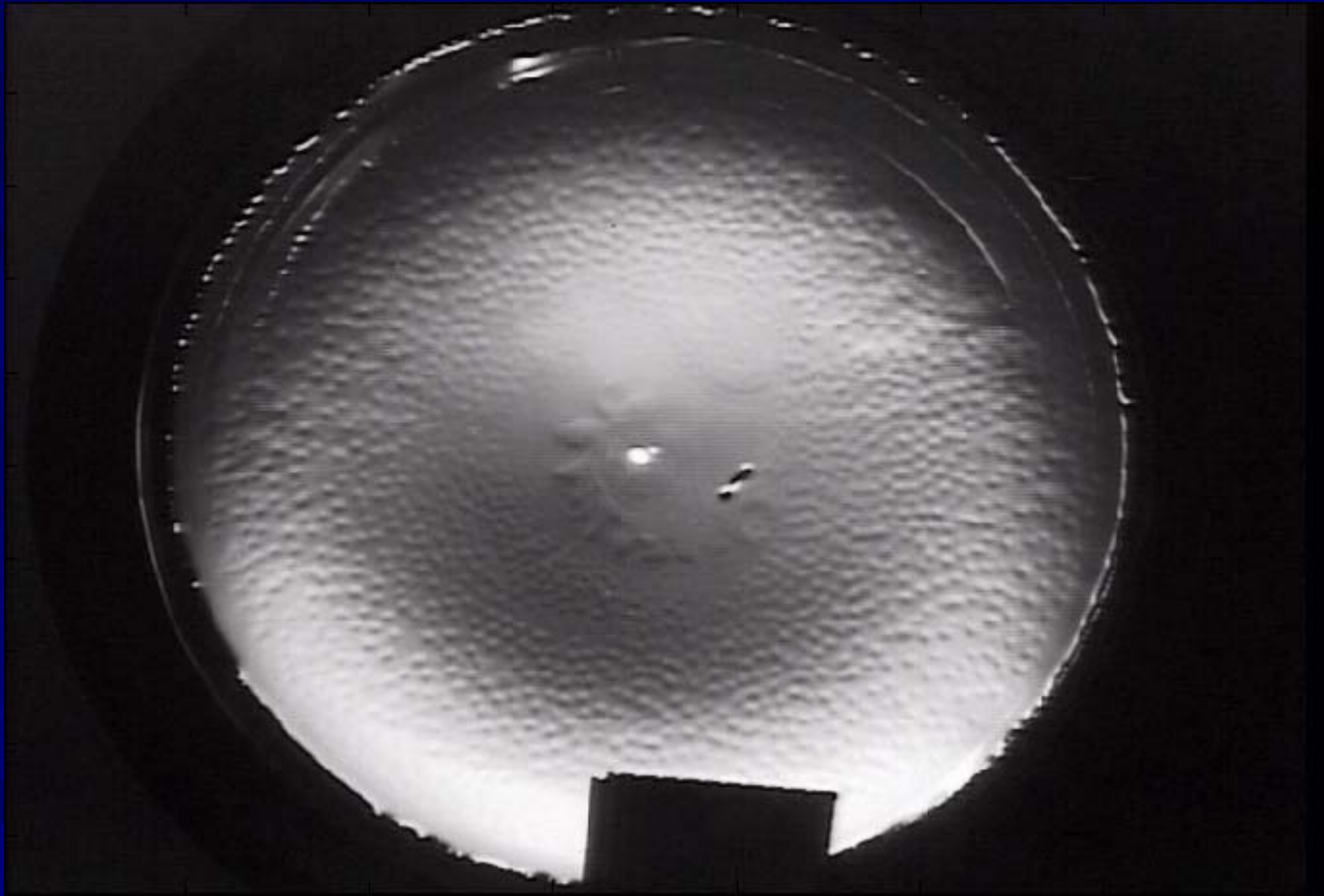


- Cyclonic vorticity in a rotating-fluid mountain wake



shed cyclone

A field of tornadic convection cells as seen in SSH. Here the amplitude of the elevation features is  $\sim 10^{-6}\text{m}$  (1 micron).





Dye tracer view of the same convection cells



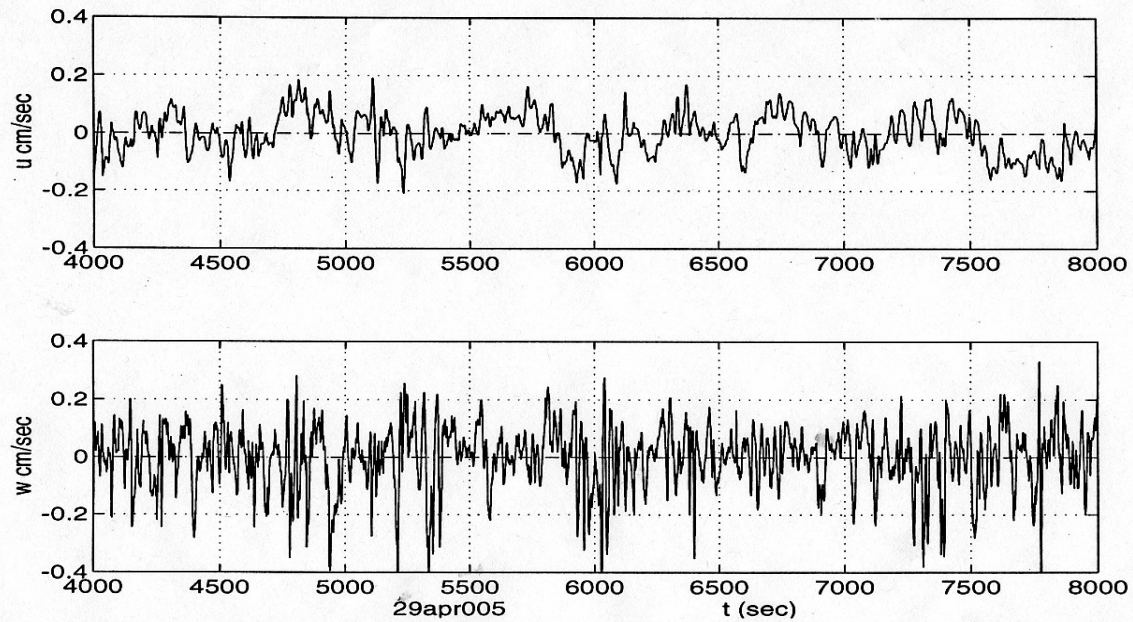
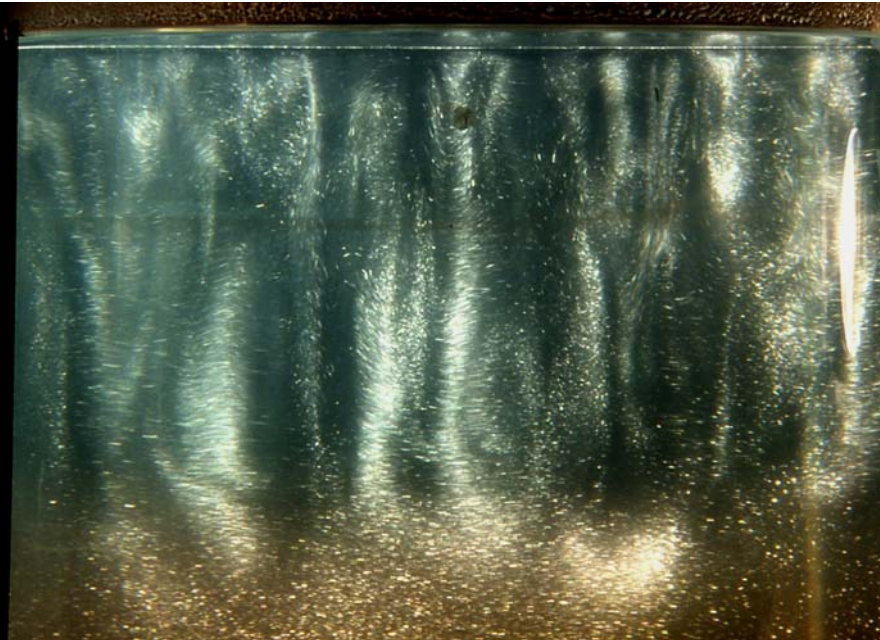


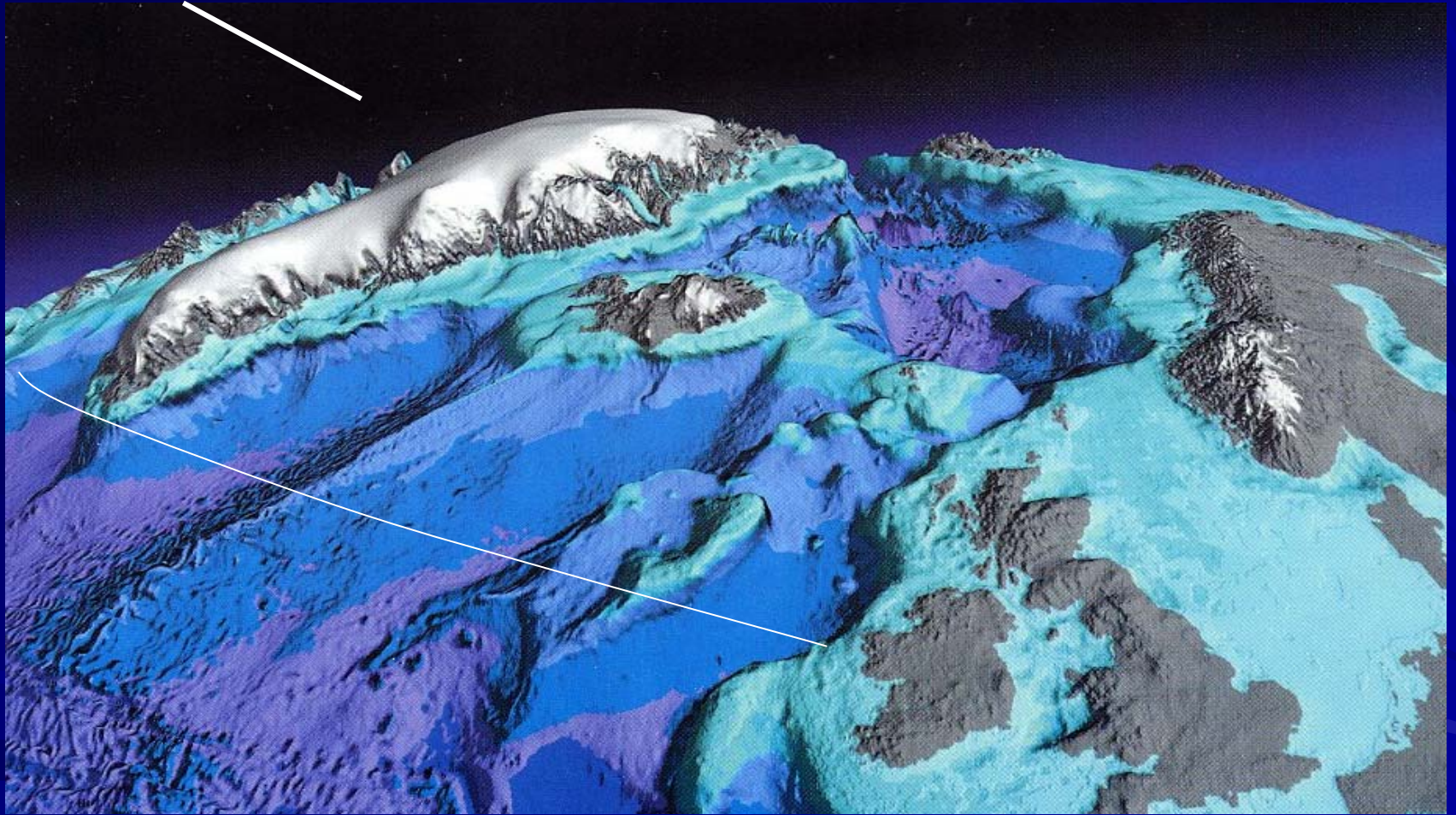
Figure 3. Laser Doppler Velocimeter velocities for simple rotating convection, showing intense spiking of vertical velocity, and longer time- (and length-) scale horizontal velocity.





# Subpolar Atlantic

*stirring rod?*

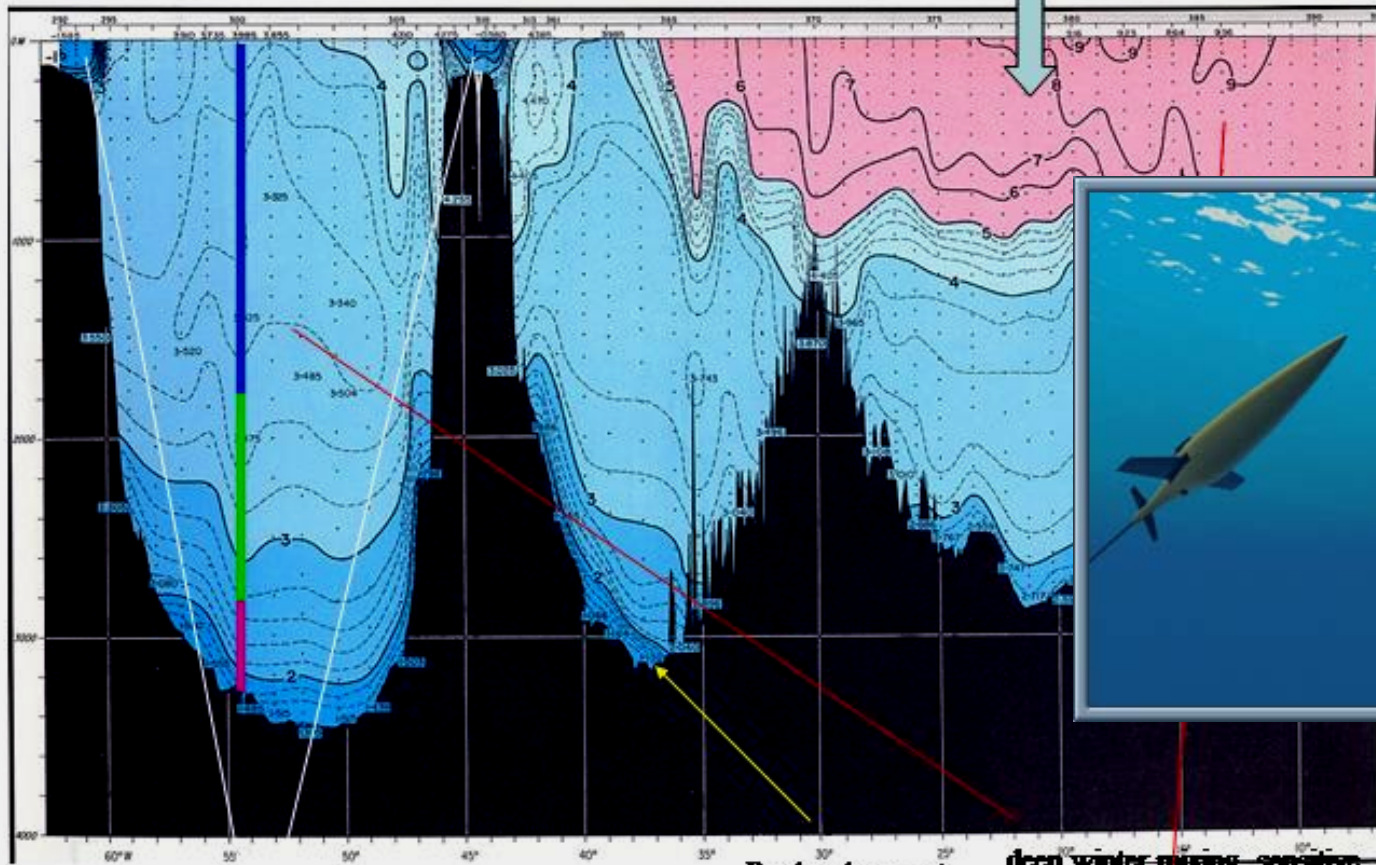


*AGU, 2003*



**Erika Dan temperature section, 60°N  
 Labrador-Greenland-Rockall-Ireland  
 Worthington+Wright, 1970**

**warm, saline water moving  
 north from the subtropics**



**Shallow continental shelf circulation provides shallow southward flow and FW transport. *Global climate models do not have continental shelves!***

**Deep boundary current less on Greenland's continental slope: Denmark Strait Overflow Water**

**deep winter mixing sensitive to upper ocean low-salinity waters**

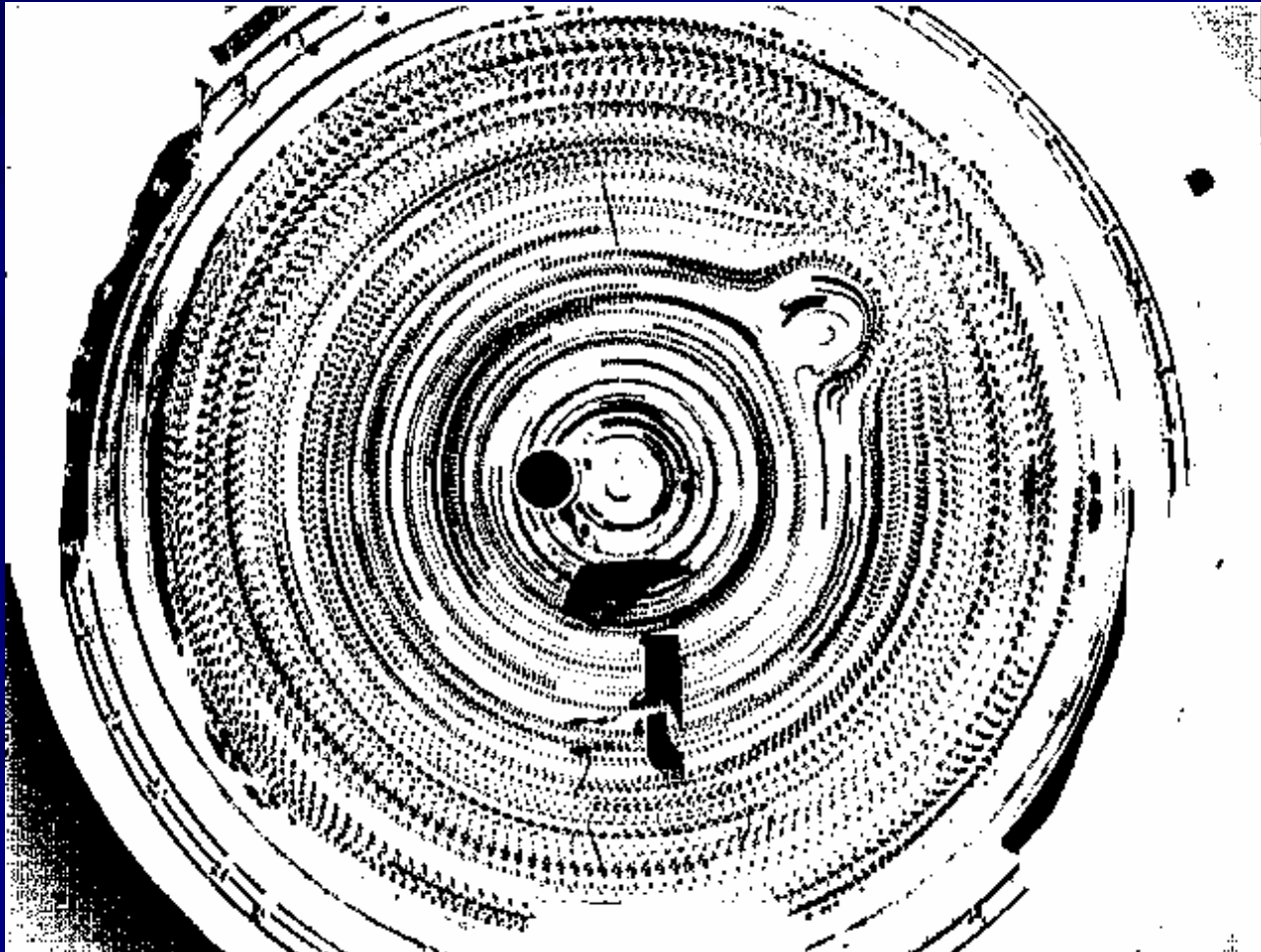




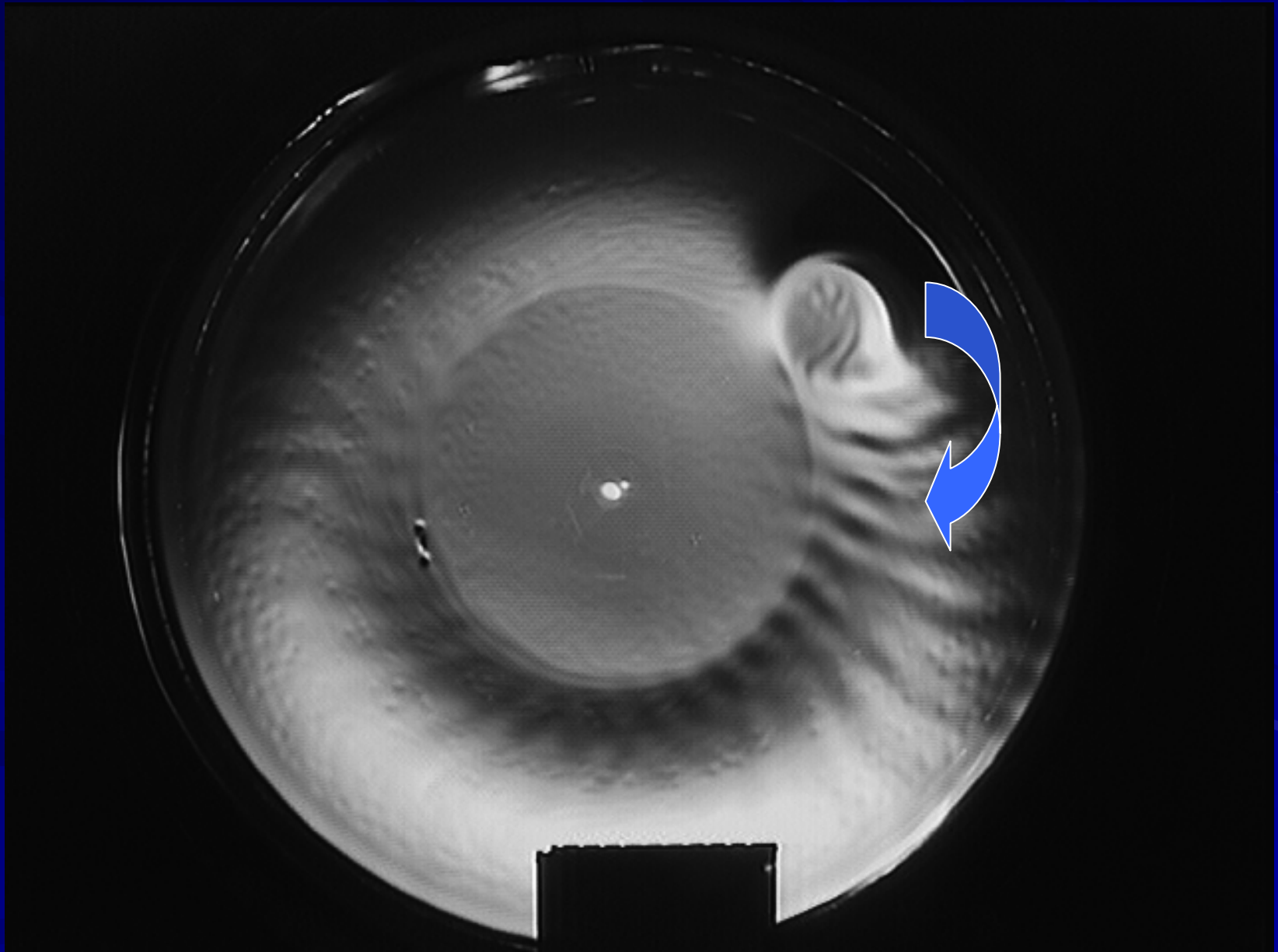
Altimetry works by expanding the image of a light source to fill the entire fluid domain



As in earlier slides, here we have zonal flow past a spherical-cap mountain with height about  $1/3$  the depth of the fluid. The flow is produced by changing the rotation rate (often ramped by computer control, so as to avoid viscous spindown). The mean flow is anticyclonic (easterly, westward) producing a Taylor column above the mountain. Particle tracking (one-sec. intervals) shows the streamlines.



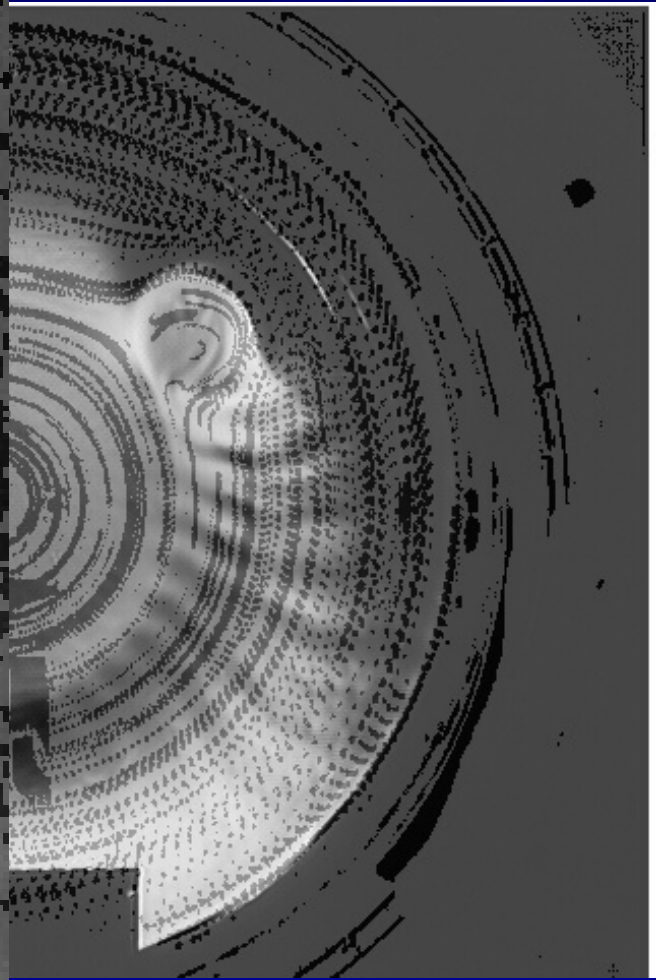
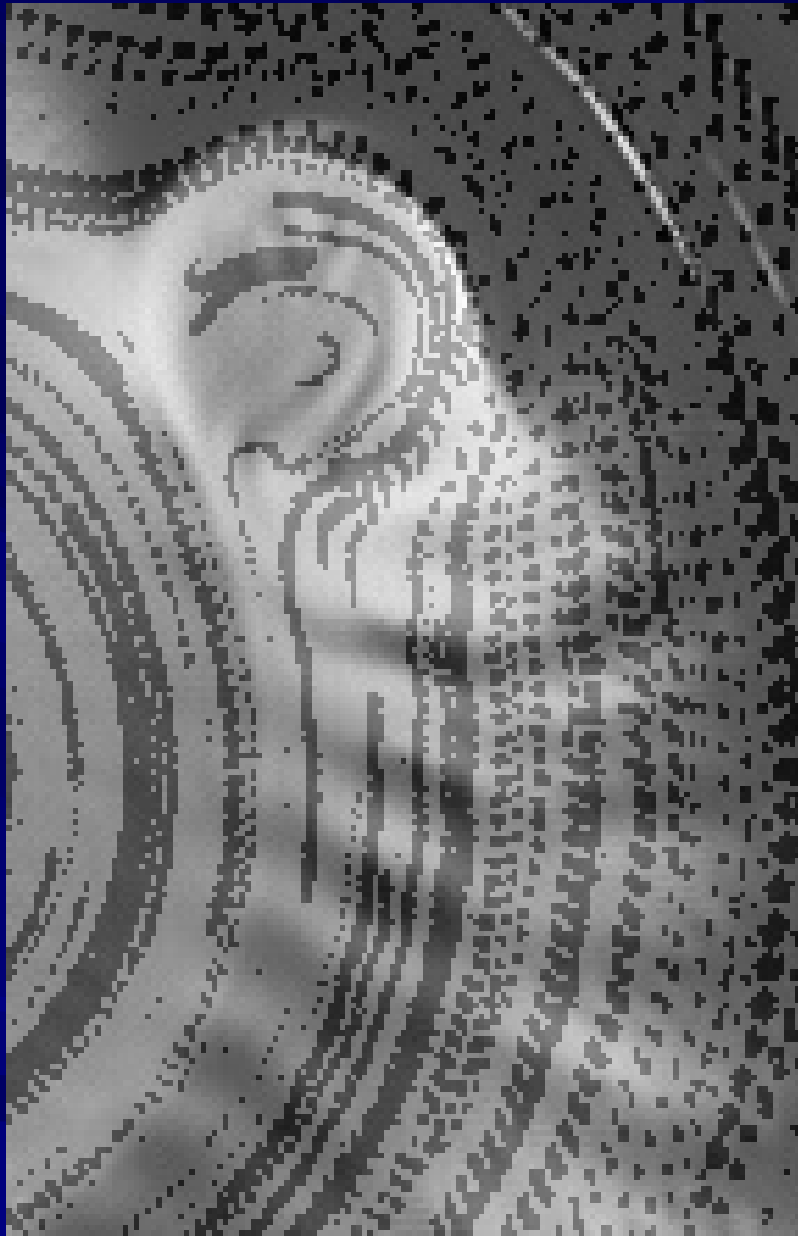
the rather dull picture of particle tracks becomes more interesting viewed through the altimetric height field





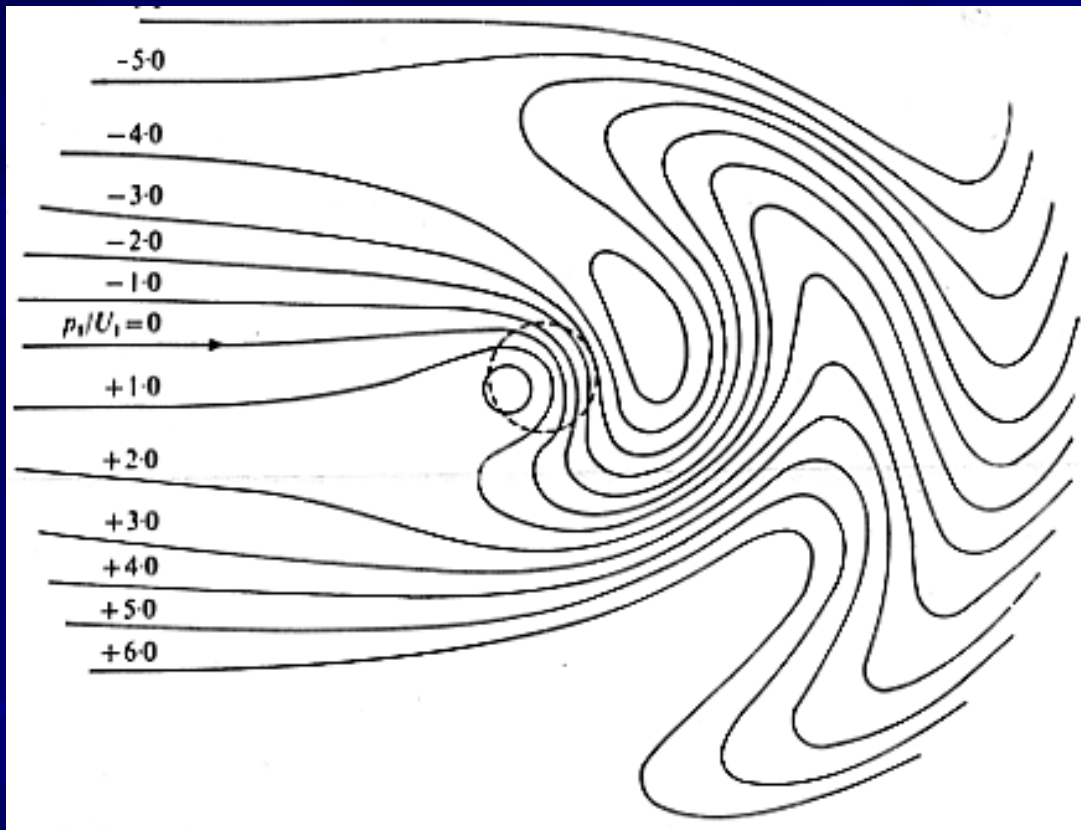
standing inertial waves form in the lee of the mountain, and are ducted along a sharp shear line on the poleward side of the mountain.





- Rossby waves and jet streams: the same experiment repeated with the mean zonal velocity cyclonic (westerly; eastward) about the North Pole on this polar  $\beta$  plane allows standing Rossby waves to exist. It is interesting that given the choice of inertial or Rossby waves, the fluid chooses the latter.

# Lee Rossby-waves in the wake of a cylindrical mountain (McCartney JFM 1976)



Rossby waves are ‘one-way’: their phase propagation has a westward component relative to the fluid: thus they exist as lee waves for an *eastward* flow but not a westward flow. Wave drag peaks at:

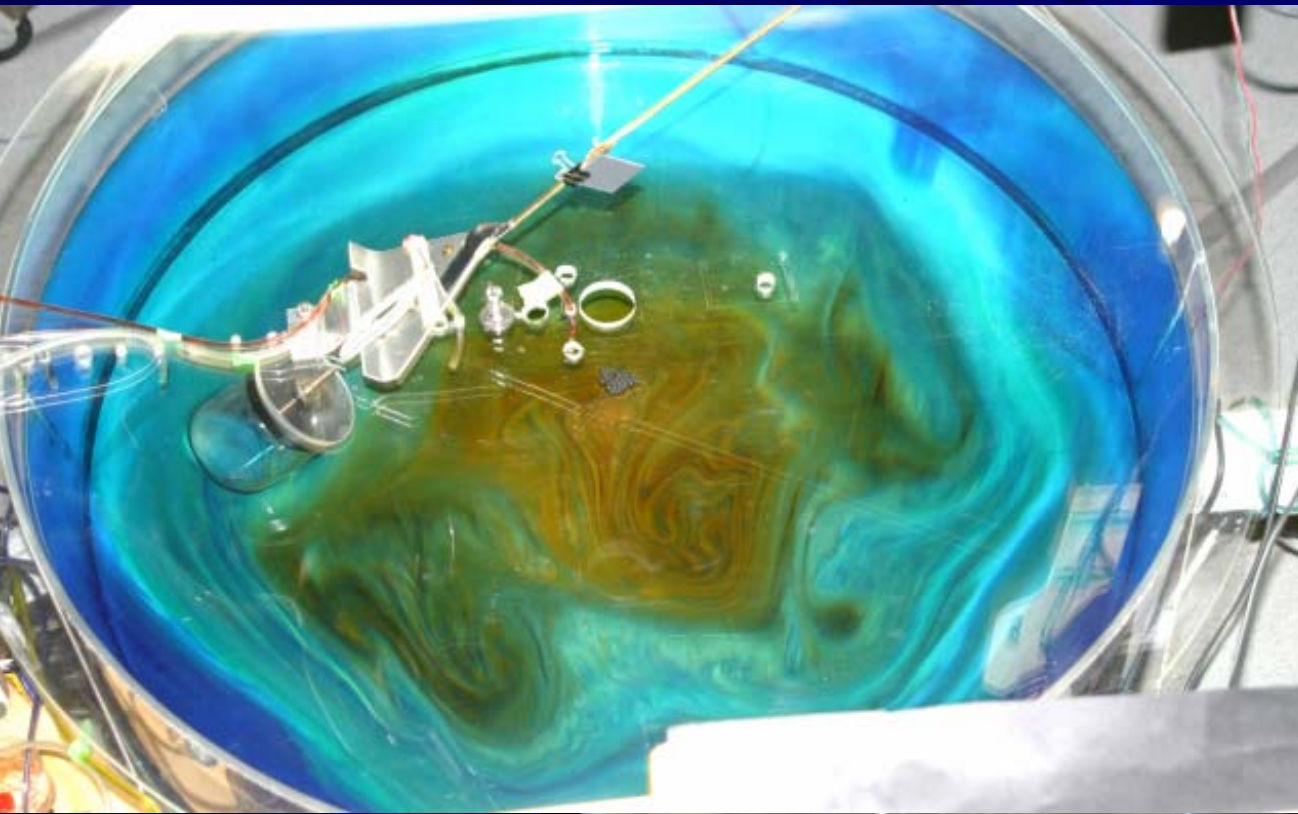
8.2  $\delta/\varepsilon$  times the ‘naive estimate’,

$$\rho f U L^2 \delta H$$

where  $\delta = h/H$  is the fractional mountain height,  $\varepsilon$  the Rossby number,  $U$  the mean flow,  $L$  the radius and  $H$  the total fluid depth

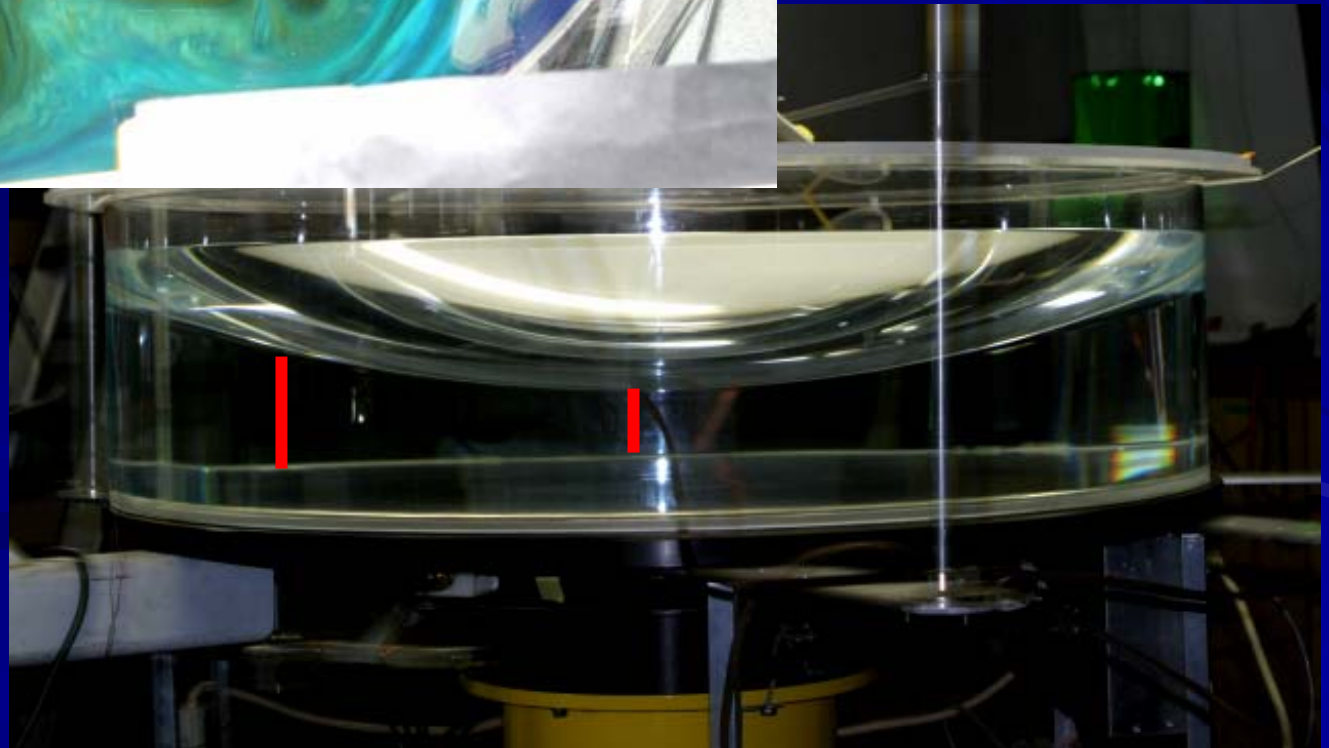
note strong correlation of meridional velocity and topographic height.....wave drag





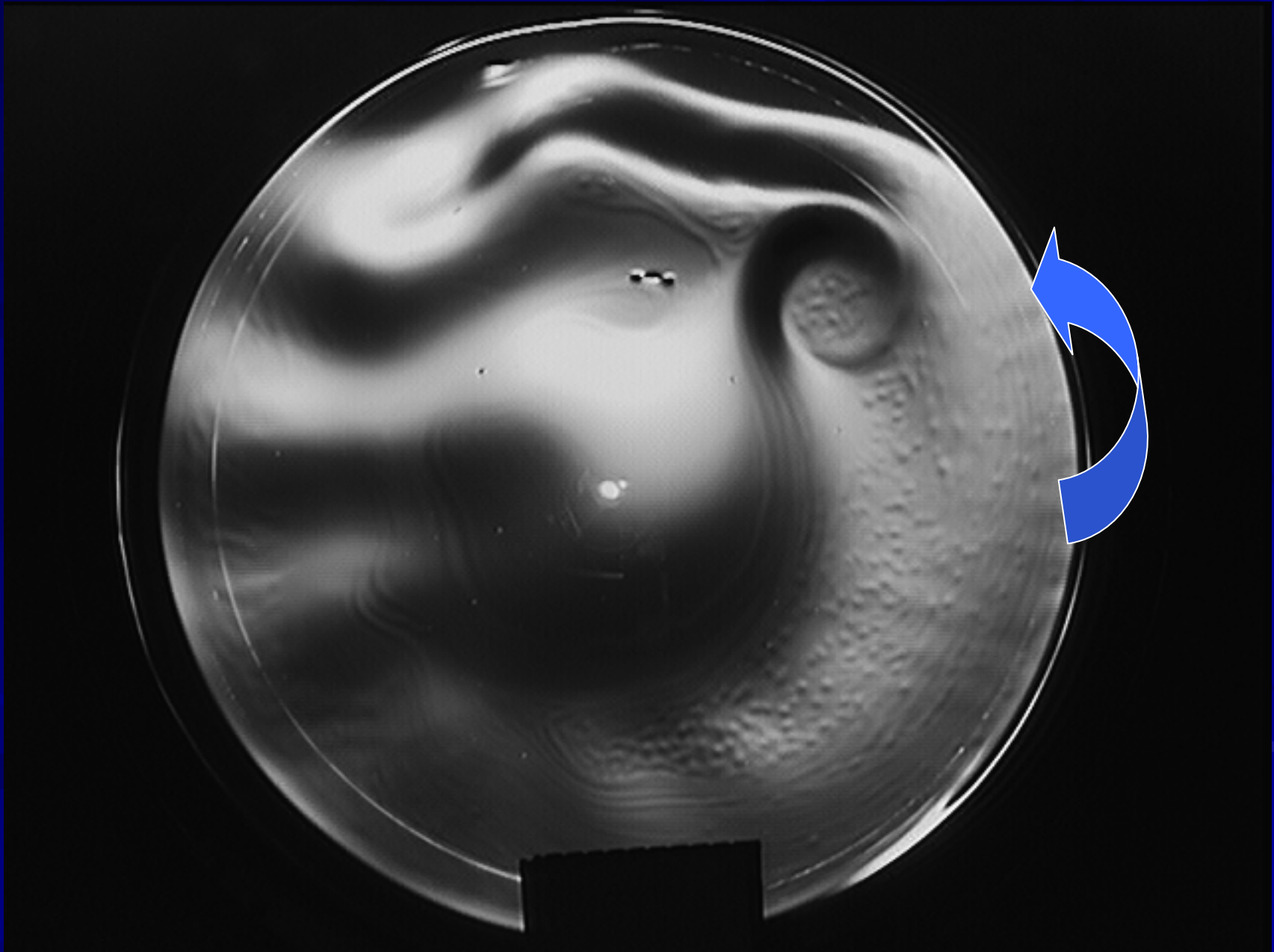
*the laboratory polar  
 $\beta$ -plane  
(GFD lab, Univ. of Washington)*

*stiffness along  
the rotation axis:  
2D ribbons of  
tracer*





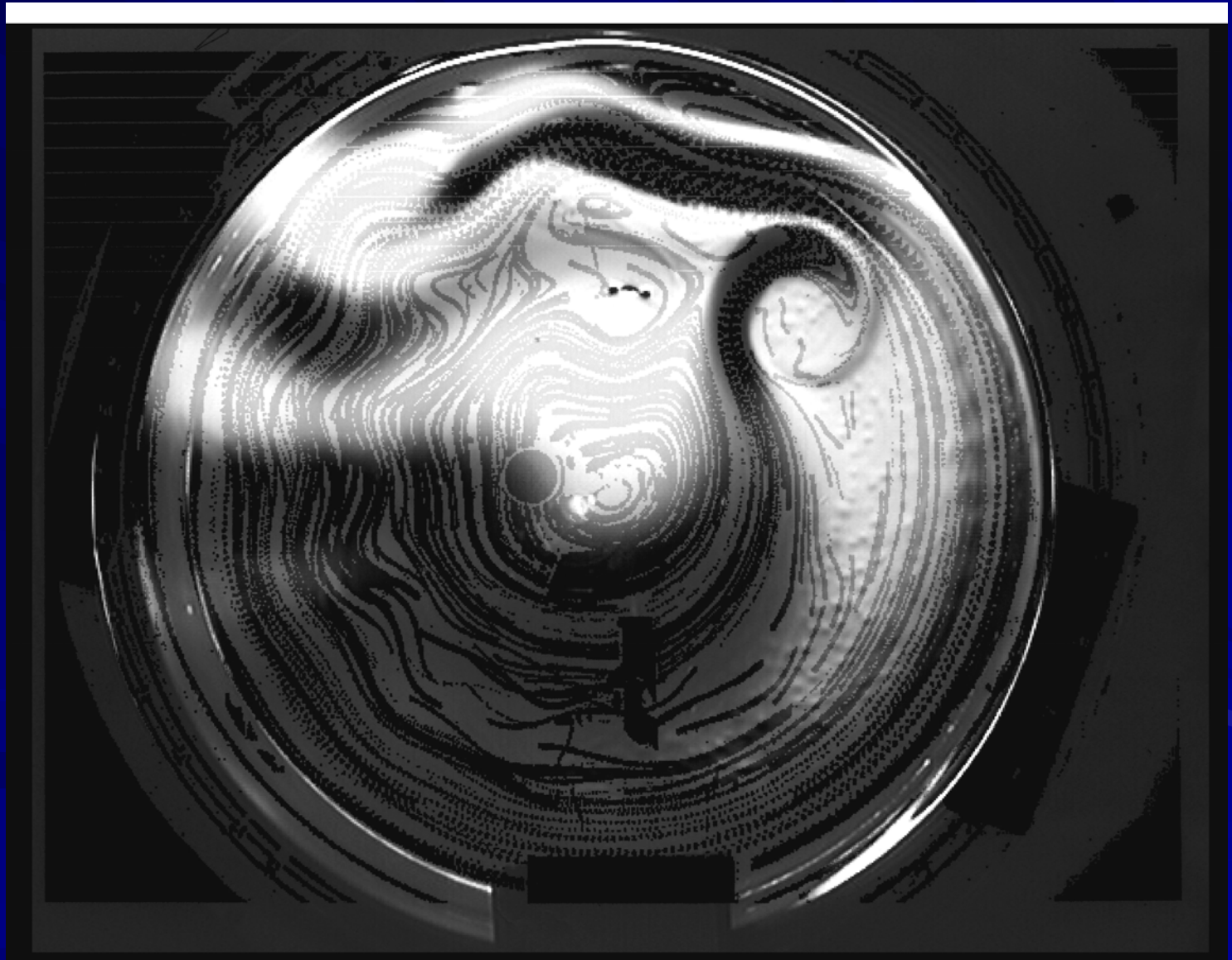
upstream waves become a 'Lighthill' block, west of the mountain, and the topographic Rossby waves form a concentrated 'tip jet' southward/leeward of the mountain.





mature  
th = 50





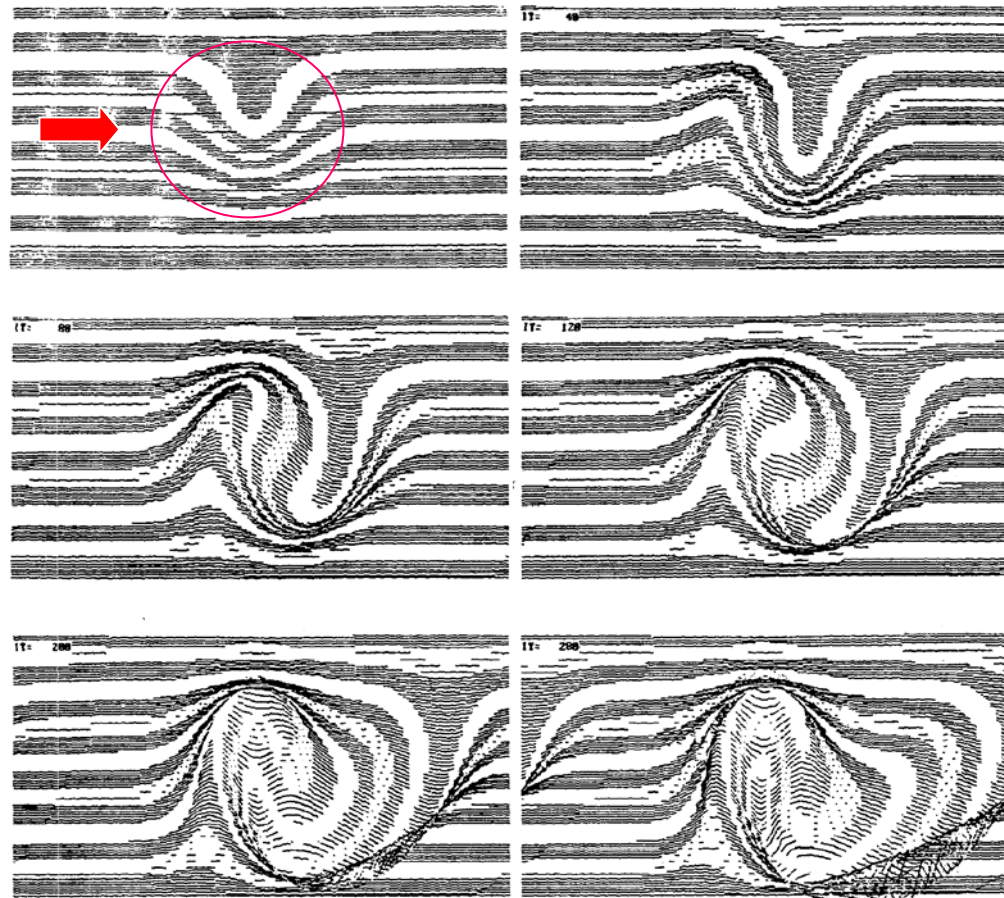


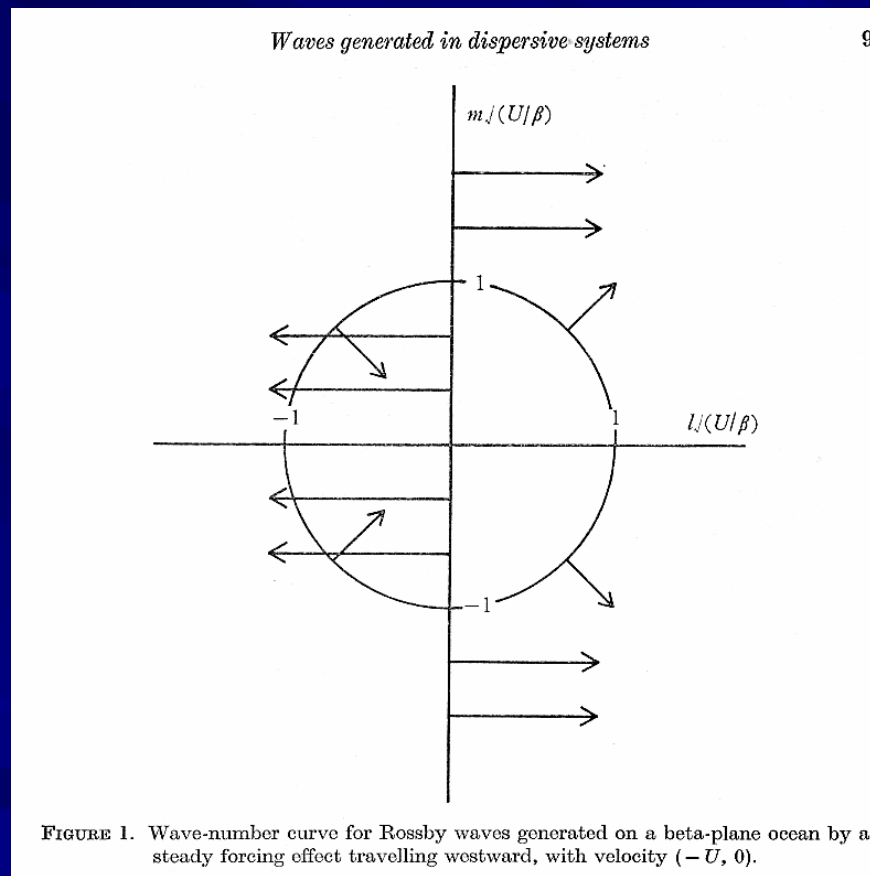
FIG. 9. *Nonlinear supercritical*. Read across, then down. Evolution of an initially uniform eastward barotropic flow over 280 days. Strong eastward flow, as in Fig. 8, except with a broader ridge (600 km half-width in the  $y$ -direction) and slightly faster flow ( $0.08 \text{ m s}^{-1}$ ). Potential vorticity contours, shown as bands superimposed on the interface surface plot, are wound into the region above the ridge. The slope of  $\eta$  increases, and correspondingly, the velocity. The free vortex moving eastward is connected to the bound vortex above the ridge by a long trough, which draws in high potential vorticity fluid from a great distance poleward.

pressure field  
and (stripes)  
PV field

Detail of the winding of PV contours above the mountain, producing jets both up- and downstream. Planetary-geostrophic regime: exact solution by integration along time-dependent characteristics *Rhines, JPO 89*



Linear stationary waves: circular lee Rossby waves plus upwind and downwind wake blocks. (though strictly linear topography does not generate them). Analogous to linear blocking in a stratified fluid approaching a mountain ridge *Lighthill JFM 1968*



Charney-Drazin theory for a stratified atmosphere: wavenumbers lie on an ellipsoid whose base plane is this circle,

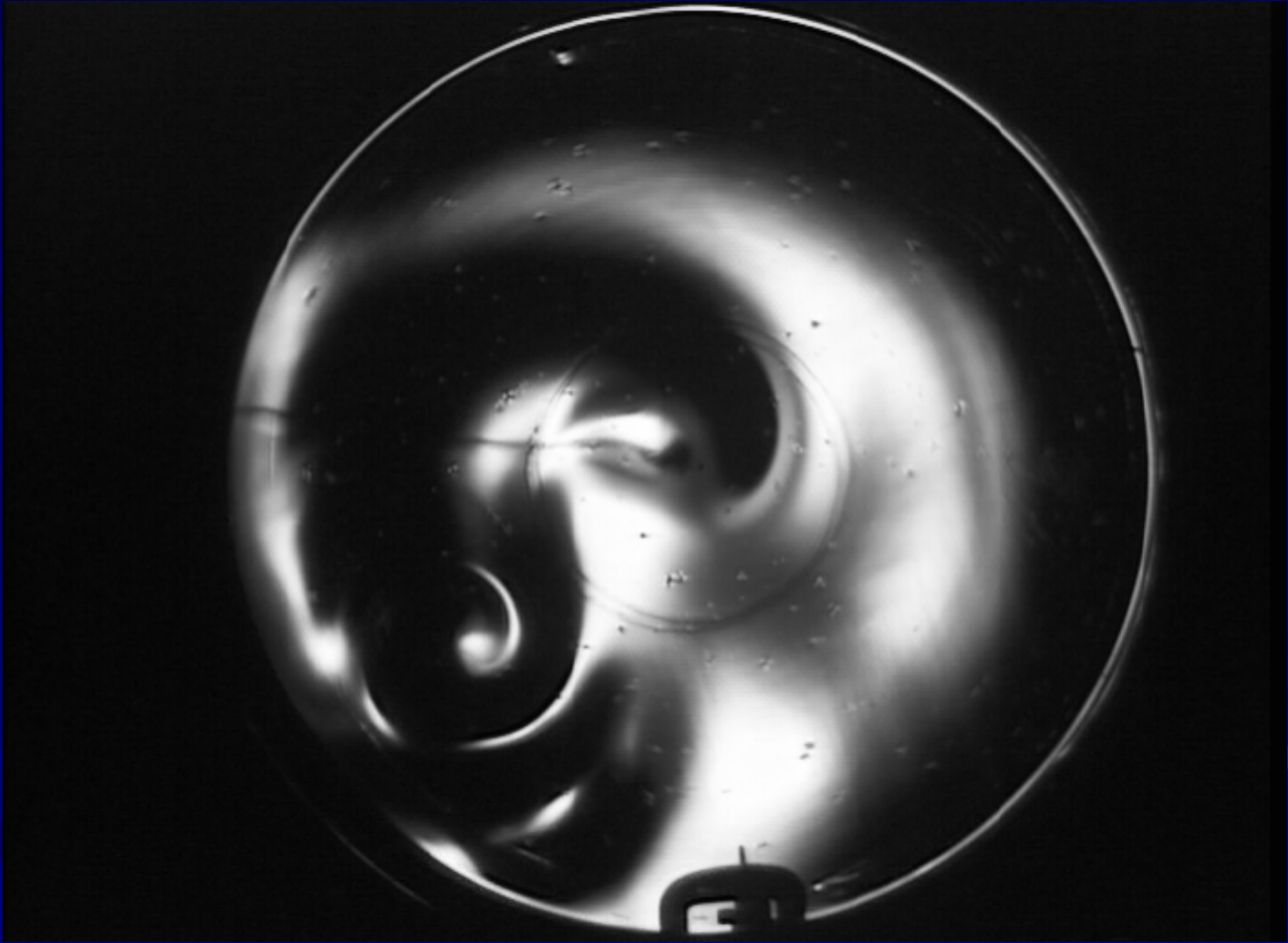
Blocking 'tubular modes' are not standing waves but propagate non-dispersively upstream if  $\beta a^2/U > 1$ .

Connections with nonlinear solitons, KdV solutions for small aspect ratio (tubular,  $l \gg k$ ).

*In a confining channel, these ideas lead to a hydraulic theory of Rossby wave controlled flows (R.R.Long, L.Armi, P.Haynes).*

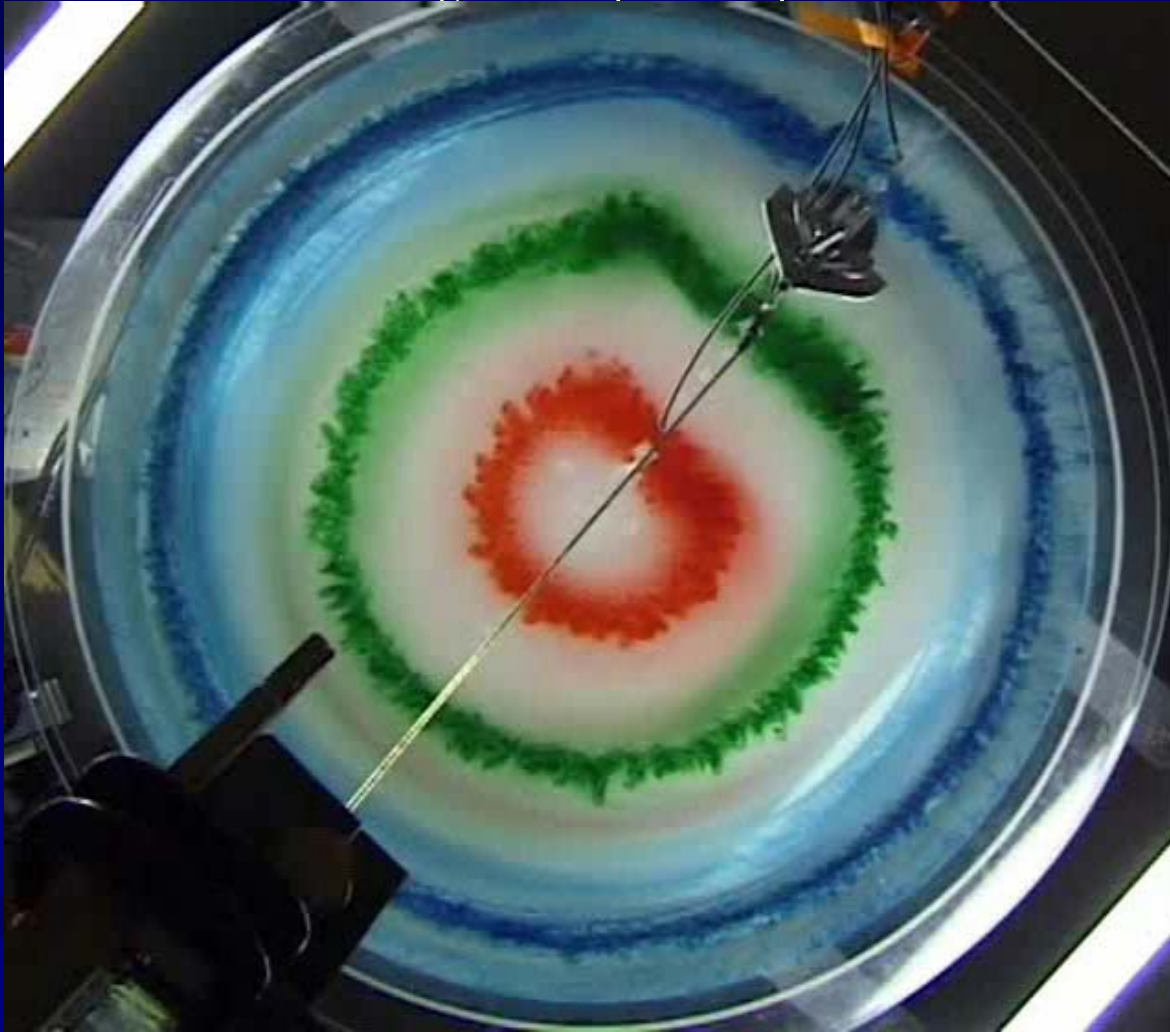
time development of the upwind blocking and  
downwind Rossby waves





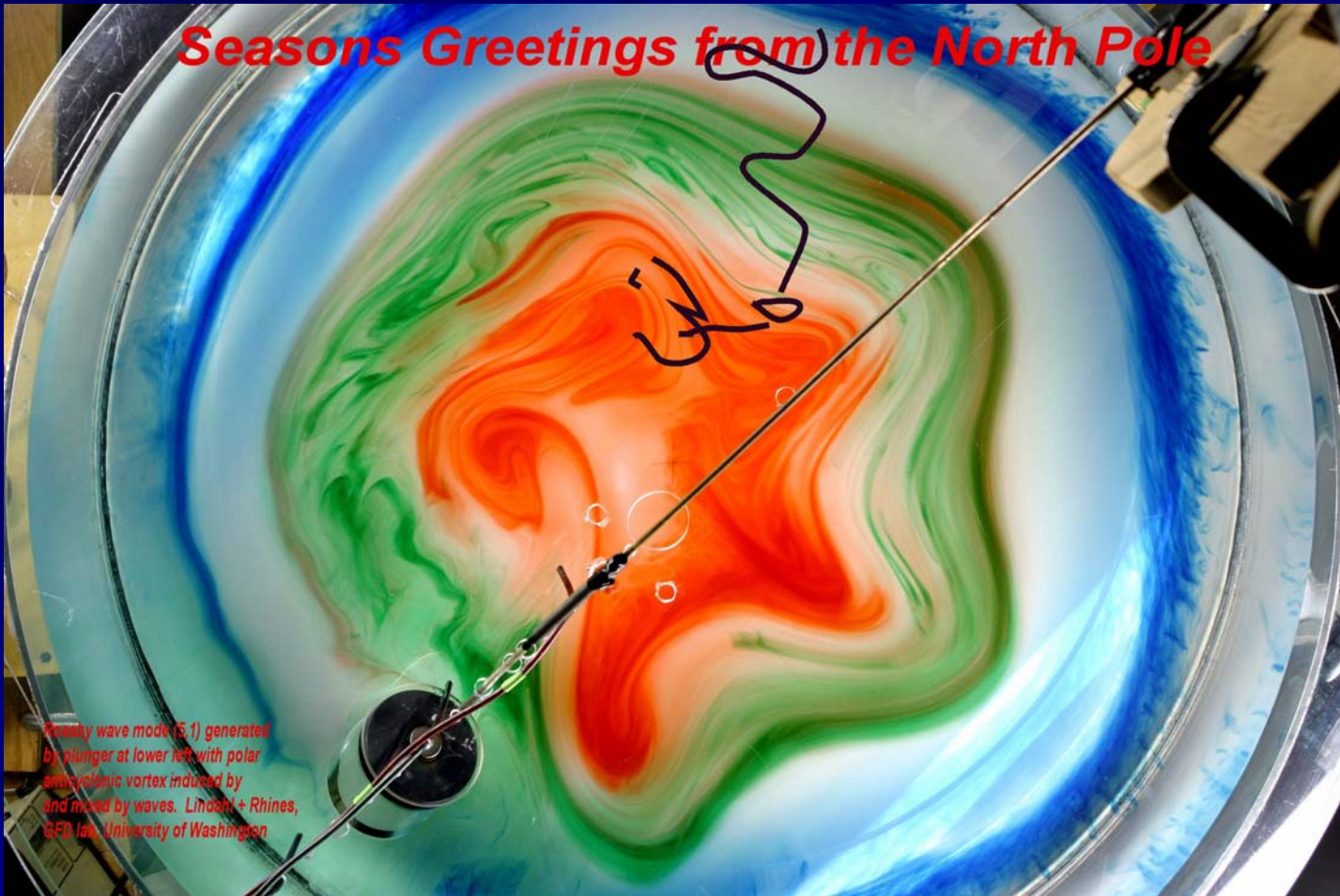


Polar  $\beta$ -plane oscillating Rossby wave source, no initial mean zonal flow: illustrating PV elasticity, Rossby wave group velocity, induced anticyclonic polar vortex, westerly jet at the latitude of the wave forcing and ozone-hole-like resistance to mixing of the polar cap

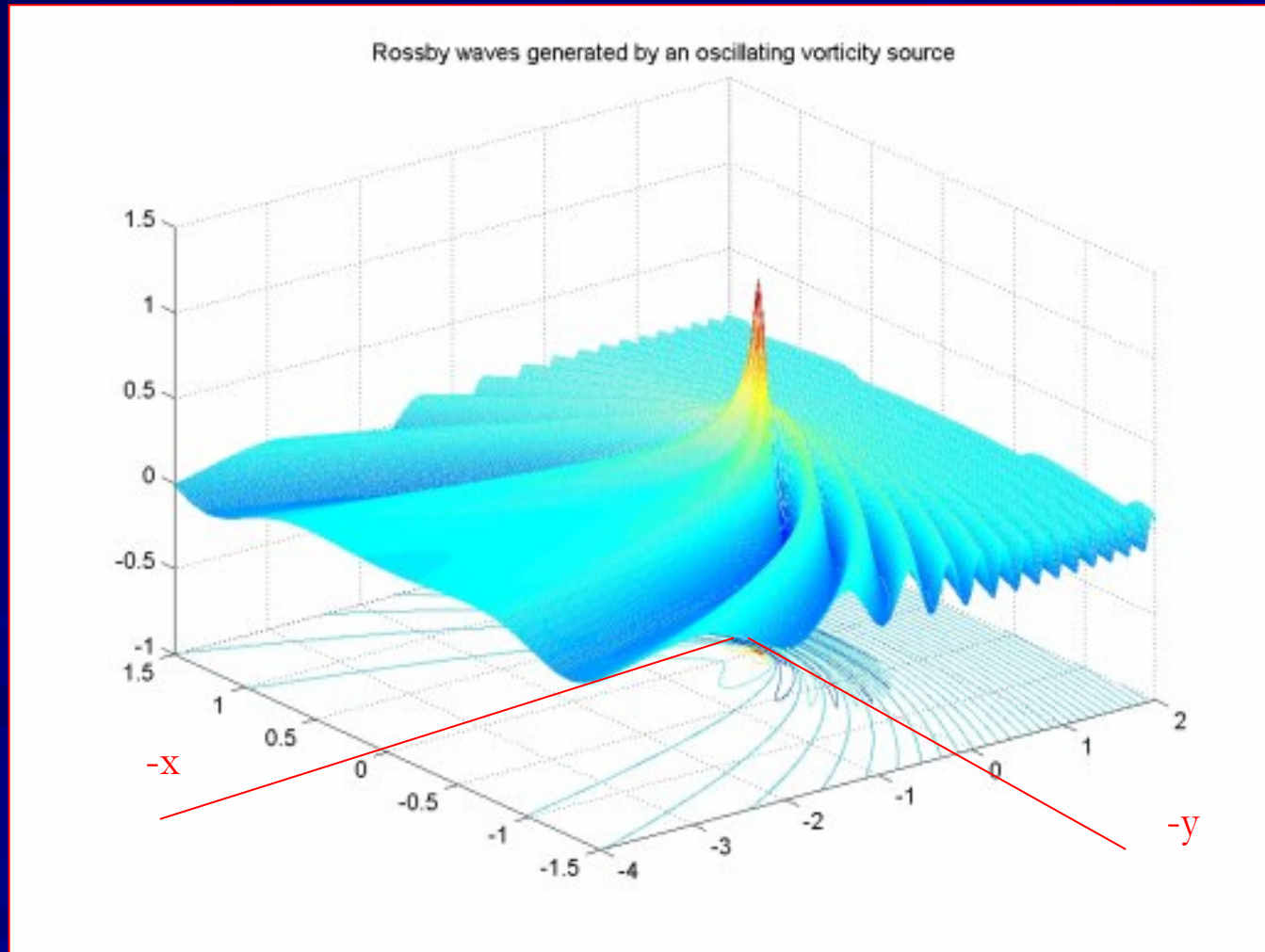


The PV elasticity...the restoring effect for Rossby waves...is very scale-dependent

A well-developed mode (1,5) makes a nice Christmas card

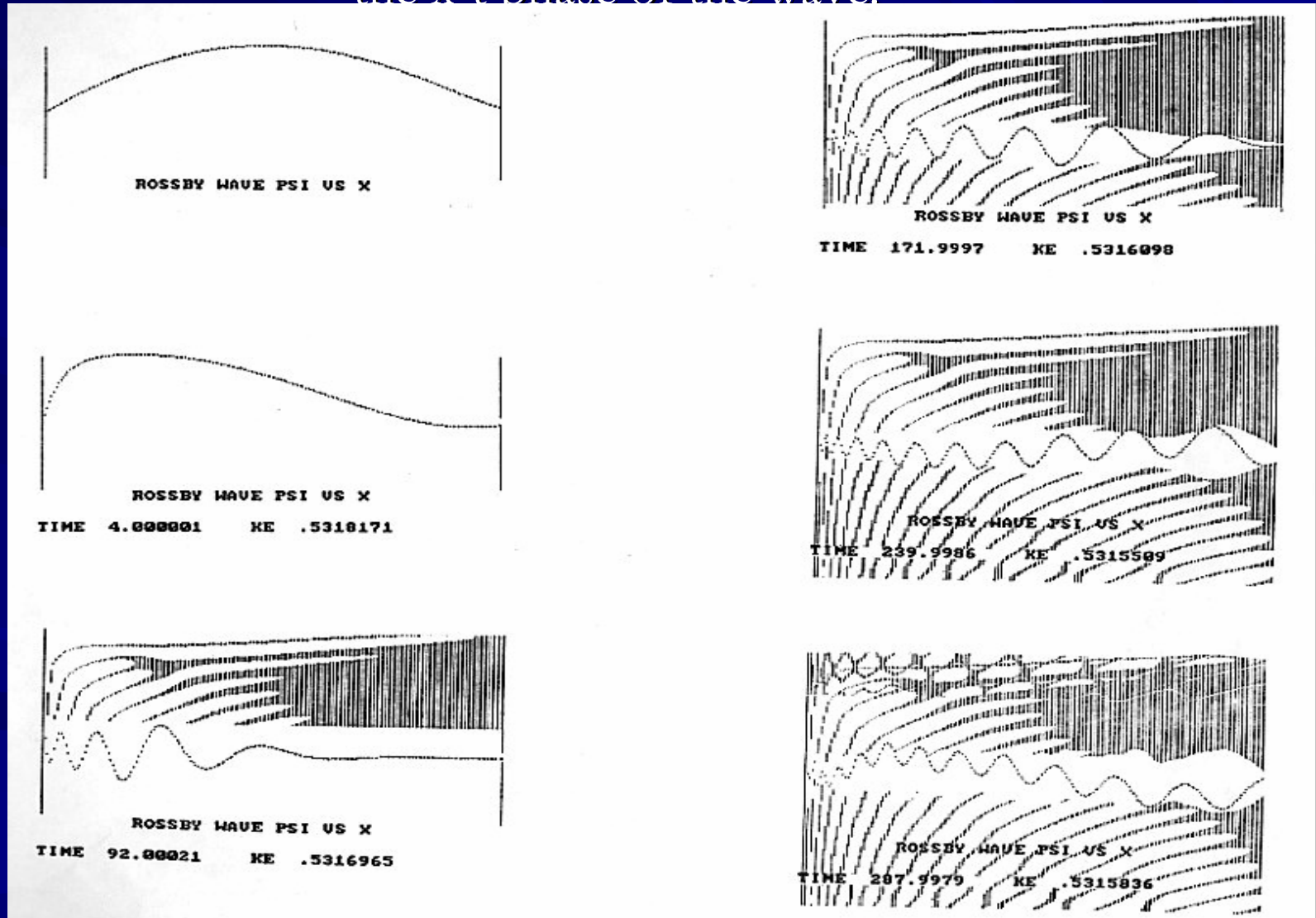


the barotropic Rossby wave Green function is simply a Bessel function times a traveling sine wave

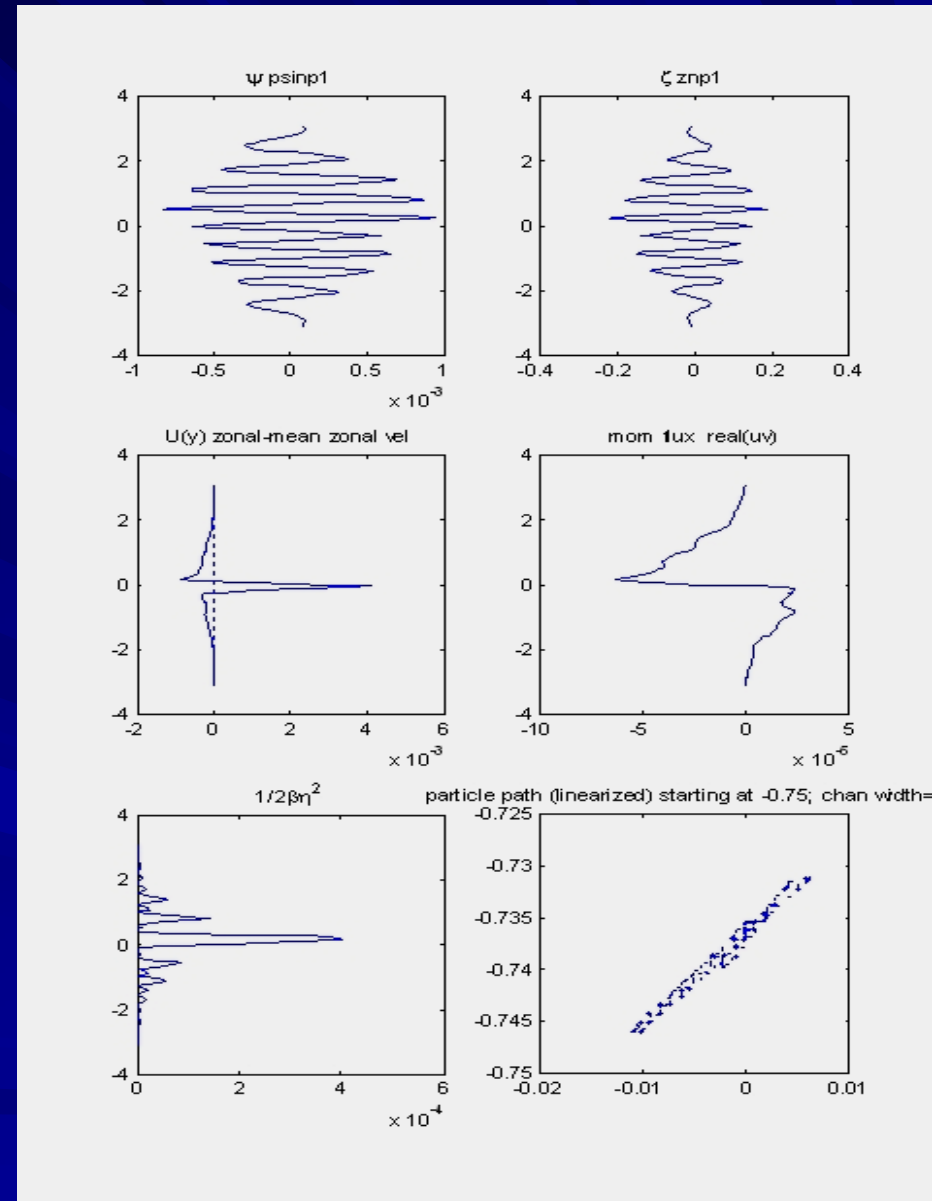




the barotropic problem makes a speedy numerical model on a laptop...here a Rossby wave develops from initial conditions with north-south walls at both ends; a Hovmoeller plot is added showing the x-t phase of the wave.

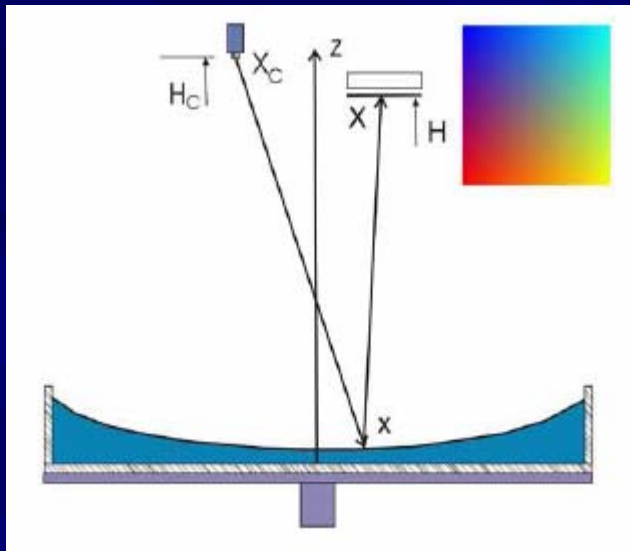


An equally simple numerical model illustrates the development of mean zonal flow as seen in the experiment, due to Rossby wave radiation from a narrow strip of latitude via a matlab m-file. Here PV stirring produces broad easterly acceleration at everywhere except at the latitudes of forcing where equal and opposite westerly acceleration creates a strong jet. The forcing is a single wave in  $x$  times a Gaussian in  $y$ , with a single frequency in time. The upper panels are streamfunction and vorticity. The lower left is the pseudo-momentum, based on north-south particle displacement (see Rhines, *The Sea*, v.6, 1977)



color altimetry





For quantitative inversion of surface elevation, velocity, potential vorticity we use colorometric mapping with a light source in the form of a square multi-hued panel: the imaged color field encodes the surface slope.

CIE (Commission Internationale d'Eclairage)  $L^*a^*b$  color space.

# Inversion from surface elevation to velocity

$$\frac{\partial \vec{V}}{\partial t} = -\nabla\left(\frac{1}{2}V^2\right) - g\nabla\eta + (\vec{k}f_0 + \nabla \times \vec{V}) \times \vec{V}.$$

$$\vec{V}_g = (u, v) = \frac{g}{2\Omega}(\eta_y, -\eta_x).$$

geostrophic

$$\vec{V} = \vec{V}_g - \kappa \frac{V_g \vec{V}_g}{f_0}.$$

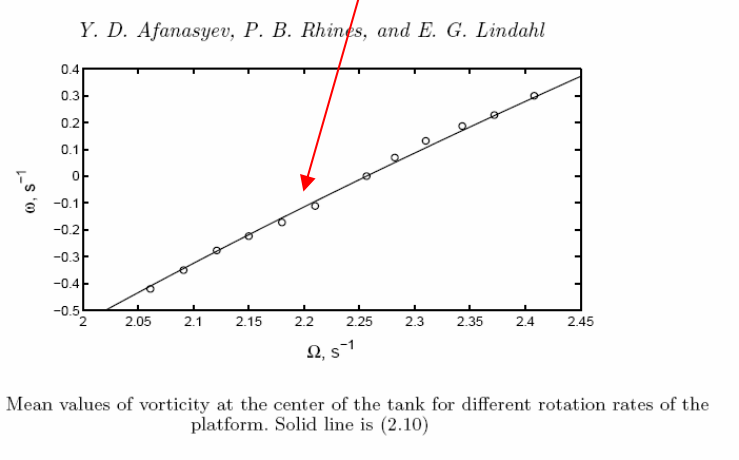
gradient

$$\vec{V} = \frac{g}{f_0} \vec{k} \times \nabla\eta - \frac{g}{f_0^2} \nabla\eta_t - \frac{g^2}{f_0^3} J(\eta, \nabla\eta).$$

semi-geostrophic

accuracy of the method: simply change the rotation rate over a known range...altimetry accurate to 0.05% (std)

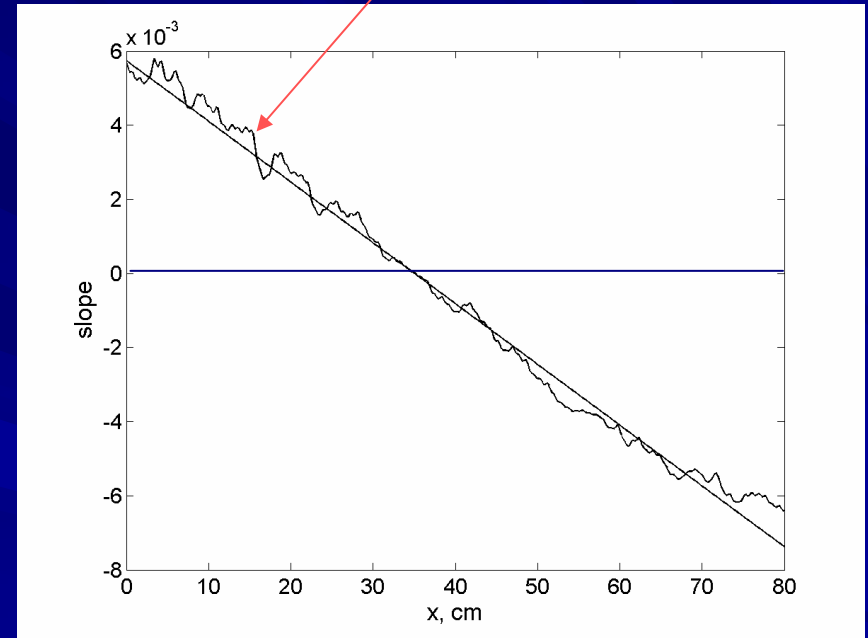
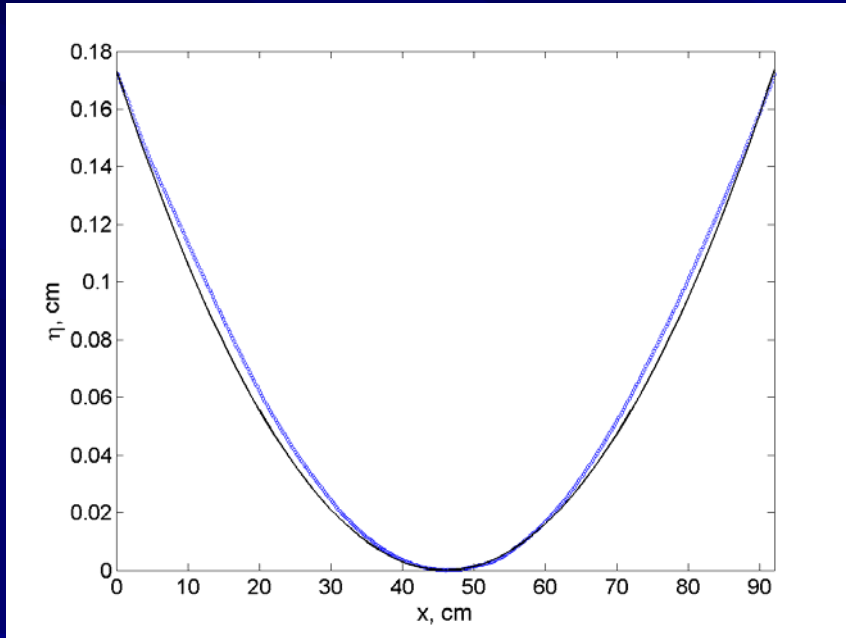
$$\zeta = \frac{\Omega^2 - \Omega_0^2}{\Omega}.$$



$$h(r) = H_0 + \frac{\Omega^2}{2g}\left(r^2 - \frac{D^2}{8}\right),$$

....PV inversions

calibrating the altimetric elevation and slope against known solid body rotation: snapshot; std of slope =  $2.0 \times 10^{-4}$  corresponding to velocity of  $0.5 \times 10^{-3} \text{ m sec}^{-1}$  temporal smoothing readily increases the accuracy by at least a factor of 10. (The azimuthal velocity at mid radius is  $8 \times 10^{-3} \text{ m s}^{-1}$ .) *high frequency surface waves*





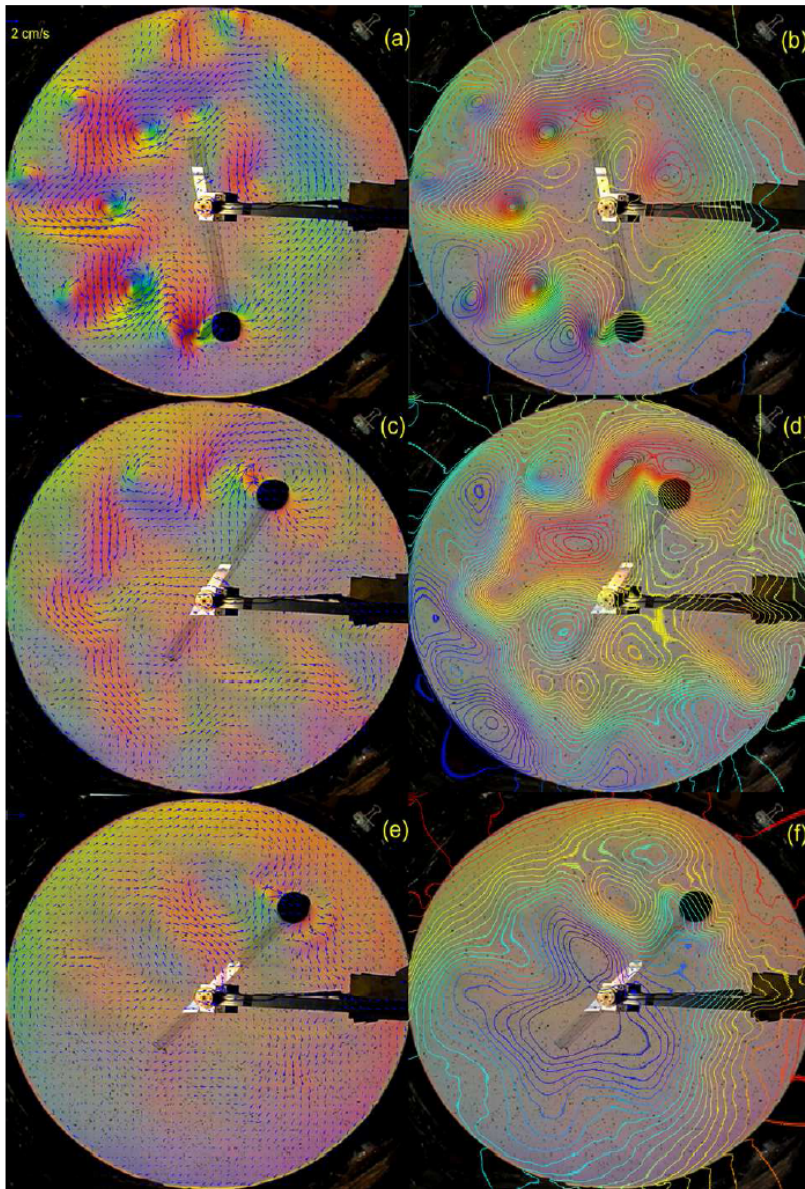


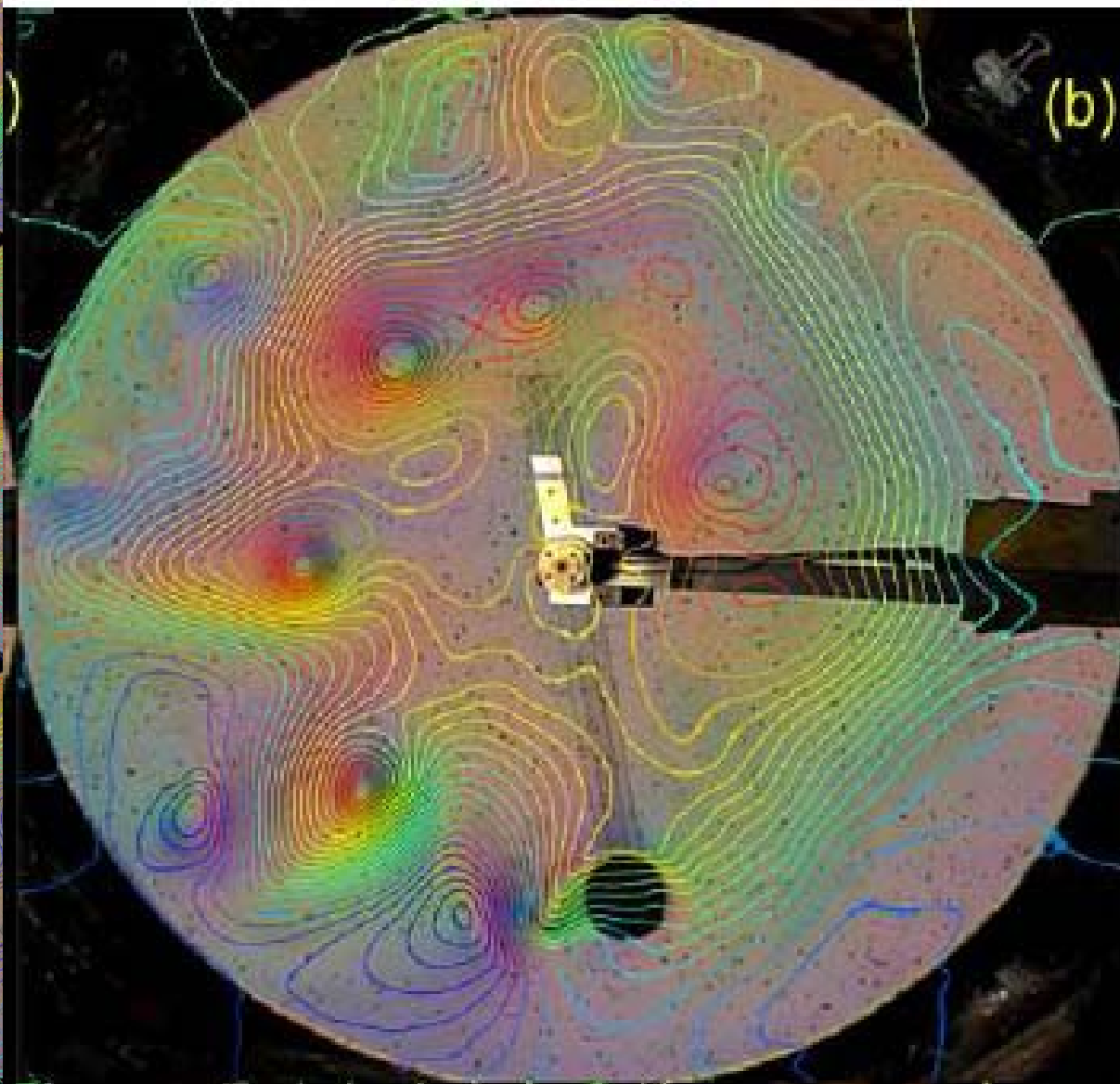
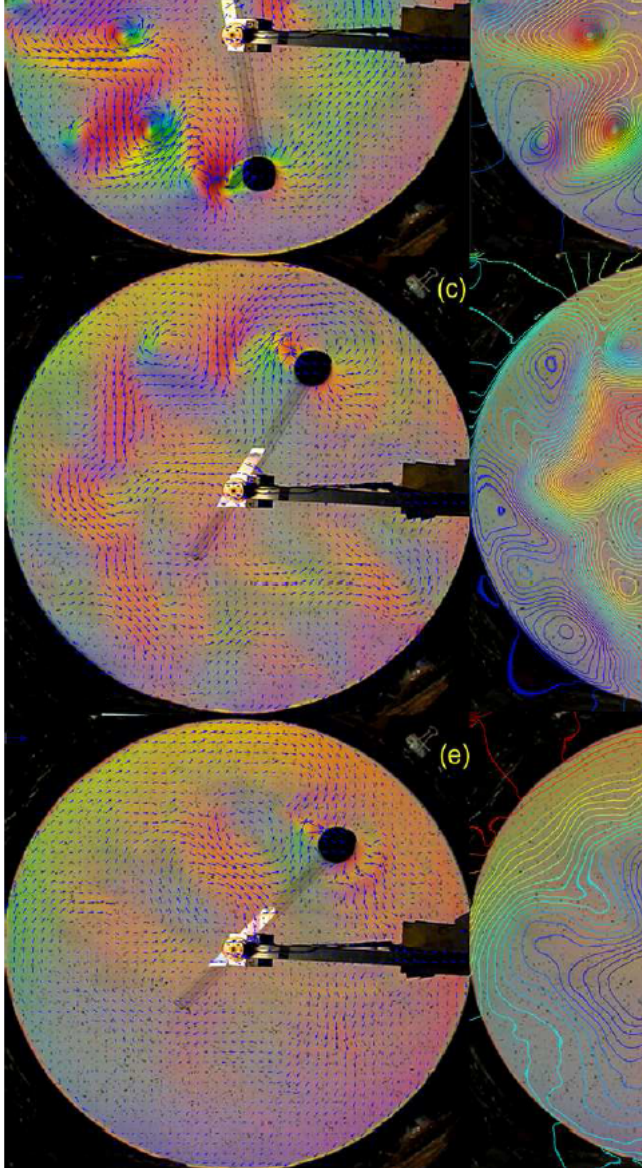
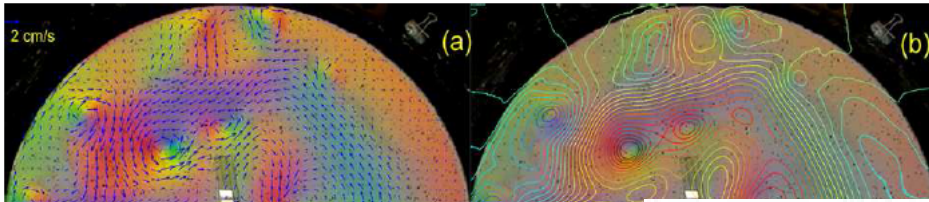
FIGURE 3. gradient wind velocity vectors and isolines of the surface elevation for three different experiments with the cylinder of diameter  $d = 6$  cm. The background color images are video frames showing the color-coded slope field. Only every 100th velocity vector is shown. (a, b) eastward translation of the cylinder,  $U = 3.6$  cm/s,  $\beta^* = 1.7$ ,  $Re = Ud/\nu = 2200$ ,  $Ro = 2U/(df_0) = 0.3$ , isolines are drawn for  $\eta = -0.07:0.005:0.07$  cm; (c, d) westward translation,  $U = 2.4$  cm/s,  $\beta^* = 1.1$ ,  $Re = 1400$ ,  $Ro = 0.2$ ,  $\eta = -0.042:0.002:0.04$  cm; (e, f) westward translation,  $U = 1.3$  cm/s,  $\beta^* = 0.6$ ,  $Re = 800$ ,  $Ro = 0.1$ ,  $\eta = -0.06:0.0025:0.0$  cm.

- Here the colormetric altimetry scheme shows SSH gradient as a perturbed color field. The quantitative inversion gives SSH (right panels), velocity (arrows on left panels) and potential vorticity. (Every  $1/100^{\text{th}}$  velocity vector is plotted).

The flow is generated by towing a circular cylinder rapidly eastward (upper panel), rapidly westward (middle panel) or slowly westward (lower panel) about this polar  $\beta$  plane, generating

both a vortex wake and Rossby waves





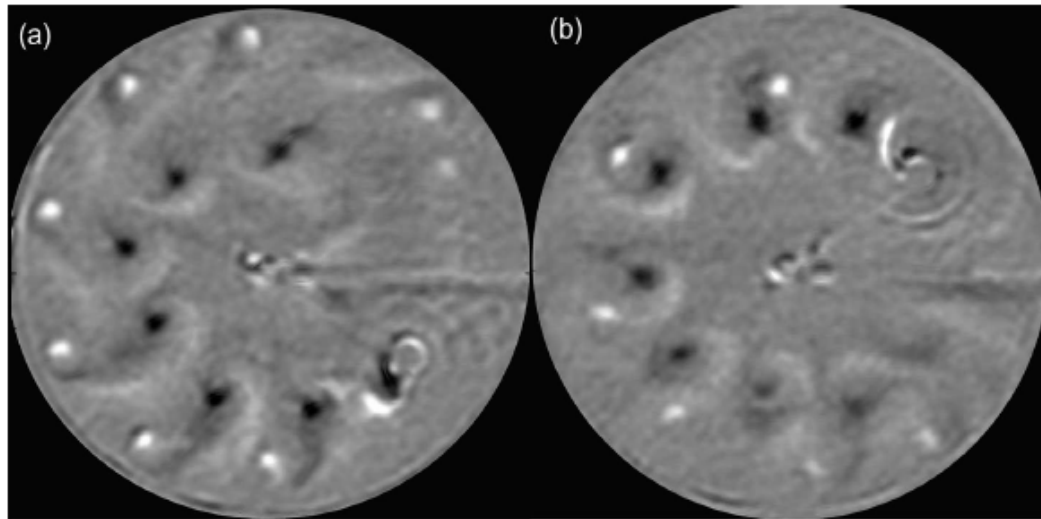


FIGURE 7. Vorticity maps for two experiments corresponding to figure 6 a and c. Vorticity is normalized by the Coriolis parameter and varies from  $-0.5$  to  $0.5 \text{ cm}^{-1}$  in (a) and (b).

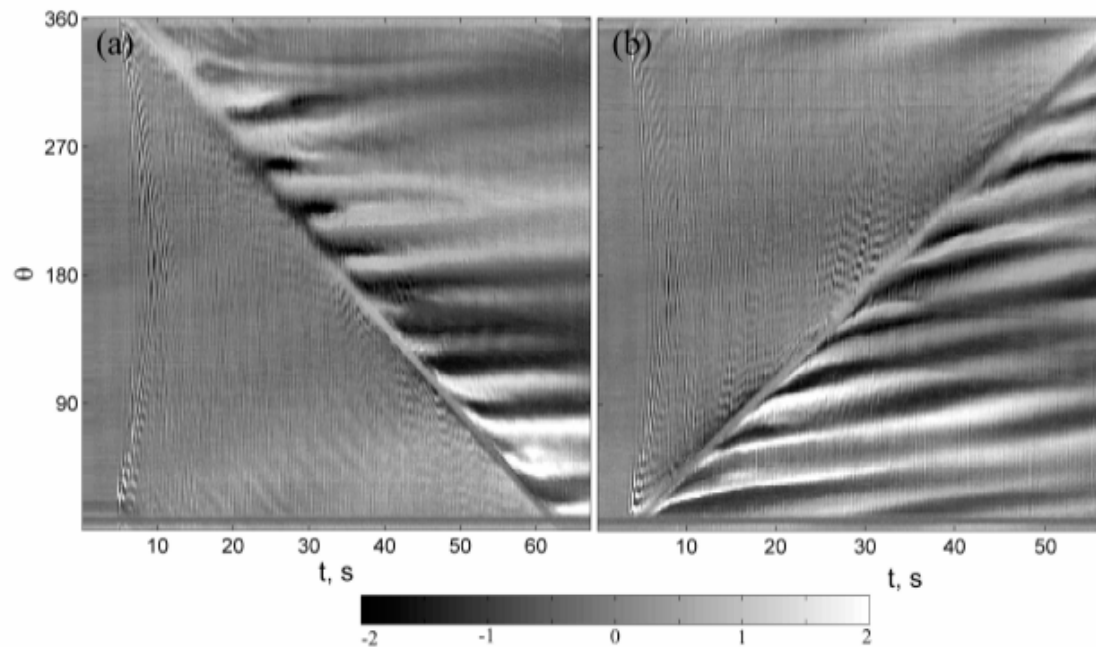


FIGURE 8. Hovmöller diagrams for two experiments corresponding to figure 6 a and c. Azimuthal angle  $\theta$  increases in westward (clockwise) direction. Grayscale shows radial velocity component in  $\text{cm/s}$ .

on a  $\beta$  plane cyclonic eddies drift poleward (as in Dudley Chelton's analysis of altimetric SSH), while anti-cyclones drift equatorward.

This is seen here, with the vortices in the cylinder wake for eastward (left) and westward (right) moving cylinders.

The lower Høvmøller plot shows the wake propagation speed for the respective cases..almost always westward regardless of the direction of motion of the cylinder



# Altimetry in the real world: Topex-Poseidon/JASON/ERS satellites

- A key discovery using satellite altimetry is the Rossby wave/nonlinear eddy structure of the upper km of the ocean (Chelton and collaborators). Almost everywhere mesoscale eddies drift westward, as large-amplitude Rossby waves similar in structure to the baroclinic eddy describe in the MODE 1973 experiment in the western N Atlantic. The Antarctic Circumpolar Current is the main exception where eddies are systematically advected eastward.

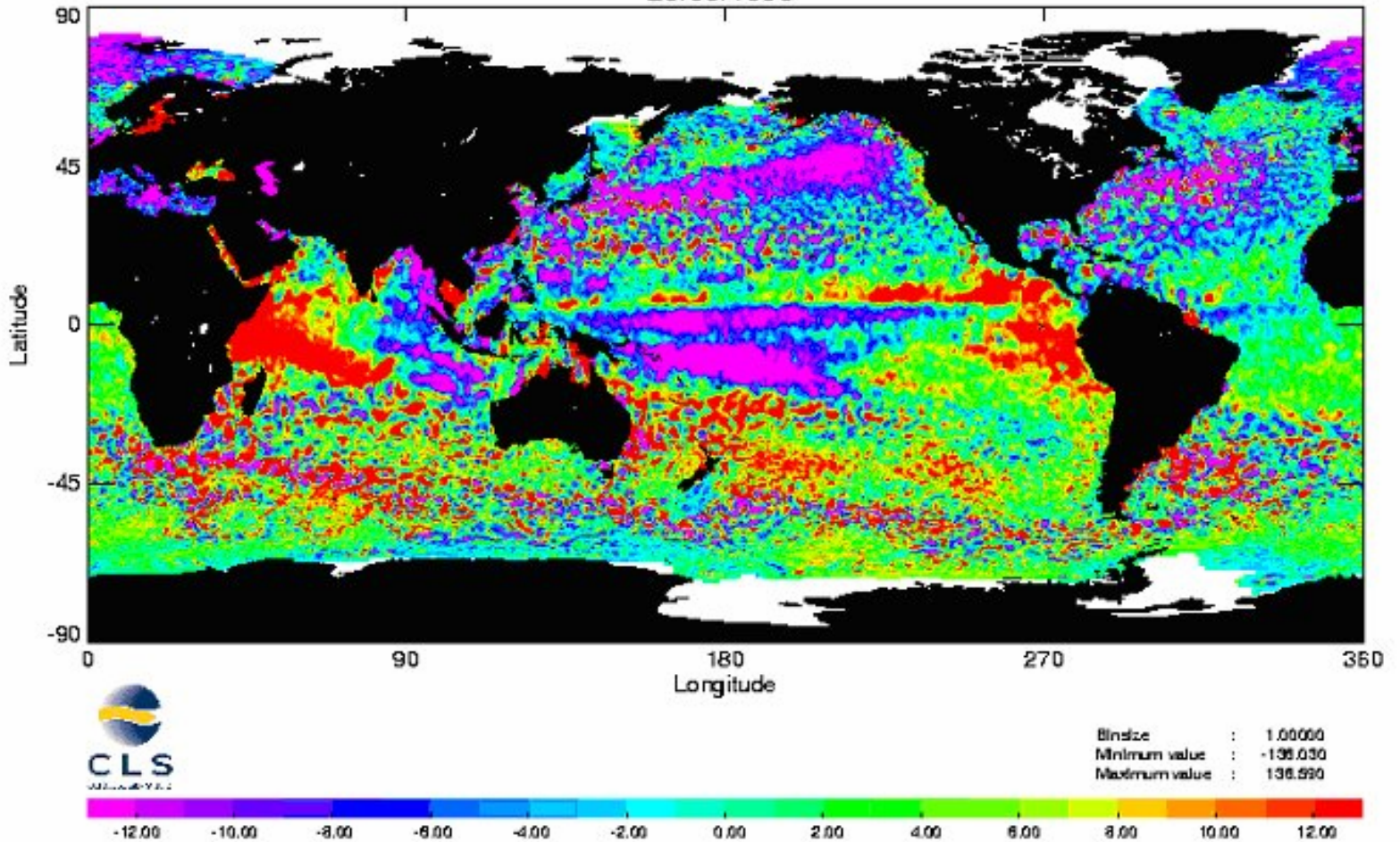
And, many of these eddies carry fluid with westward with them, in what amounts to a new form of general circulation. They have been tracked with RAFOS floats and, tentatively, with their own potential vorticity signature.

We have carried out a series of experiments to investigate the mixed wave/eddy properties using barotropic and baroclinic disturbances generated by a towed circular cylinder

*(Afanasyev, Rhines & Lindahl Phys. Fluids 2008; Exps in Fluids 2008; preprints at [www.ocean.washington.edu/research/gfd](http://www.ocean.washington.edu/research/gfd)).*

# SEAL LEVEL ANOMALY - T/P + ERS - (cm)

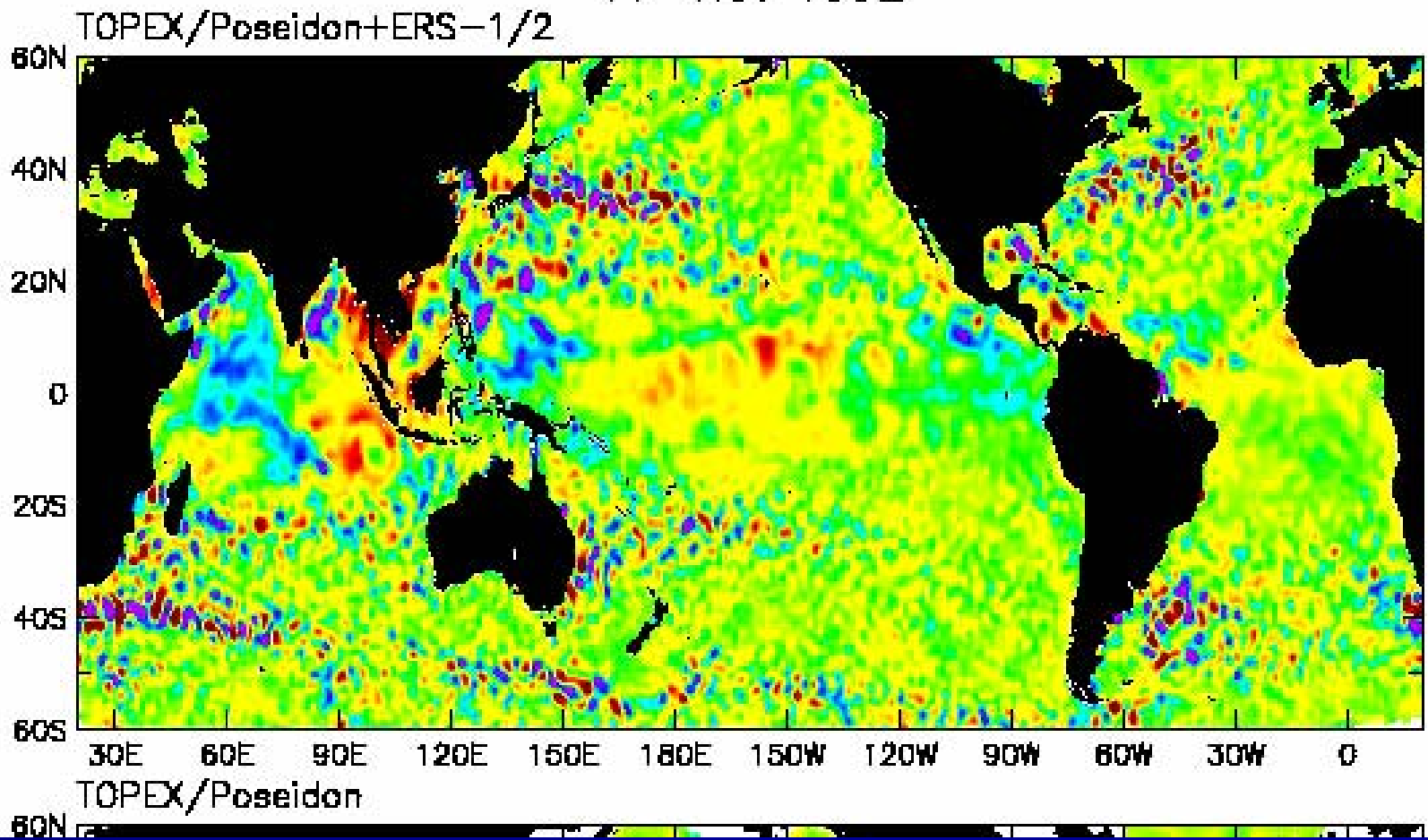
25/03/1998



*Dudley Chelton*

Topex/Poseidon/JASON satellite  
altimetry (JASON-2 launch this Friday!) (Dudley Chelton video)

11 Nov 1992





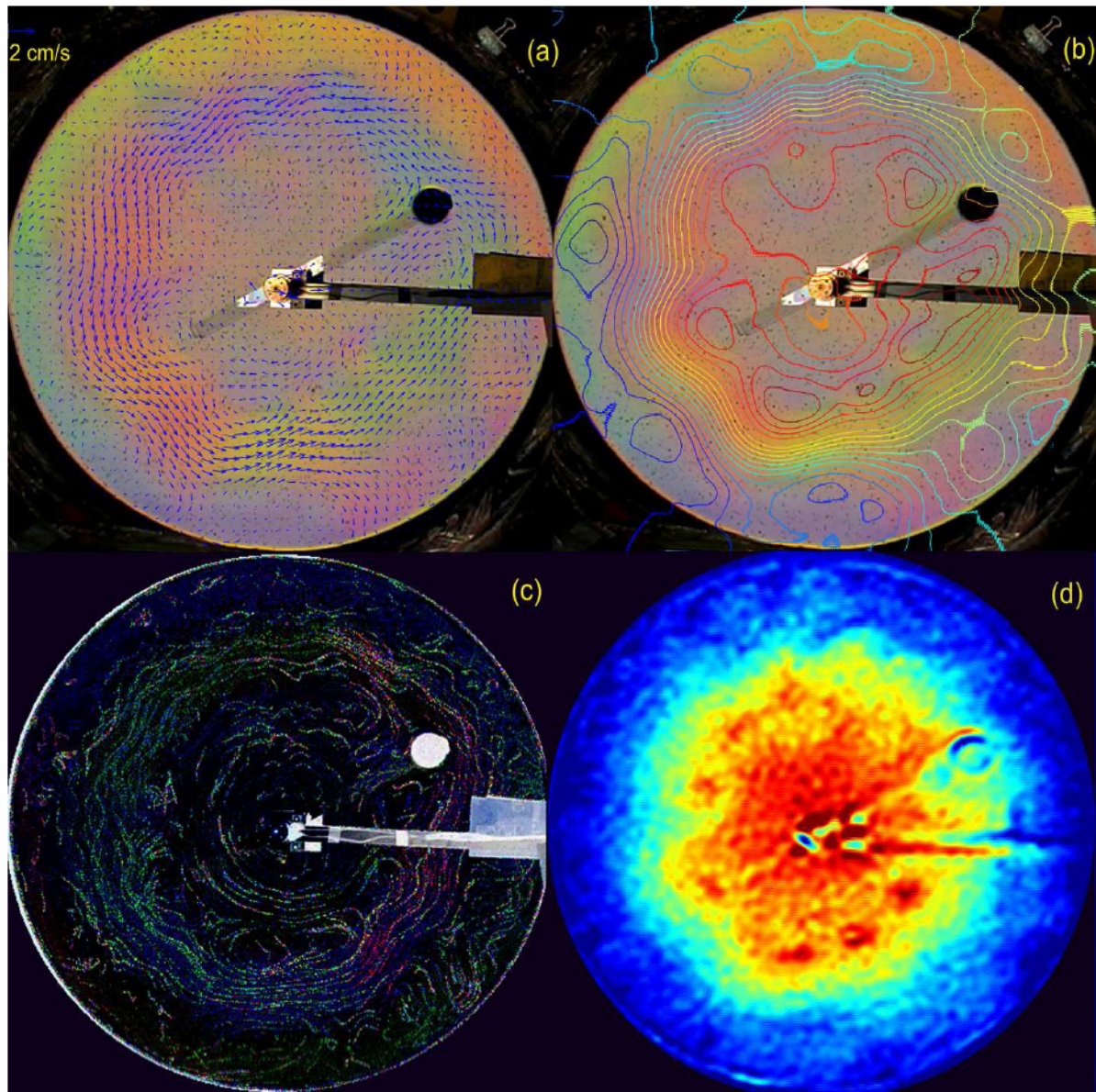


FIGURE 9. Eastward jet at  $t = 75$  s after the cylinder was stopped. Cylinder performed one full cycle in eastward direction,  $d = 4.8$  cm,  $U = 4.8$  cm/s. (a) gradient wind velocity; (b) surface vorticity  $\eta = -0.025:0.004:0.045$  cm; (c) particle tracks for the period of 30 s; (d) PV varies from 0 to 0.5 (cms)<sup>-1</sup>



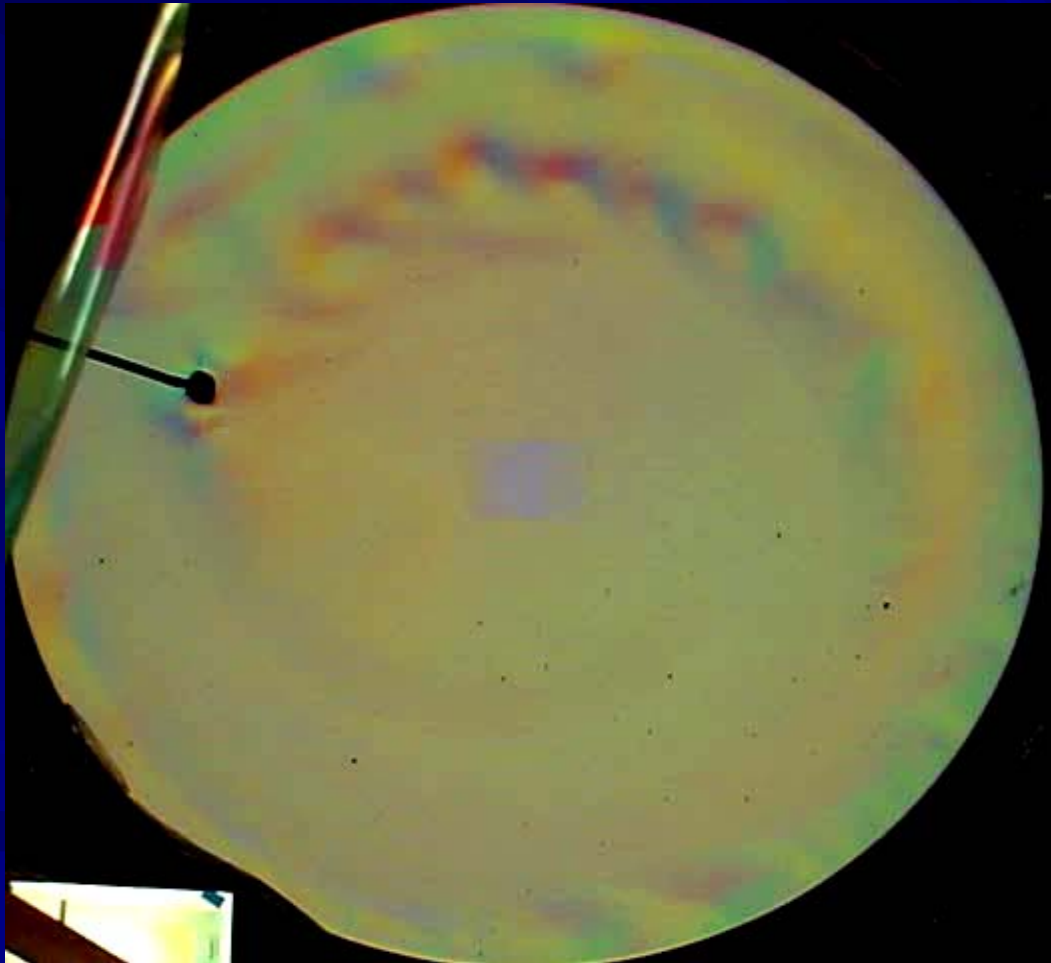
## Baroclinic flows

- Barotropic modes remain potent in stratified ocean and atmosphere. 'Barotropization' is a key process of geostrophic turbulence which sends energy into tall eddies (the troposphere has too much surface drag for this to go to completion, yet synoptic clustering and excitation of the stratospheric polar vortex is readily seen).

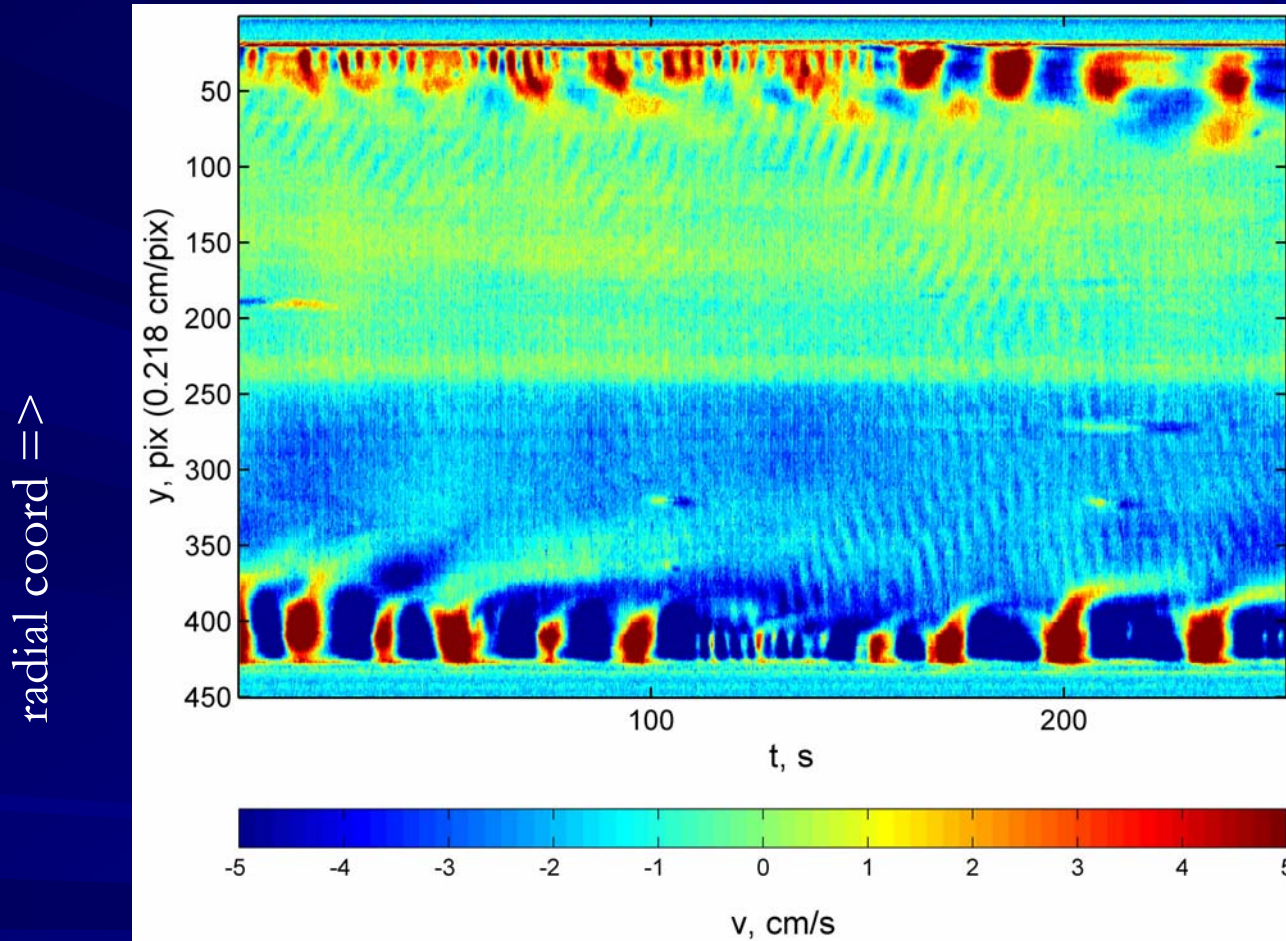
Early ref: *Rhines, The Sea vol. VI 1977; Ann. Revs Fluid Mech 1979*)



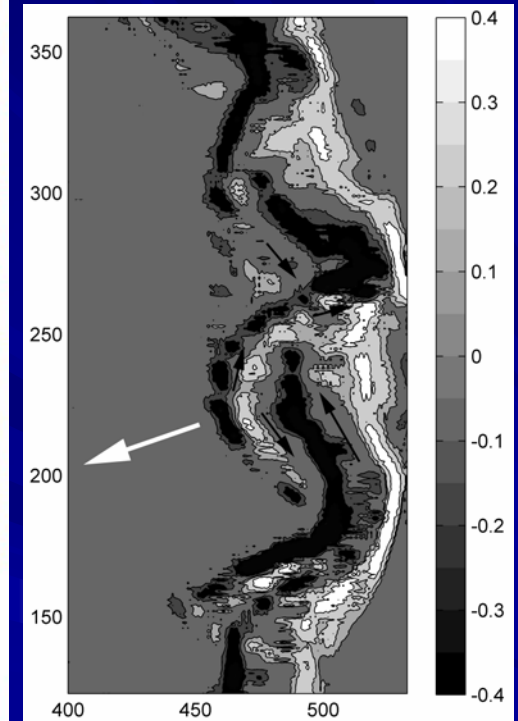
Buoyant source of fluid produces a ' $\beta$ -plume' in a thin surface upper-ocean surface layer, radiating west of the source and producing an unstable boundary current.



The boundary current's baroclinic instability radiates near-inertial waves  
(*Afanasyev, Rhines & Lindahl, J Atmos Sci 2007*)

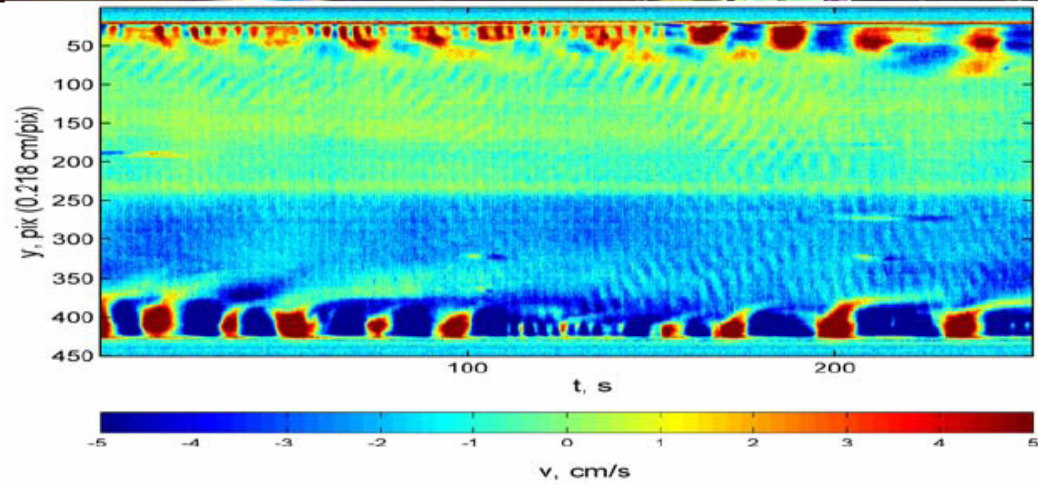
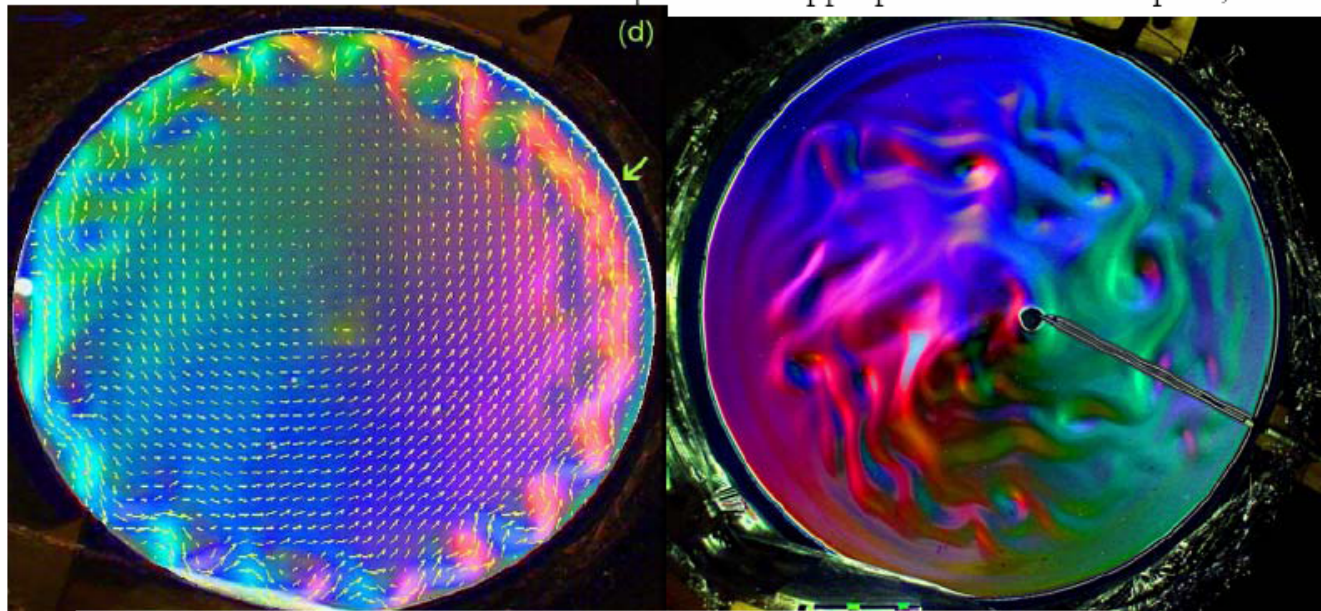


time =>

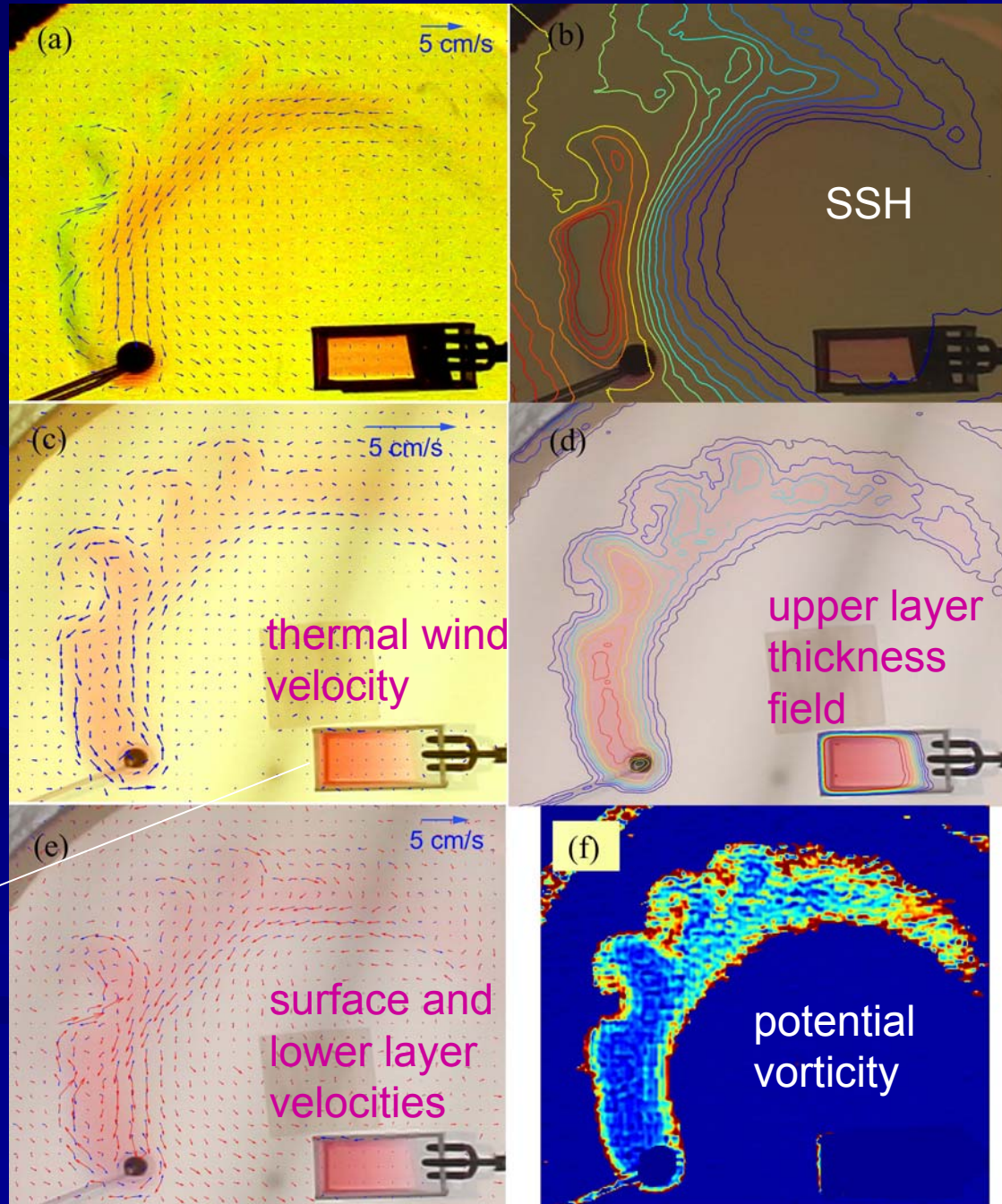


zoom of the boundary current reconstructed from altimetry. The wave radiation site is shown.





SSH, surface velocity  
(every 100<sup>th</sup> vector)

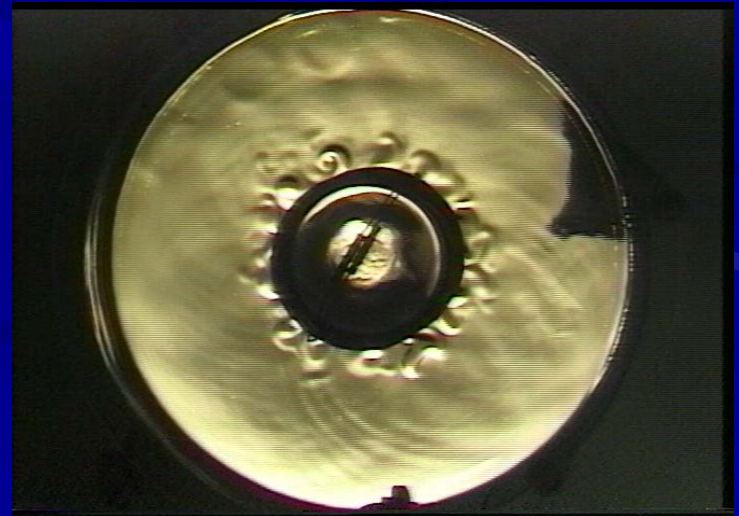
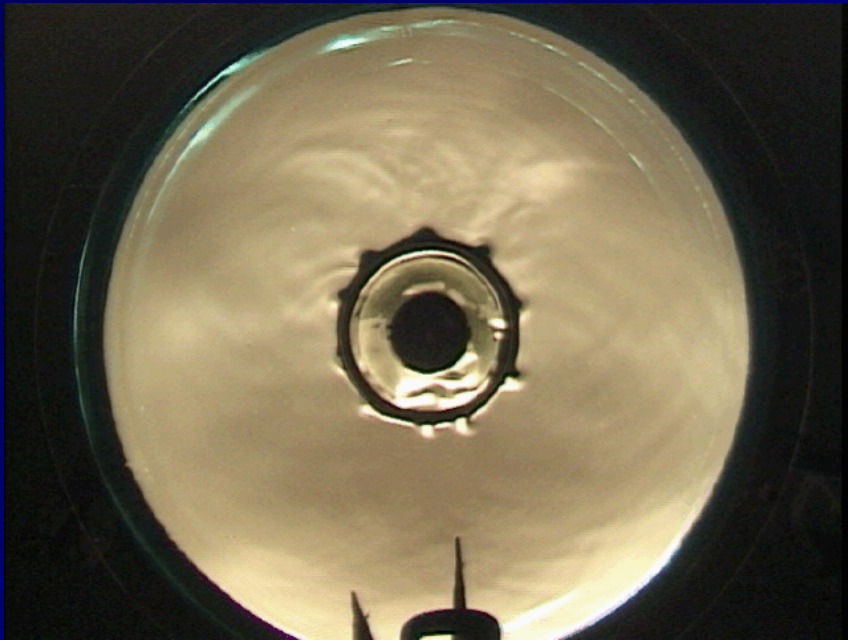


We combine alimetry with an optical thickness measurement of the upper layer of a stratified fluid, giving both barotropic and baroclinic velocity fields, which is complete in the case of 2 layers.

a wedge-shaped cuvette with uniformly dyed fluid calibrates the optical layer thickness



convective mesoscale eddies from a hot inner wall (with rotation)

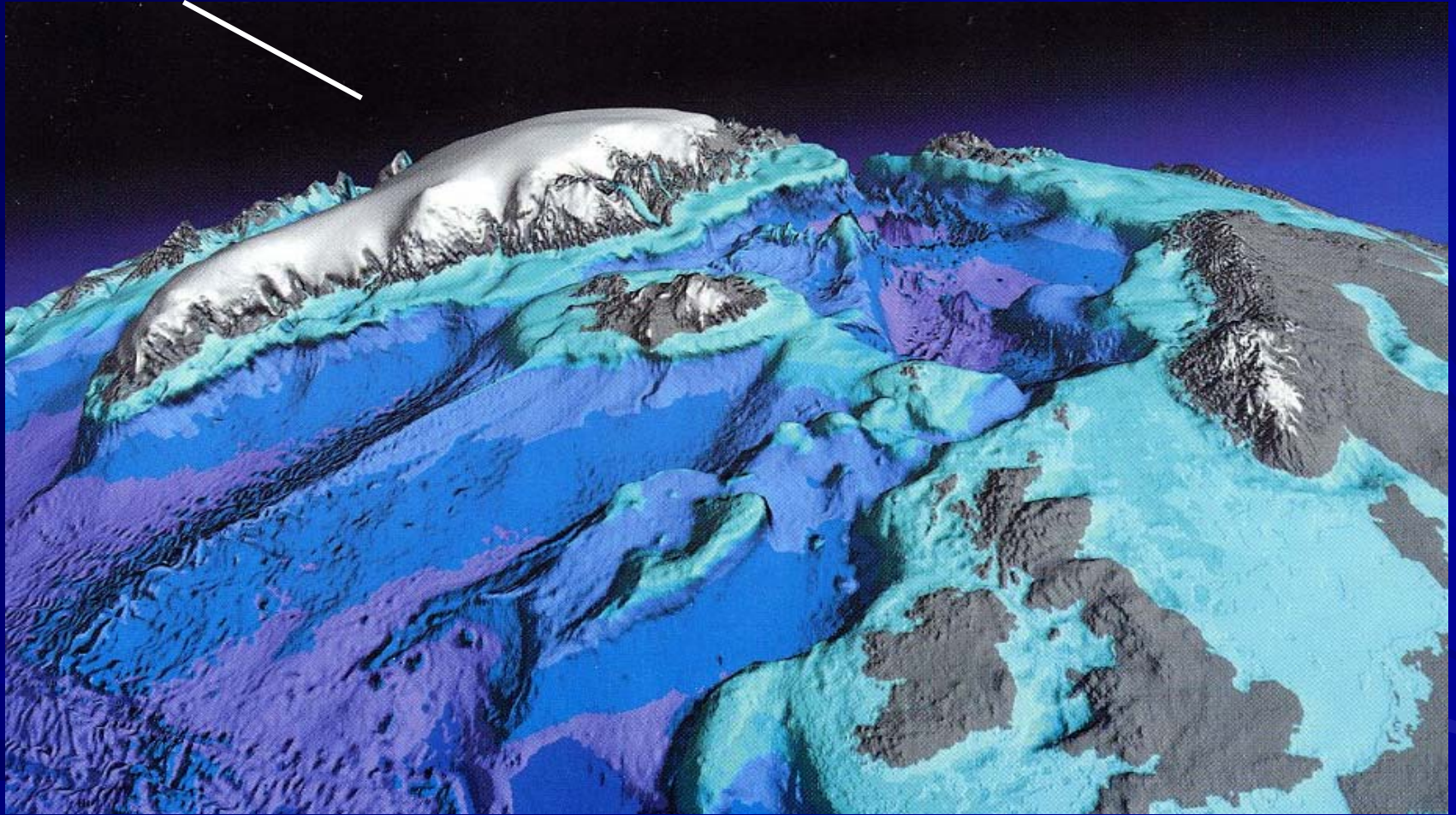


# Effects of bottom topography



# Effects of complex Earth topography Taylor-Proudman and 'PV waveguides'

*stirring rod?*



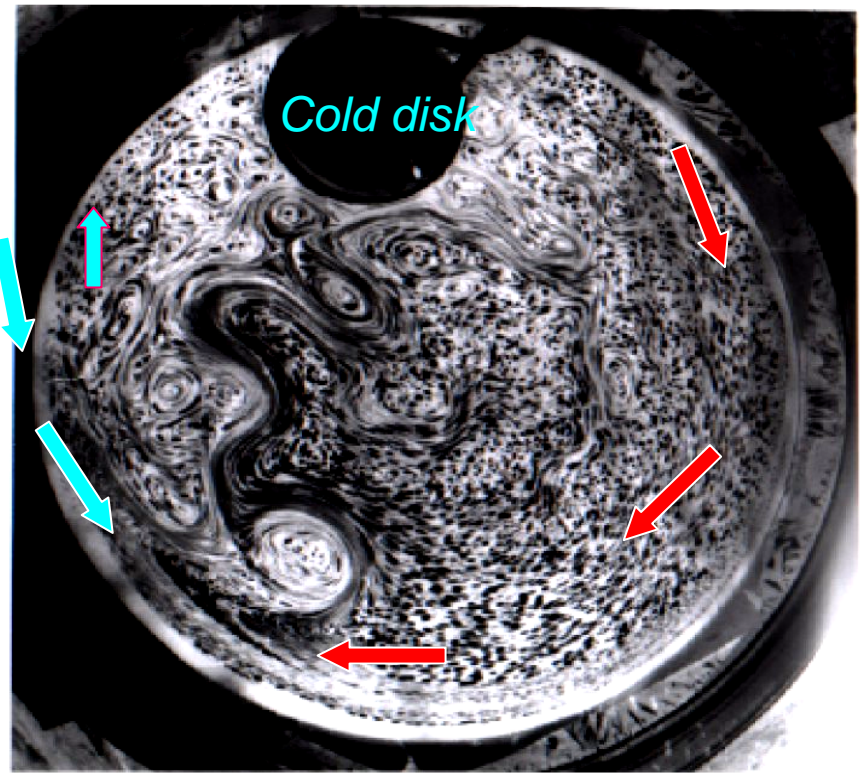
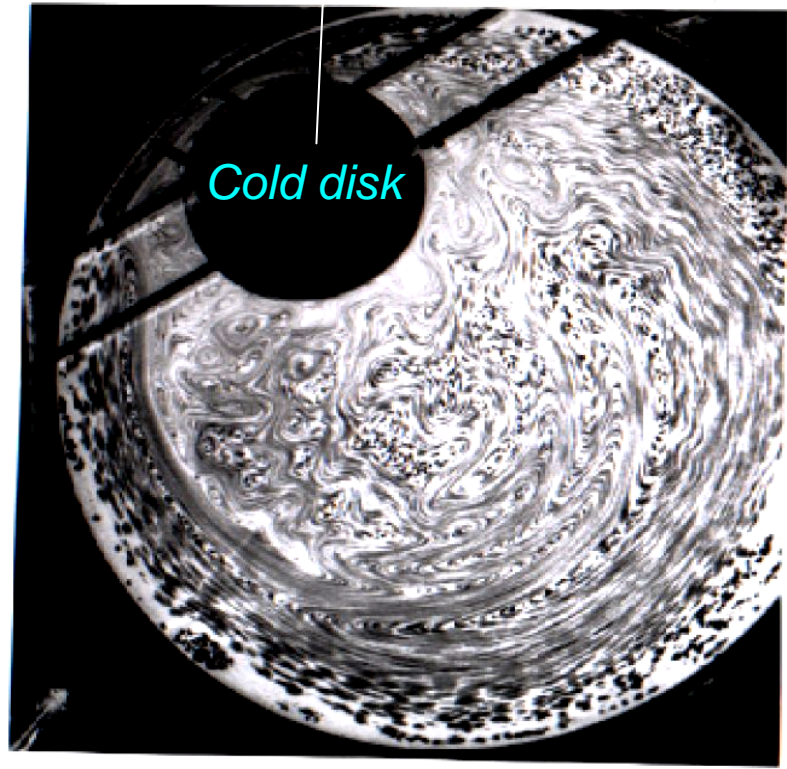
*AGU, 2003*



Forcing of a rotating bowl-shaped basin by a disk of surface cooling...the circulation is most intense far from the convective energy source. Boundary currents, gyres and deep convection develop from this compact source

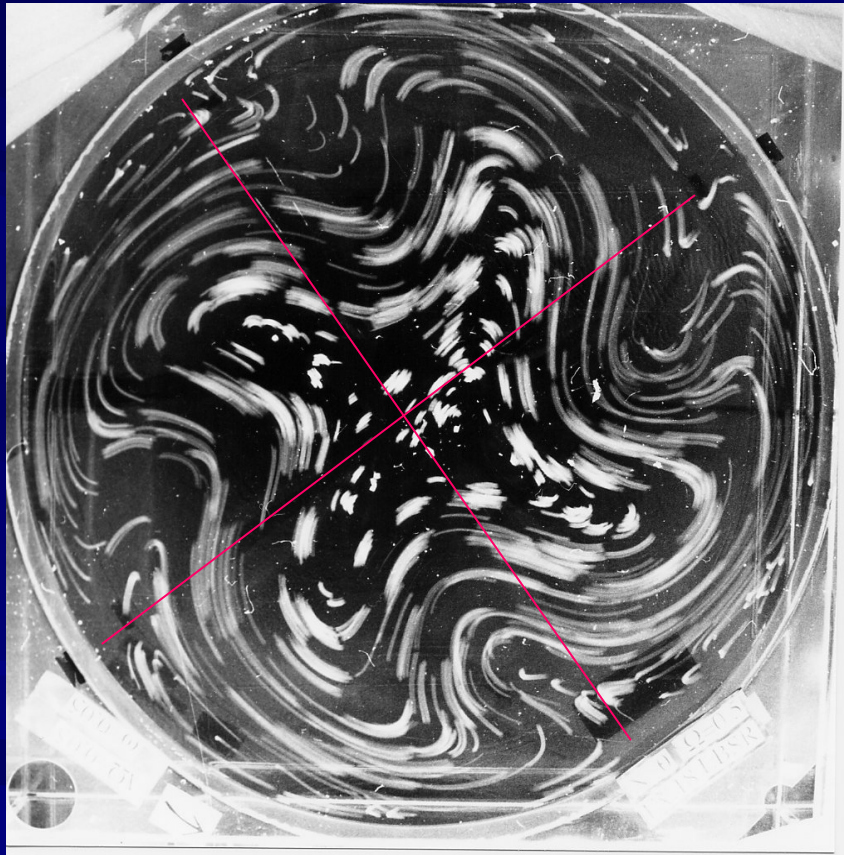
*rapid rotation*

*less rapid rotation*



*Condie & Rhines 'Topographic Hadley Cells JFM 1994*

# Surface flow in rotating bowl with 4 ridges (spoke-like along red lines)

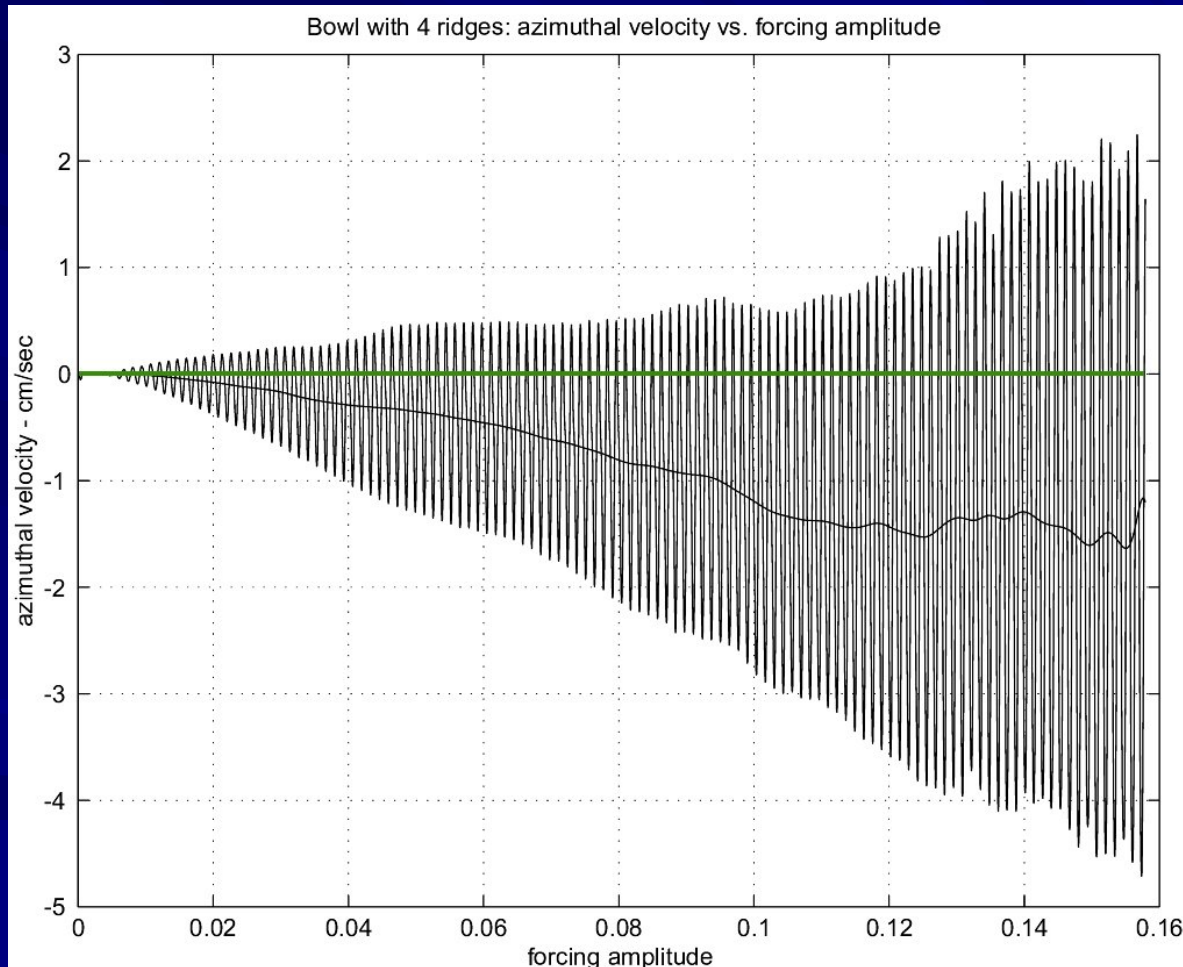


Slow flows follow contours of constant depth; here the clover-leaf pattern is shifted off the ridges by finite zonal velocity, as part of a topographic Rossby-wave pattern





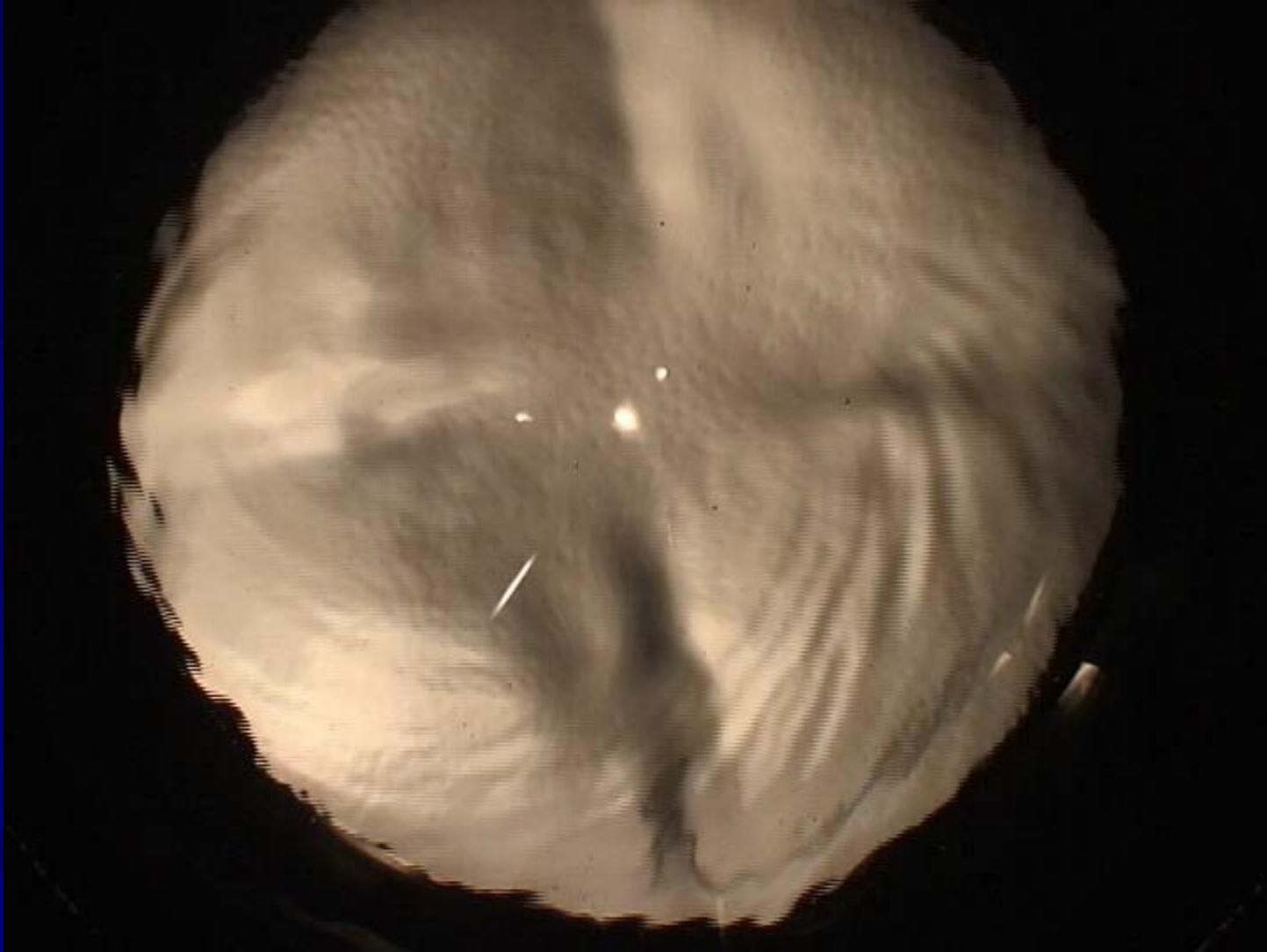
**Azimuthal velocity vs. forcing amplitude: the induced mean flow is ‘pseudo-westward’, (thinking of Rossby waves) or in the direction of topographic wave propagation, with shallow water to the right.  
(laser velocimeter record of azimuthal velocity vs. time as the oscillation is ramped up in amplitude)**

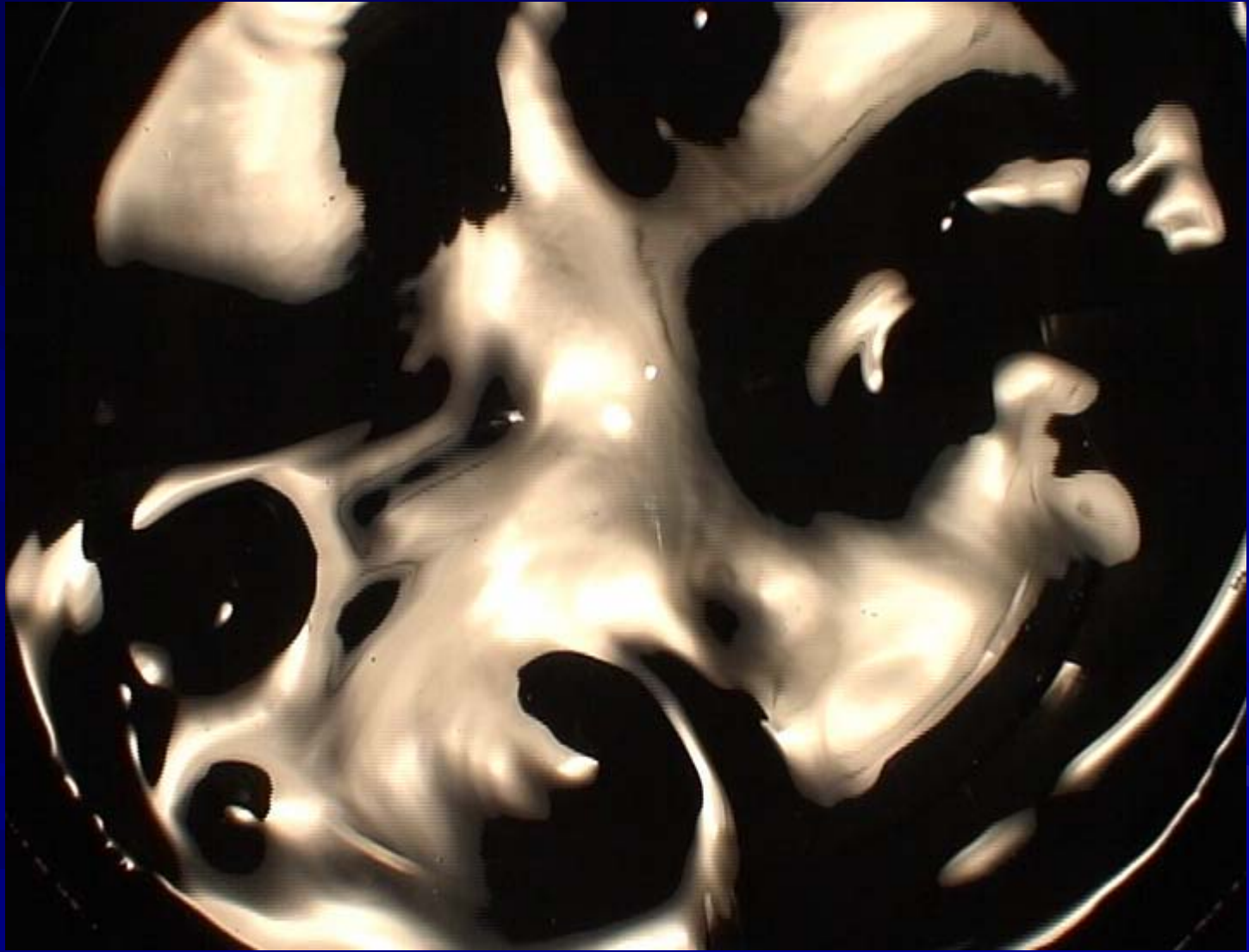


With sine-wave topography an elegant 3-mode nonlinear system emerges: the Charney-deVore problem



snapshots from topographic flow experiments









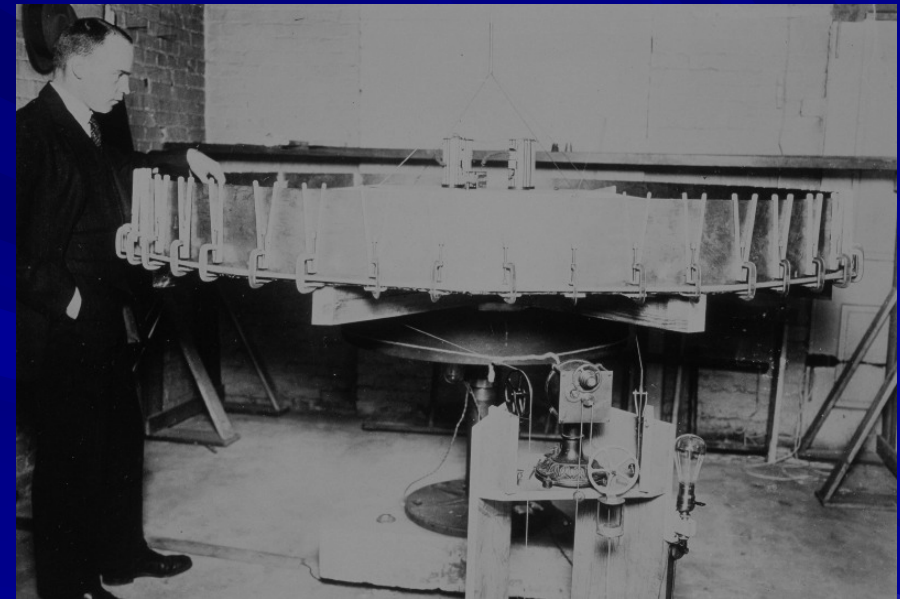
The entire free-surface elevation field of a rotating fluid in the laboratory can be imaged and analyzed, by using it as a parabolic telescope mirror (*Newton & Huygens 1672*)

This ‘optical altimetry’ readily achieves a precision of better than 1 micron of surface elevation. The surface topography corresponds to the pressure field just beneath the surface. It is the stream-function for the geostrophic, hydrostatic circulation, which can be resolved to better than 0.1 mm sec<sup>-1</sup>.

*Rhines, Lindahl & Mendez, J. Fluid Mech, 2007*

*Gharib & Dabiri, Exp. Fluids, 2001, slope detector probe*

*Afanasyev, Rhines & Lindahl, Physics of Fluids (accepted 2008); Experiments in Fluids (accepted 2008)*



[www.ocean.washington.edu/research/gfd](http://www.ocean.washington.edu/research/gfd)

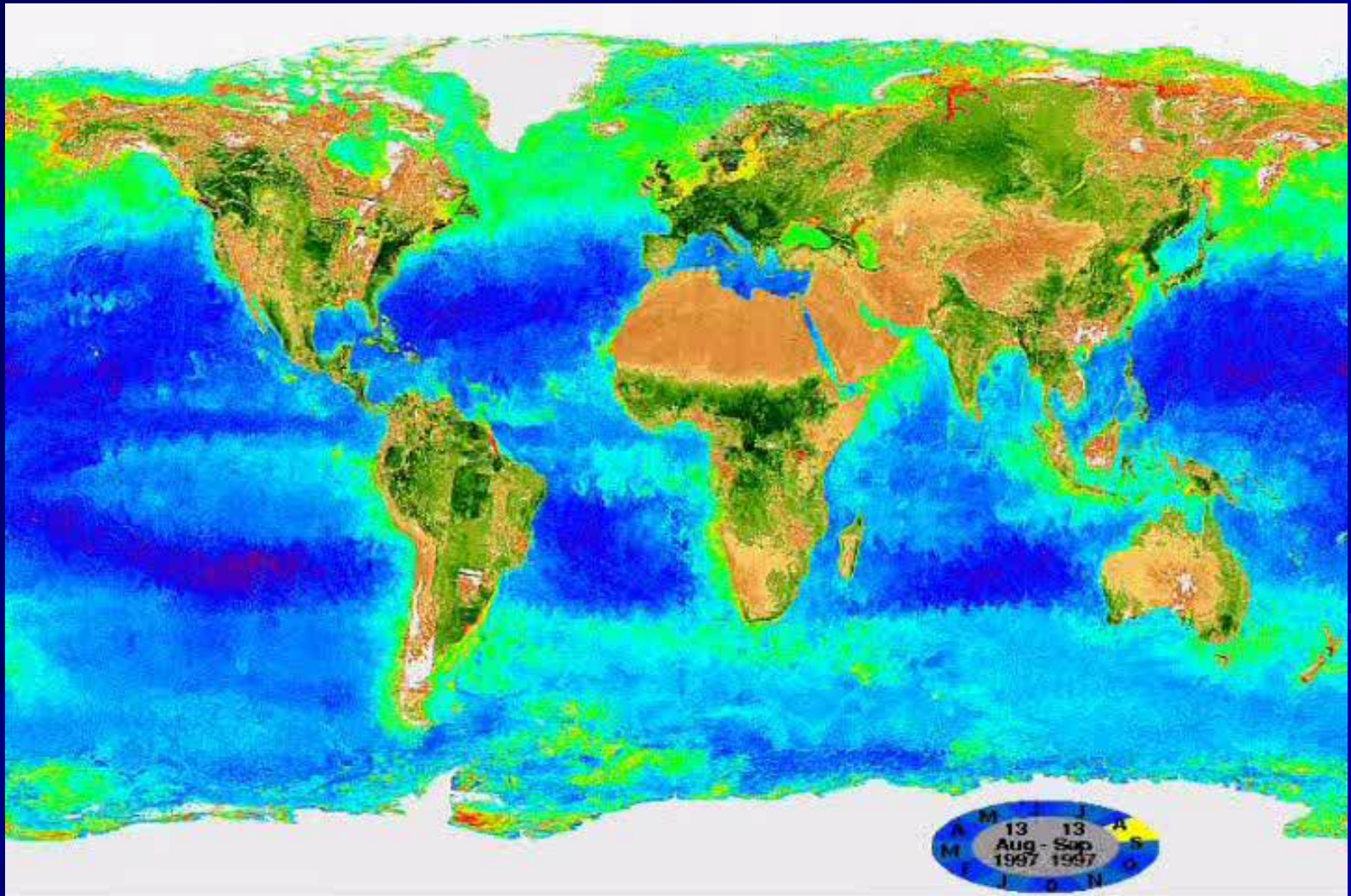
Carl-Gustav Rossby in the mid 1920s, with a large rotating platform for gfd experimentation: such an apparatus can ‘calculate’ barotropic polar  $\beta$ -plane circulations and f-plane baroclinic circulations with high resolution

# Conclusions

- It is important that laboratories complement numerical models rather than duplicate them.
- Except in health sciences/biology, labs are disappearing from universities. They are expensive in manpower. In my university there is not funding to support a lab course with, say 15 to 30 students, a senior instructor, a lab engineer and a TA.....but we do it anyway. NSF has some education money but ...
- Our students now have grown up without benefit of wood-shops, metal shops, car repair, dress-making that used to be a part of the home. They can benefit by learning to build things. Arduino boards....
- Lab work and demonstrations use different brain functions than classroom learning.
- Students doing field observations can profit by a parallel lab simulation
- You are more often surprised by a lab experiment than by a numerical experiment
- In research GFD labs need to break new ground, looking at phase-change physics, air-water interfaces, chemical/physical interaction, biological/physical interaction.
- The biggest challenge to our world at present is the integrity of the global biosphere. The lab can be used to teach both underlying science (for example following the flow of energy beginning with the sun) and merge this with 'deep ecology', culture, economics and public policy.
- Labs are aesthetically and socially exciting



This is what it's all about: the integrity of the global biosphere

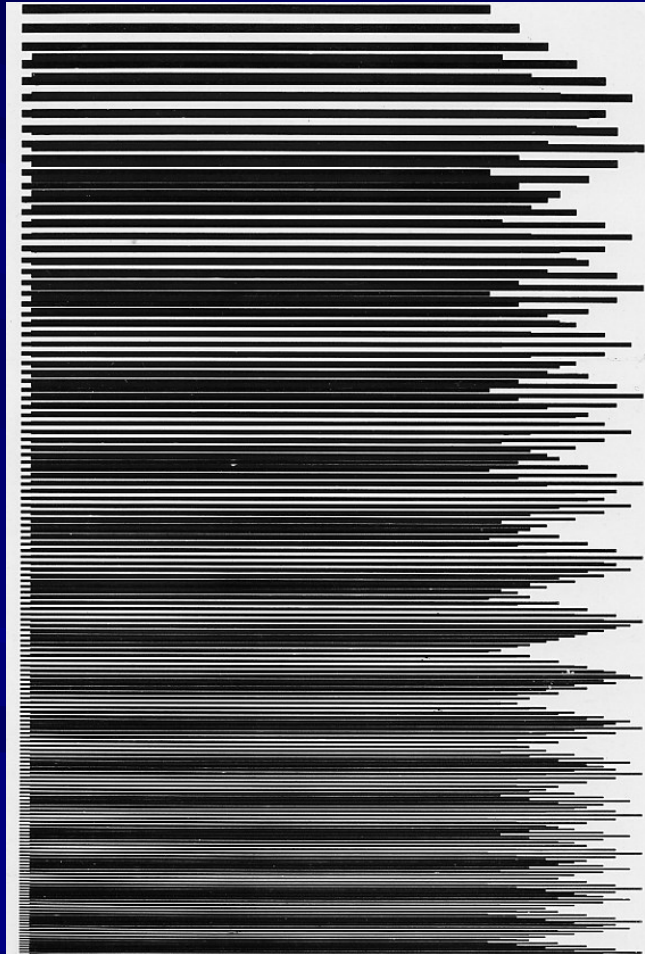




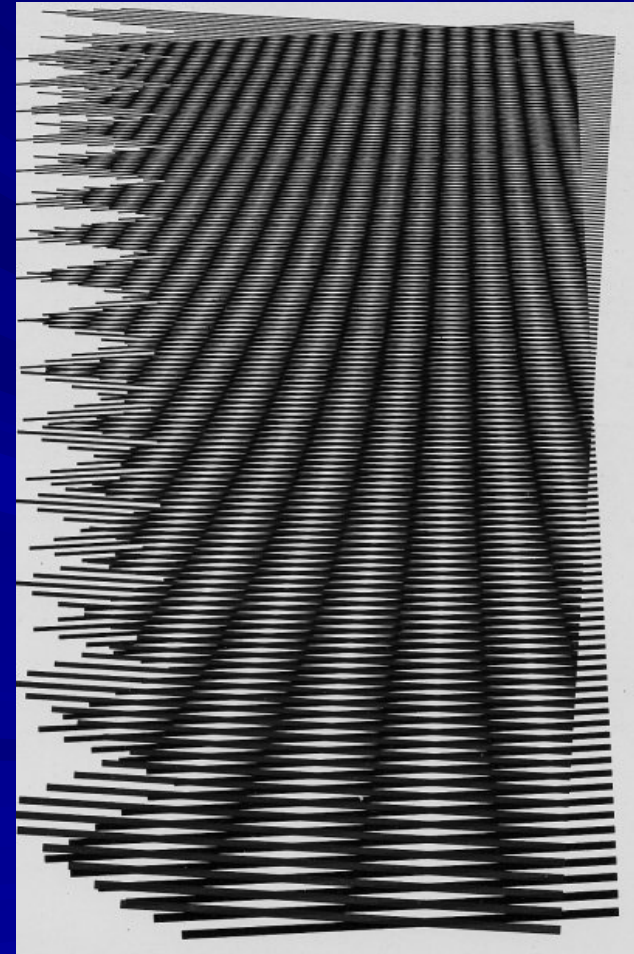
During discussions, the following came up:

Moiré and group velocity: we handed out transparencies with a bar pattern (the wavecrests); superimposing two of these and sliding one relative to the other illustrates group velocity (the constructive interference pattern). It is interesting to work out the details. The case of internal gravity waves is achieved by tilting one pattern relative to the other, then sliding. Full 2D wavepackets can be built up with 3 such sheets. The variation in wavelength gradually along the sheet allows one to show a variety of situations; for internal gravity waves keep the wavelength the same so that the dispersion is directly along the wave crests.

isotropic waves (gravity...)



anisotropic waves (internal, Rossby...)



During discussion we mentioned how easy it is to use simple digital cameras to explore wave dynamics...here streak photos of white particles showing the streamlines in a standing gravity wave (nicely contrasted with the traveling wave case).



)











# Undular bore: GFD Lab, University of Washington





# overhead projector-rotating table

